ARCHMAT (ERASMUS MUNDUS MASTER IN ARCHaeological Material Science)

A Multi-Analytical Study of Ceramics from the Chalcolithic Period and the Early Bronze Age IB from Tell El-Far'ah North – Palestine

Mervat Akrmawi
Matricola: 1947475

Supervisors:

Dr. Laura Medeghini

Dr. Michela Botticelli

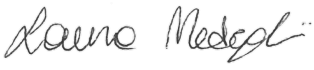

ARCHMAT Edition 2019/2021

ABSTRACT

The focus of this work is the characterization of ceramic fragments unearthed more than 60 years ago from the archaeological site of Tell El Far'ah North (west Bank), dated back to the Chalcolithic period (4500-3200 BC) and the Early Bronze Age I (3100-2900 BC). The ancient ceramics found at Tell El Far'ah North are considered fundamental archaeological material remains in reconstructing the cultural development. Indeed, they can provide insight into socio-economic backgrounds through their material culture and technological knowledge.

Mineralogical, petrographic and chemical analyses are applied by means of optical Microscopy (OM), X-Ray Powder Diffraction (XRPD) and Scanning Electron Microscopy coupled with Energy Dispersive Spectroscopy (SEM-EDS). The aim of this study is the identification of petro-fabrics that may allow the assessment of the nature of the raw material used and their provenance, in addition to the technological level, such as the firing temperature.

Keywords: Chalcolithic, Early Bronze, Um Hammad ware, Ceramics, Southern Levant, XRPD, OM, SEM-EDS.

ACKNOWLEDGMENTS

My sincere thanks and graduate goes for ARCHMAT EMMC International Selection Committee for accepting me in this master program and all the professors that contributed in my learning process throughout this masters.

I would like to thank my supervisor Dr. Laura Medeghini for her patience with me throughout my numerous revisions. She helped make some sense of the confusion with her useful comments, remarks and engagement through the learning process of this master thesis. Furthermore I would like to thank my Co-supervisor Dr. Michela Botticelli who shared her time to guide me .

I am grateful for my parents' constant love, support, and encouragement that kept me motivated and confident. Many thanks to my siblings for keeping me grounded, reminding me of what matters in life, and encouraging me to keep going. And special thanks to Yasmine for being there for me whenever I needed.

Last, but not least, my warm and heartfelt thanks go to my ARCHMATIAN friends for their support, light and hope that they had given me.

LIST OF FIGURES

LIST OF TABLES

TABLE OF CONTENTS

OVERVIEW

The thesis will be composed of six chapters which will present the result of my thesis work. The first chapter will focus on presenting the study object, the research context and the research aim, to describe the problem and to present the work of the thesis. The second chapter is dedicated to the research background, the archaeological context, the archaeological excavations, and the geological setting of the area. The third chapter includes a description of the investigated ceramic material and the methods applied in the thesis. The fourth chapter will present the results of macroscopic analysis, Optical microscopy, X-Ray Powder Diffraction (XRPD) and Scanning Electron Microscopy coupled with Energy Dispersive Spectroscopy (SEM-EDS), whereas the fifth chapter will include the discussion of the results to define the nature of the raw materials used in the production and their provenance, as well as the technological level of this ceramic production. Finally, the sixth chapter will include the conclusion.

Chapter 1 : INTRODUCTION

1.1 Study Object

Material culture gives the opportunity to reconstruct the cultural development of ancient societies, based on what they consumed, produced, and manufactured, which reflects their lifestyles. In addition, other aspects such as economic, social and cultural issues can be also taken into account.

The abundance and variety of pottery scattered across archaeological sites helps us to understand the lifestyle, past social systems of production and exchange as well as the socio-political structures of past communities and societies. The characterization of pottery involves numerous studies, from sample typology - which includes the study of shape, colour, drawings and decorations, as well as the texture of the material - to the determination of its chemical composition. Typology is useful when applied to whole or reconstructed vessels or objects, but it is proved to be less helpful with the fragmented objects, which are mostly found at any archaeological site and seem to be closely similar when examined under the microscope. The advantages of archaeometry in this case are in determining the mineralogical composition and answering questions on the nature of the raw materials, dating, use, place of production, and technology assessment (Munita et al. 2003).

In this research, twenty-one pottery sherds, excavated from Tell El Far'ah North, are examined to define their mineralogical, petrographic and chemical composition, answering questions regarding the technological aspects, the nature and the provenance of the raw materials.

1.2 Research Context:

Tell El Far'ah North was first identified by Albright in 1931 as Tirzah the biblical site and later excavated under the direction of de Vaux of the *École biblique et archéologique française de Jérusalem*, in a total of nine campaigns, from 1946 until 1960 (Amiet et al,1996).The political situation in Palestine led to an instability in the archaeological research in this area. However, in the past couple of years several expeditions led by the college of Liceo Franciscano and Universidade Nova de Lisboa, along with the Palestinian Ministry of Antiquities, provided new data on the Iron Age (10th-8th century BC).

A relevant archaeometric investigation conducted in 2019 by the Department of Earth Sciences - Sapienza University of Rome, on ceramics from the archaeological site of Tell El-Far'ah North (West Bank), dated from Early Bronze I-II (EB I-II, 3300–2700 BC) reconstructed the nature of the raw materials used in the manufacture of some ceramic typologies, as well as their provenance. According to the results of this study two petro-fabrics were distinguished by the inclusions of calcareous rock fragments, calcite, quartz, iron oxides and categorized by the presence (fabric A) or absence (fabric B) of coarse grains of calcite as predominant inclusions. The optical activity of the matrix and the presence of calcareous inclusions indicate a maximum firing temperature lower than 850 °C and in the range 700–850 °C for those ceramics showing an initial decarbonation process of calcareous inclusions. The nature of the inclusions supported a local supply of raw materials (Medeghini, et al. 2019).

1.3 Research aim

Archaeometry links different scientific fields such as chemistry, geology, evolutionary biology, physics, to support archaeology in the study of archaeological ceramics (Neff, 1993). In fact, the study of artifacts produced by human beings is one of the best instruments that researchers have in order to reconstruct the cultural development of ancient societies.

In this thesis, twenty-one diagnostic ceramic samples, unearthed in the 1950s at Tell El Far'ah North and preserved by the *École biblique et archéologique française de Jérusalem* (EBAF) are analysed by OM, XRPD, and SEM-EDS. Among the fragments under investigation, seven are dated back to the Chalcolithic period (4500-3200 BC) and others to the Early Bronze Age I (3100-2900 BC).

The aim of the study is to define the mineralogical, petrographic and chemical composition of these ceramic sherds which could help to reconstruct the technological level as well as nature and provenance of the raw materials. The significance of this study would shed light on the sum of actions performed to produce a specific object, which reflects both the material and technological knowledge achieved by the manufacturer. The choices, tools, and capability of the individual to obtain a specific product are all essential information for an in-depth study of the cultural background of an ancient community.

Chapter 2 : RESEARCH BACKGROUND

2.1 Chronology

The Chalcolithic period in the Southern Levant

The Chalcolithic period in the Southern Levant extends from the 5th to the mid-4th millennium BC. It is a fundamental period that witnessed a change in the socio-political structure, craft production and subsistence economy (Rowan & Golden, 2009). This period is featured by the use of copper and painted pottery vessels. Albright (1931) first labelled the 4th millennium BC as the Chalcolithic period and according to Moore (1985) the 4th millennium BC is used as a chronological synonym for the Levantine Chalcolithic as he dated the end of the Levantine Neolithic societies to about 4000 BC. The best-known and most homogeneous archaeological entity of the 4th millennium BC is the Ghassulian culture of the Southern Levant, first found in the site of Tulailat Al-Ghassul (Mallon et al., 1934) and later in Western Negev (Macdonald, 1932) and Beer Sheva regions (Perrot, 1955).
When describing the Chalcolithic period, the architecture and thick accumulation of painted pottery indicates that the sites were sedentary and occupied for a long period of time. The communities could be described as rural with a low degree of social complexity up until the revolution of metallurgy during the late 4th and early 3rd millennium BC. After that, the area witnessed a rapid cultural change influenced by Egypt and Mesopotamia, which impacted the rural and provincial Levantine Chalcolithic societies, contributing to more complex social organizations (Gilead, 1988).
Chalcolithic pottery is characterized by coarse, usually mild-buff and sometimes red-slipped vessels. It includes large bowls with straight sides, occasionally decorated with a painted band on the outer rim or with a shallow pedestal base; bow-rim jars and hole-mouthed jars decorated with bands of finger impressions under the rim. Mat-impressed bases, thick horizontal ledge handles with large finger impressions, loop handles with an enlarged attachment to the vessel's body and occasionally incised herringbone-pattern decorations

are all features of the Chalcolithic pottery at Tell El Far'ah North (Miroschedji &Chambon, 1993). According to Garfinkel (1999), typologically these pottery vessels belong to the middle and late Chalcolithic periods.

The Early Bronze Age in the Southern Levant

The Early Bronze Age (3300– 2000 BC) in the Southern Levant is generally assigned to three subperiods: EB I, ranging between ca 3300-3050 BC (Miroschedji, 2013) and 3300-2950 BC (Braun and Gophna, 2004); EB II (2900-2700); EB III (2700– 2300 BC) and EB IV (2300– 2000 BC), often labelled as separate periods. EB is characterized by a distinct material culture as well as a somewhat unified social structure, which has traditionally been viewed as relatively short.
Former EB I settlements may be described as extensive and dispersed. Social groups were small and segmented; a limitation of specialized crafts and long-distance contacts were observed. The earliest phase of the Levantine Bronze age, EB IA, has only recently been recognized as a separate archaeological entity. As far as social and economic organization is concerned, it is considered post Chalcolithic. It is quite dissimilar to the agglomerated villages that provided the basis for urbanism in late EB I (or EB IB), and represented the emergence of village societies in the EB IA. EB IA is characterized by numerous villages scattered across the landscape, some of which contain substantial populations and where only a few functioned as regional centres (Braun 2001, 2011a,b). However, the ceramics unearthed from Tell El Far'ah North has been labelled as EB IB production.
The EB IB is characterized by the emergence of large cemeteries marked by multiple burial tomb caves, where most of the ceramic assemblages were unearthed from. Regionally distinctive fabrics and styles are featured in the ceramic industry (Braun 2001, 2011a,b; Regev et al.,2012).

The Um Hammad Ware, which is also associated with the EBI, was firstly identified by Glueck in a survey performed in (1951) and later by de Contenson (1960) and Mellaart (1962) at Tell Um Hammad esh-Sherqi in the Jordan valley, east of the river. Mellaart (1962) introduced the term 'Um Hammad esh-Sherqi Ware', which came to be known as Um Hammad Ware. It was thought to be concentrated mostly around the site of Tell Um Hammad in the eastern Jordan valley (Miroschedji, 1971; Braun, 1996). According to Rice (1987), the Um Hammad ware includes several morphological types including excellently crafted forms and well-levigated fabrics ranging in colour from shades of red to dark brown and grey. Bowls, *kraters*, hole-mouths and other jar types belong to Um Hammad Ware. The Um Hammad Ware is characterized by thick walls, decorated rims and unique rope decorations applied to the bodies of the vessels. In assemblages recovered from the Wadi Far'ah North area, there was a dominance of this ware, which was not present at any known large cemetery sites in the area, indicating that this was most likely a local common ware, not a luxury item (Bar, 2010).

Chalcolithic and Early Bronze as a transitional period

Stratigraphically, the Early Bronze Age I is separated from the Chalcolithic by a thin layer of sterile earth, but it shares the same stratigraphic features such as the layers of small stones presumably from mid-walls of pit dwellings. Although these two phases are separated, some scholars contend that material culture remained the same during both periods (Milevski, 2013).

Basing on mixtures of archaeological material from different phases of occupation, some scholars have argued that some transitional assemblages or continuity of traditions from the Chalcolithic into the Early Bronze existed (Golani, 2004; Golani and Nagar, 2011; Rosenberg

and Golani, 2012). According to Milevski (2013), there is no real transition, but rather "false transitions" derived from a misunderstood archaeological record. Thus, he attempted to distinguish the features of each period in the ceramic production and supplying processes.

2.2 Location

Figure 1 Location of Tell El Far'ah North (Beller, et al, 2016)

Tell El Far'ah North is located 11 km northeast of Nablus, in the north-eastern part of West Bank (Figure 1). It is bordered by Tammun village to the east, Tubas city and El Far'ah Camp to the north, Yasid village (Jenin Governorate) to the west and Wadi Al Bathan to the south (Arij,2006).

Its geographical location is important for its dimensions: it includes the incline, which is 600 m long by 300 m wide, on a rocky plateau, which descends towards the northeast, where the human occupation first settled. The location of the archaeological site in this place conforms to three fundamental reasons: easy natural defence (except in the west flank) given by the surrounding valleys, which guaranteed an easy fortification from the south and the east; a good water supply, due to two natural water resources nearby ('Ain ad-Dlaid and 'Ain El-Far'ah); and the control over the communication route which connected the Jordan valley (situated 20 km west) to the region of the ancient city of Shechem (currently Tell Balata, in Nablus) and towards Beth Shan to the North (Amiet et al., 1996).

2.3 Archaeological Excavations

In 1946, a project of excavations with the permission of Jordan's Department of Antiquities started in Tell El Far'ah North by the director of the *École Biblique et Archéologique Française de Jérusalem* (EBAF), Roland de Vaux. Between the 1st of June 1946 and the 22nd of October 1960, a total of nine archaeological campaigns were conducted. In the 1970s, EBAF tried to re-establish the project but was not successful. The site was first inhabited in the pre-pottery Neolithic B and then abandoned until the second half of the 5th millennium. During the Chalcolithic period the site was not heavily occupied while in the Early Bronze Age I and II it was intensely occupied. The site was abandoned during Middle Bronze Age IIA; however, some graves indicate that the occupation resumed by the end of that period. In the Middle Bronze Age IIA and IIB, it was a small rural settlement which later became a fortified city. Thereafter, occupation continued up until the Iron Age. De Vaux's work has led to the establishment of an occupation sequence, formed by seven major periods in the time range from ca. 8500 to 600 BC: pre-pottery Neolithic (8500-5500 BC), pottery Neolithic (5500-4500 BC), Chalcolithic (4500-3500 BC), Early Bronze I (3500-2900 BC), Early Bronze II (2900-2600 BC) Middle Bronze I (2000-1800 BC), Middle Bronze II (1800-1550 BC), Late Bronze I (1550-1400 BC) Late Bronze II (1400-1200 BC), Iron I (1200-1000 BC), Iron II (1000-586 BC), Roman period (63 BC-325 AD), Byzantine period (325-638 AD), and Arab period (11th to the 13th centuries AD).

According to (De Vaux's, 1976), the site could be divided into four designated areas (Figure 2):

- Area I, which was excavated between 1946 and 1947. Located in the northern part of the site towards the Far'ah Spring. De Vaux labelled it as 'Eneolithique Moyen', 'Eneolithique Superieur', 'Ancien Bronze I', 'Ancien Bronze IIa', 'Ancien Bronze IIb' and 'Moyen Bronze II'. These periods were later distinguished as Chalcolithic Moyen and Chalcolithic Superieur, and correspond to the Late Chalcolithic and Early Bronze Age I in current terminology, respectively. The Eneolithique Superieur was ascribed to a single period known as Ancien Bronze I. This period corresponds to the beginning of the Early Bronze II or Ancien Bronze IIA and IIB.
- Area II, excavated from 1950 to 1959, is located in the northwest area of the site. It consists of a succession of strata from the earliest Neolithic to the Chalcolithic period. In the sequence of the 'Ancient Bronze I' and 'Ancient Bronze II', six phases of occupation were recognised and called from period 1 to period 5 and final period. Similarly, six phases of occupation were identified in the Middle Bronze Age II that were called Strata A1 to A2 and B1 to B5.
- Area III, excavated in 1960, is located to the southwest of the site. Above the bedrock containing Early Bronze Age I sherds, four phases of the Early Bronze Age II and at least five phases of the Middle Bronze Age II occupation were discovered. This area was also extramural after the Early Bronze Age.
- Area IV is the extension of area II outside the line of the Early and Middle Bronze Age fortifications. Above the Early Bronze Age fortifications, two phases (A1 and A2) of the Middle Bronze Age II occupation prior to the erection of the Middle Bronze Age Rampart were identified (Miroschedji & Chambon,1993).

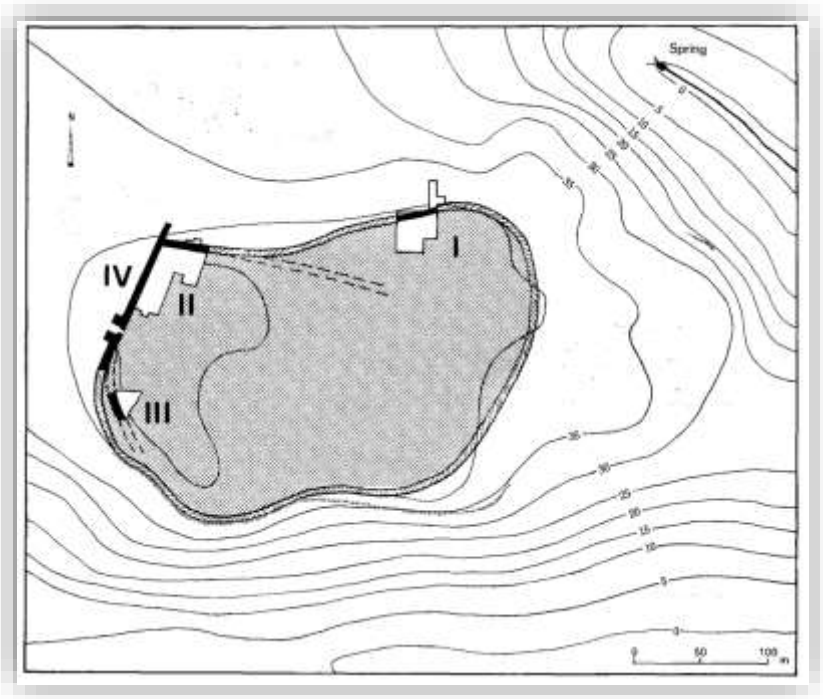

Figure 2 Tell El Far'ah North: plan of the mound and excavated areas between 1946 and 1960 with the subdivisions of the site, labelled I, II, III and IV (Miroschedji & Chambon,1993).

At the present, the archaeological materials exhumed by the French team are conserved in several institutions: EBAF, Rockefeller Museum (Jerusalem), Museum du Louvre and the Jordan Museum (Amman) (Amiet et al.,1996). In 1931, William F. Albright was the first researcher to propose the identification of Tell El Far'ah with the ancient city of Tirzah, mentioned seventeen times in the Old Testament (Albright, 1931). In October 2016, the Universidade da Coruña, Universidade Nova de Lisboa and the Ministry of Tourism and Antiquities of Palestine signed a cooperation agreement in order to start a new research phase at Tell El-Far'ah North. The first field campaign took place in October 2017 and it continued until the present day focusing on the Iron age period of the site.

2.4 Geological setting

The archaeological site of Tell El-Far'ah North is located in the Nablus district (Figure 3). The neighbouring outcrops include Cretaceous and Tertiary marine carbonate sedimentary rocks such as limestone, dolostone, chalks, marls, chert, alluvium, quartzite and rare Jurassic outcrops. The Ramali formation exposed in Wadi Far'ah includes the lower Cretaceous rocks, which consists of sandstone between the Maleh and Beit Kahil formations, a prominent craggy limestone.

The main outcrop in the Wadi Far'ah is a massive iron-stained limestone alternated with sandy marls and shales characterized by the deposition of Beit Kahil which is considered in the Cenomanian age, the lowest stage of the Upper Cretaceous series (Figure 4).

Marl, chalky limestone, clay and thin interbedded dolomitic limestone are the Uppermost part of this formation which characterizes the Yatta Formation that is covered by the Hebron Formation with blue-green limestone and dolomitic limestone. Dolostones, limestones, chalks and marls are exposed on the flanks of the Far'ah district where the Cenomanian age ends with the Bethlehem Formation.

Two main Jurassic formations are identified in Wadi Maleh over an igneous basement. Lower and upper formations are identified in the Maleh formations; the lower formation includes mainly limestone and basalt whereas the upper formation embodied by marl with chalky limestones or chalk with chalky limestone. The first igneous event, which took place at the end of the Jurassic period, can be observed in Wadi Far'ah in the basaltic layers that are interbedded with yellow-red sandstone.

The Jerusalem Formation, exposed in narrow strips along the Far'ah anticline, is predominantly made of limestones, dolostones and chalk, which were deposited during the Turonian period. Chalk may be associated with chert, which represents the Cretaceous-Tertiary transition phase.

Among the Tertiary rocks, we find the Bayda Formation. The Jenin subseries covers one third of the district of Nablus. Five facies of limestone and chalk are distinguished: chalk with interbedded limestone, limestone with minor chalk, chalk with minor chert, bedded massive limestone and limestone. Conglomerates are found in the Bayda Formation, which were produced by a second igneous event that occurred at the end of the Eocene and originated deposits similar to those found in Wadi Far'ah at the end of the Jurassic period. In the Quaternary, the Lisan Formation (laminated marls and gypsum), alluvium (unconsolidated marls with siliceous sands) and Nari Formation were deposited (Medeghini et al., 2019).

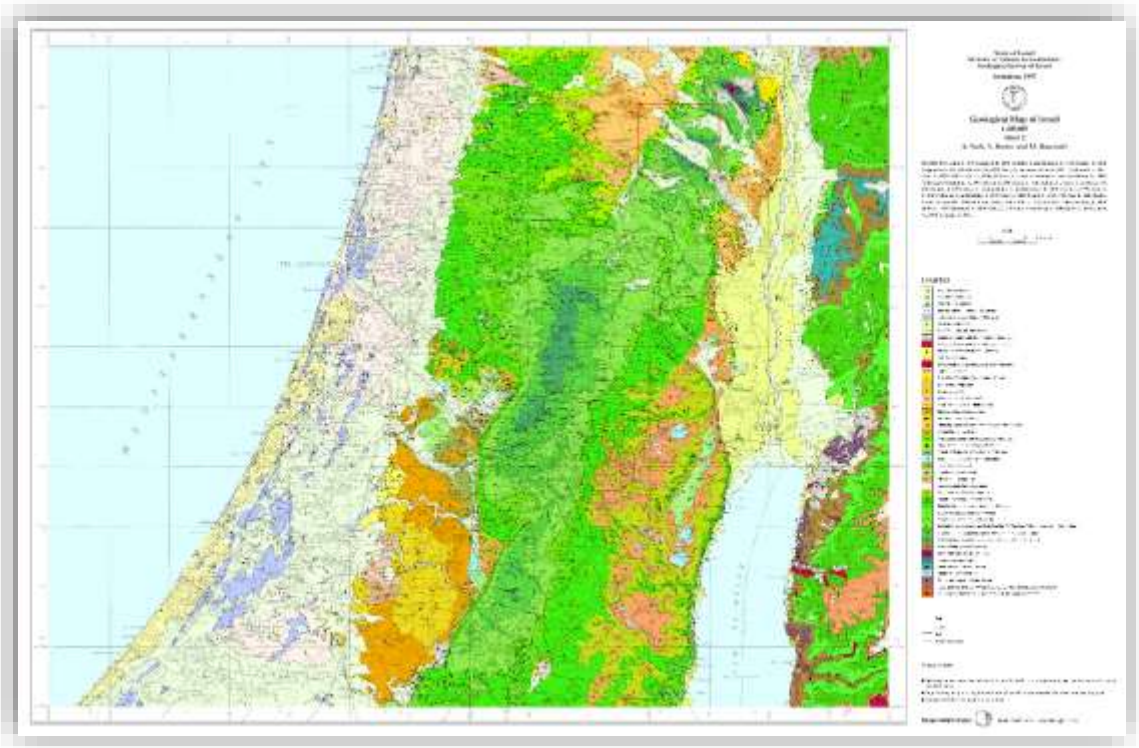

Figure 3 A geological map labelling Tell El- Far'ah as Tirzah (the biblical name) (Sneh, et al, 1998)

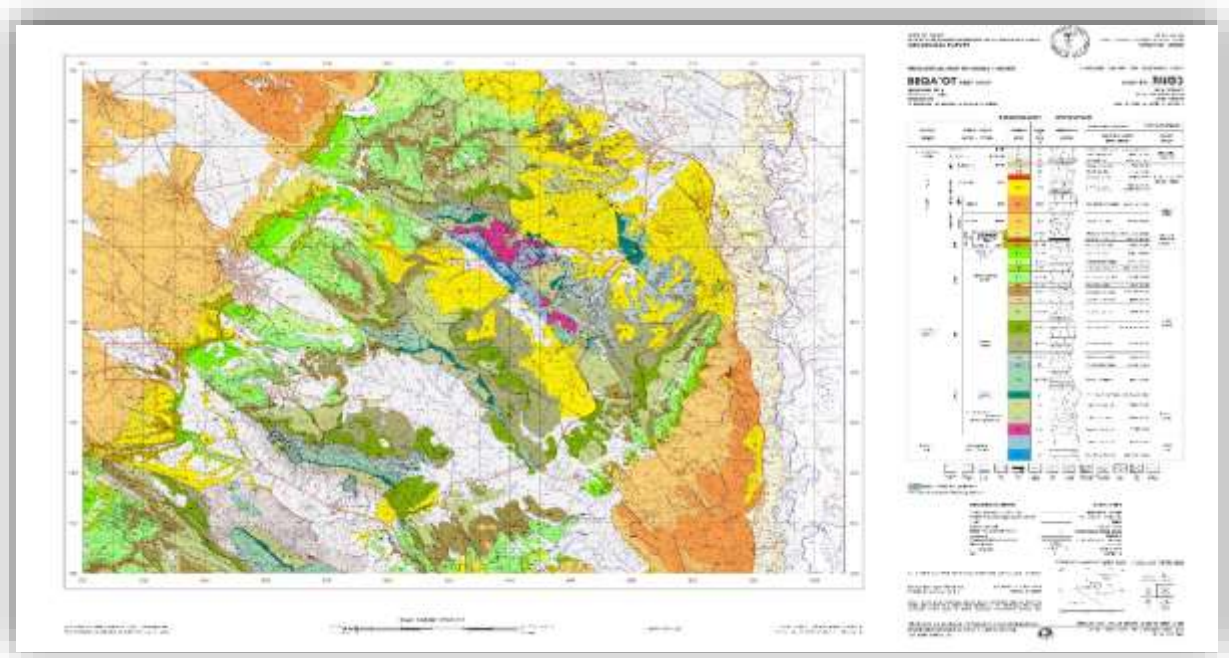

Figure 4 Beqa'ot, Wadi El Far'ah labelled as Al Holocene stage, 2 m thickness and mapping units corresponding to Alluvium, colluvium, soil in the Dead sea group (Mimran et al., 2016).

Chapter 3 : MATERIALS AND METHODS

3.1 Materials

Twenty-one diagnostic samples were selected to be studied. Seven are dated to the Chalcolithic period (4500-3500 BC) mostly consisting of tableware, simple ware bowls, storage ware jars, storage ware holemouth jars and red slip bowls. Other fourteen were dated to the EB IB (3500-2900 BC) and divided typologically into two groups: the first is labelled Early Bronze IB Um Hammad ware, which includes storage ware jars, tableware and simple ware jars; the second is labelled Early Bronze IB (other wares) including tableware/red slip bowls, tableware/red slip amphoriskos, storage ware jars with ledge handle, storage ware pithos with grain-wash decoration, storage ware holemouth jars and red burnished ware bowl.

3.2 Methods

Optical microscopy

A small fragment of each sample is collected, fixed to a glass microscope slide and ground with a diamond lap or with an abrasive powder until it is exactly 30 μm thick. With this thickness most of the minerals become transparent to be studied under a petrological microscope.
A Zeiss D-7082 Oberkochen polarized optical microscope at the Department of Earth Sciences, Sapienza University of Rome, Italy, was used for the analysis of thin-sections according to Whitbread's scheme (1995), which facilitates the classification of pottery based on its porosity, matrix and inclusions.

Scanning Electron Microscopy coupled with Energy Dispersive Spectroscopy (SEM-EDS)

The microstructural features, deep morphological analysis of tempers and qualitative chemical description have been performed using a FEI Quanta 400 electron microscope (Department of Earth Sciences, Sapienza University of Rome, Italy), equipped with an EDS unit for microanalysis.

X-Ray Powder Diffraction (XRPD)

The ceramic sherd samples were scratched using a raiser and then hand grinded into the agate mortar using a pestle. Once the loose powder is obtained, it is loaded into the sample holder for random orientation of crystallites, thus minimizing the effects of preferred orientation. X-Ray powder diffraction data were collected at the Department of Earth Sciences of Sapienza University of Rome, using a Bruker D8 Advance diffractometer, with CuKa radiation Spectra were taken in the range 5°–60° 2θ, with steps of 0.02° 2θ and step-times of 1 s/step.

Chapter 4: RESULTS

4.1 Macroscopic analysis

SAMPLE TFN.1959.B.686/1

The sample is a fragment from a Chalcolithic tableware bowl. The sherd is from the neck and partially from the rim of the vessel. It appears to have a range of brownish to reddish luster on both the outer and inner surfaces, which gives it a smooth surface. However, the core colour is light brown to beige Khaki (Figure 5).

Figure 5 Sample TFN.1959.B.686/1 (inner surface to the left and outer surface to the right)

SAMPLE TFN.1959.B.686/3

The sample is a fragment from a Chalcolithic storage ware jar. The sherd comes from the bottom body of the jar and possibly includes part of the base of the vessel. It appears to have a homogenous reddish luster on the outer surface, which gives it a smooth surface. The inner surface appears to be rough but almost homogenous in colour. However, the core colour resembles the inner surface, with khaki to light brown colour (Figure 6).

Figure 6 Sample TFN.1959.B.686/3 (inner surface to the left and outer surface to the right).

SAMPLE TFN.1959.B.686/7

The sample is a fragment from a Chalcolithic storage tableware. It is a holemouth jar. The sherd is from the neck and partially from the rim of the vessel. It appears to have some residues of a brownish luster on the upper part of the outer surface, which gives it a smooth surface. Below the luster there is a thumb print decoration in a horizontal line along the vessel. The outer surface colour is lighter khaki than the inner surface colour (Figure 7).

Figure 7 Sample TFN.1959.B.686/7 (inner surface to the left and outer surface to the right)

SAMPLE TFN.1959.L.689sup./1

The sample is a fragment from a Chalcolithic storage ware. The sherd is from the body of a jar. It has a rough surface. The colour is almost homogenous and light brown on both the inner and the outer surfaces (Figure 8).

Figure 8 Sample TFN.1959.L.689sup./1 (inner surface to the left and outer surface to the right)

SAMPLE TFN.1959.L.689sup./2

The sample is a fragment from a Chalcolithic simple ware. The sherd of this holemouth jar is from the neck and partially from the rim of the vessel. It has traces of a brownish luster on the outer surface which gives it a smooth surface. The colour of the rim is reddish brown while the rest of the neck is light khaki, on the outer surface. The inner surface has a more homogenous khaki colour, while the core is dark beige (Figure 9).

Figure 9 Sample TFN.1959.L.689sup./2 (inner surface to the left and outer surface to the right)

SAMPLE TFN.1959.L.689sup./3

The sample is a fragment from a Chalcolithic storage ware. A holemouth jar, the sherd is from the neck and partially from the rim of the vessel. It appears to have a brownish-to-reddish luster on both the outer and inner rough surfaces. It appears to have spots of a brownish patina attached to both surfaces which gives it a rough appearance. The colour is light brown, however the inner surface appears to be darker than the outer (Figure 10).

Figure 10 Sample TFN.1959.L.689sup./3 (inner surface to the left and outer surface to the right)

SAMPLE TFN.1959.L.689sup./4

The sample is a fragment from a Chalcolithic tableware. This red slip bowl sherd is from the neck and the rim of the vessel. It appears to have a brownish-to-reddish luster on both the outer and inner surfaces, which gives it a smooth surface. However, the core colour is light brown to beige Khaki (Figure 11).

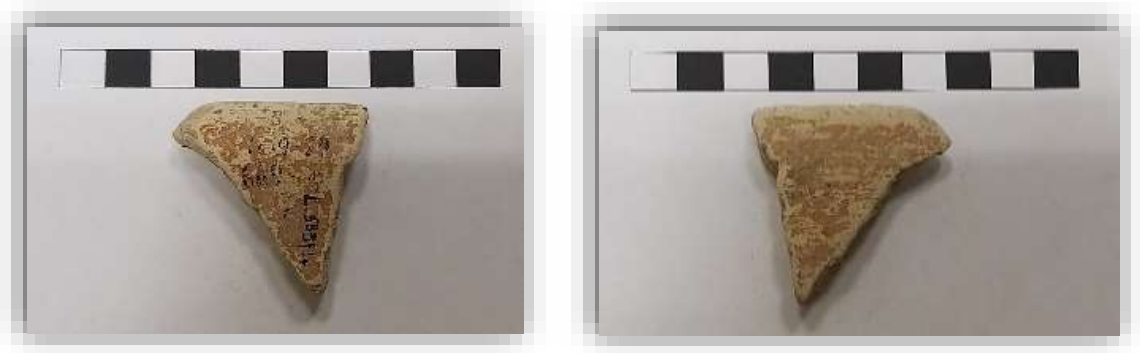

Figure 11 Sample TFN.1959.L.689sup./3 (inner surface to the left and outer surface to the right)

SAMPLE TFN.1959.L.718/9

The sample is a fragment from the Early Bronze Age (Um Hammad Ware), a storage ware jar. The jar sherd is from the neck and the rim of the vessel. Below the rim there is a strip of incised clay circling the vessel horizontally. The jar colour varies from reddish to light brown-khaki. The surface of the jar appears to be rough with big grains shown to the naked eye. The core colour is a lighter khaki (Figure 12).

Figure 12 Sample TFN.1959.L.718/9 (inner surface to the left and outer surface to the right)

SAMPLE TFN.1959.L.718/8

The sample is a storage ware jar fragment from the Early Bronze Age (Um Hammad Ware). The jar sherd is from the neck and rim of the vessel. Below the rim there is a strip of incised clay circling the vessel horizontally. The outer surface colour varies from reddish to light brown-khaki, while the inner surface is more reddish. The surface of the jar appears to be rough with big grains shown to the naked eye. The core colour is lighter khaki (Figure 13).

Figure 13 Sample TFN.1959.L.718/8 (inner surface to the left and outer surface to the right)

SAMPLE TFN.1959.L.718/32

The sample is a storage ware jar fragment from the Early Bronze Age (Um Hammad Ware), and the sherd is from the body of the vessel. Two strips of incised clay circle the vessel horizontally. The outer surface is reddish and covered with some khaki patina, whereas the inner surface is dark khaki. The surface of the jar appears to be rough. The core colour resembles the inner surface (Figure 14).

Figure 14 Sample TFN.1959.L.718/32 (inner surface to the left and outer surface to the right).

SAMPLE TFN.1959.L.718/33

The sample is a tableware/simple ware jar fragment from the Early Bronze Age (Um Hammad Ware) and the sherd is from the body of the vessel. Two strips of incised clay circle

the vessel horizontally. The outer and inner surfaces are reddish. The surface of the jar appears to be rough. The core colour resembles the inner surface (Figure 15).

*Figure 15 Sample TFN.1959.L.718/33 (**i**nner surface to the left and outer surface to the right).*

SAMPLE TFN.1959.L.718/35

The sample is a tableware/simple ware jar fragment from the Early Bronze Age (Um Hammad Ware), and the sherd is from the body of the vessel. One strip of incised clay circle the vessel horizontally. The outer and inner surfaces are reddish and rough. The core colour resembles the inner surface (Figure 16).

*Figure 16 Sample TFN.1959.L.718/35 (**i**nner surface to the left and outer surface to the right).*

SAMPLE TFN.1959.B.672/4

The sample is a tableware/simple ware bowl fragment from the Early Bronze Age (Um Hammad Ware) and the bowls sherd is from the body of the vessel. Two strips of incised clay circle the vessel horizontally. The outer and inner surfaces are reddish. The surface of the bowl appears to be rough. The core colour resembles the inner surface (Figure 17).

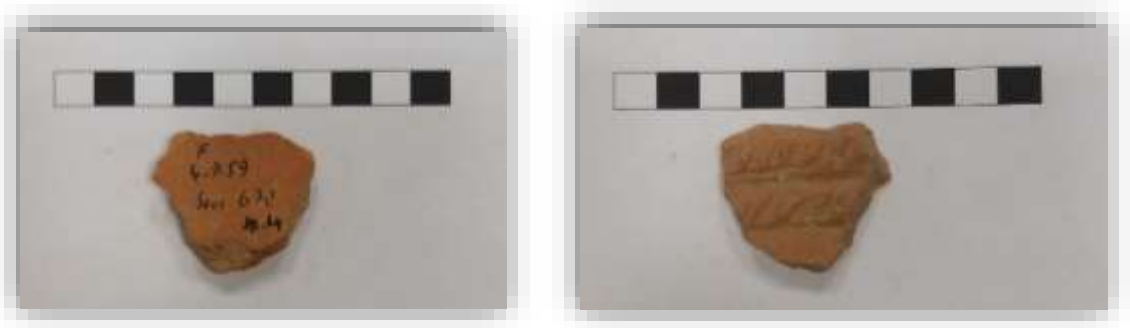

Figure 17 Sample TFN.1959.B.672/4 (inner surface to the left and outer surface to the right).

SAMPLE TFN.1959.L.686/8

The sample is a simple ware bowl fragment from the Early Bronze Age (Um Hammad Ware) and the bowl sherd is from the body of the vessel. One strip of incised clay circle the vessel horizontally. The outer and inner surfaces are reddish. The surface of the bowl appears to be rough. The core colour resembles the inner surface (Figure 18).

Figure 18 Sample TFN.1959.L.686/8 (inner surface to the left and outer surface to the right)

SAMPLE TFN.1959.L.686/6

The sample is a storage ware *pithos* with grain decoration fragment from the Early Bronze Age and the sherd is from the upper part of the body, where a ledge handle is also present. The outer surface of the vessel is grain-decorated, the grain colour is brown whereas the pottery is reddish. The inner surface of the vessel is dark khaki and on the upper part it appears to have a double layer of clay. The core is similar in colour to the inner surface (Figure 19).

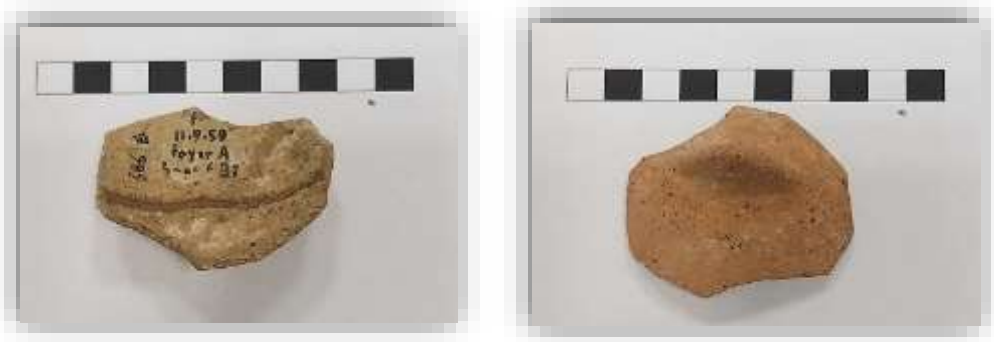

Figure 19 Sample TFN.1959.L.686/6 (inner surface to the left and outer surface to the right).

SAMPLE TFN.1959.L.718/13

The sample is a tableware red slip *amphoriskos* from the Early Bronze Age and the sherd is a loop handle. The outer surface is reddish with spots of khaki and it appears to be rough. The inner surface is more of a reddish colour. The loop is probably made with a rounded object because it looks symmetric (Figure 20).

Figure 20 Sample TFN.1959.L.718/13 (inner surface to the left and outer surface to the right).

SAMPLE TFN.1954.B.272/5

The sample is a ledge handle fragment from a storage ware jar from the Early Bronze Age, the surface appears to be rough with large-grained inclusions. The grains colour is lighter than the clay, where the clay is reddish brown and the grains are light khaki. The core is light khaki in colour (Figure 21).

Figure 21 Sample TFN.1954.B.272/5 (inner surface to the left and outer surface to the right).

SAMPLE TFN.1959.L.718/31

The sample is a storage ware *pithos* with grain wash decoration from the Early Bronze Age. The *pithos* sherd is painted with blackish stripes decorations over a light khaki slip. The sherd is lighter in weight than the other sherds. It appears to be rough. The outer surface colour is light khaki while the inner surface is greyish khaki. The cores colour resembles the inner surface colour (Figure 22).

Figure 22 Sample TFN.1959.L.718/31 (inner surface to the left and outer surface to the right).

SAMPLE TFN.1959.L.704/7

The sample is a storage ware, holemouth jar from the Early Bronze Age. The holemouth jar sherd is from the rim of the vessel. The outer surface colour is light khaki on the top whereas the bottom of the sherd has stains of reddish colour, which might be the residues of a luster and give it a smooth surface. The inner surface of the sherd has homogenous khaki colour. Both sides of the sherd have large grains. The core is similar in colour to the inner surface of the sherd (Figure 23).

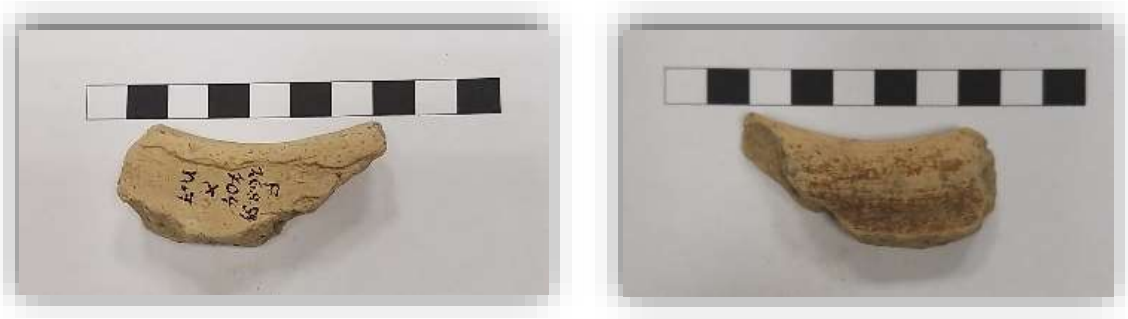

Figure 23 Sample TFN.1959.L.704/7 (inner surface to the left and outer surface to the right).

SAMPLE TFN.1959.L.718/3

The red burnished ware bowl is from the Early Bronze Age. The bowl sherd is from the neck and rim of the vessel. The outer surface has what seems to be a reddish luster and beneath it a khaki greyish colour. The surface looks smooth. The inner surface appears to be darker khaki than the outer surface, with big grains. The core colour resembles the inner surface (Figure 24).

Figure 24 Sample TFN.1959.L.718/3 (inner surface to the left and outer surface to the right).

SAMPLE TFN.1959.L.718/4

The storage ware bowl is from the Early Bronze Age and the sherd is from the body of the vessel. The outer surface is reddish with big grains. The surface looks rough. The inner surface appears to be darker brown-reddish in colour. The core colour resembles the inner surface (Figure 25).

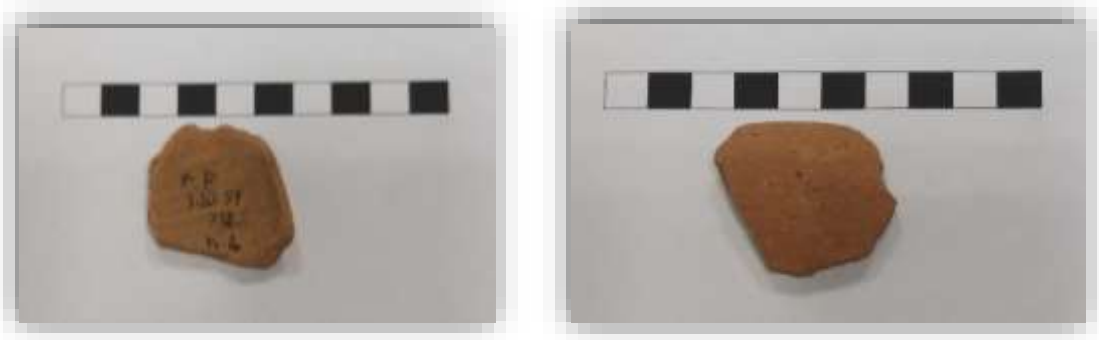

Figure 25 Sample TFN.1959.L.718/4 (inner surface to the left and outer surface to the right).

Table 1 Samples description

SAMPLE	DATE	CLASS	SHAPE	POTTERY PART	DECORATION	COLOUR
TFN.1959.B.686/1	CHALCOLITHIC	Tableware/ simple ware	Bowl	Neck and rim	No decoration	Brownish to reddish luster/core colour: light beige Khaki.
TFN.1959.B.686/3		Storage ware	Jar	Bottom body of the jar and a partial base	No decoration	Homogenous reddish luster/core colour: khaki to light brown.
TFN.1959.B.686/7		Storage ware	Holemouth jar	Neck and rim	Thumb print decoration	Covered with a brownish luster on the upper part. The outer surface colour is lighter khaki than the inner surface colour.
TFN.1959.L.689sup./ 1		Storage ware	Jar	Body	No decoration	Homogenous light khaki.
TFN.1959.L.689sup./2		Simple ware	Holemouth jar	Neck and rim	No decoration	Traces of a brownish luster on the outer surface. The colour of the rim is reddish brown while the rest of the neck is light khaki, on the outer surface. The inner surface has a more homogenous khaki colour, while the core colour is dark beige
TFN.1959.L.689sup./3		Storage ware	Holemouth jar	Neck and rim	No decoration	Brownish to reddish luster on both the outer and inner surfaces. The colour is light brown, However, the inner surface appears to be darker than the outer.
TFN.1959.L.689sup./4		Tableware	Red slip bowl	Neck and rim	No decoration	Brownish to reddish luster on both the outer and inner surfaces/the core colour is light brown to beige Khaki.

SAMPLE	DATE	CLASS	SHAPE	POTTERY PART	DECORATION	COLOUR
TFN.1959.L.718/9	EARLY BRONZE (UM HAMMAD WARE)	Storage ware	Jar	Neck and rim	Incision	The colour varies from reddish to light brown-khaki. The core colour is lighter khaki.
TFN.1959.L.718/8		Storage ware	Jar	Neck and rim	Incision	The outer surface colour varies from reddish to light brown-khaki. The inner surface is more reddish. The core colour is lighter khaki.
TFN.1959.L.718/32		Storage ware	Jar	Body	Incision	The outer surface is reddish and covered with some khaki patina. Whereas the inner surface is dark khaki. The core colour resembles the inner surface.
TFN.1959.L.718/33		Tableware/ simple ware	Jar	Body	Incision	The outer and inner surfaces are reddish. The core colour resembles the inner surface.
TFN.1959.L.718/35		Tableware/ simple ware	Jar	Body	Incision	The outer and inner surfaces are reddish. The core colour resembles the inner surface.
TFN.1959.B.672/4		Tableware/ simple ware	Bowl	Body	Incision	The outer and inner surfaces are reddish. The core colour resembles the inner surface.
TFN.1959.L.686/8		Simple ware	Bowl	Body	Incision	The outer and inner surfaces are reddish. The core colour resembles the inner surface.

SAMPLE	DATE	CLASS	SHAPE	POTTERY PART	DECORATION	COLOUR
TFN.1959.L.686/6	EARLY BRONZE (OTHER WARE)	Storage ware	*Pithos* with grain wash decoration	Body	Grain decorated	The grain colour is brown whereas the pottery is reddish. The inner surface of the vessel is dark khaki and on the upper part it appears to have a double layer of clay. The core in colour is similar to the inner surface.
TFN.1959.L.718/13		Tableware	Red slip amphoriskos	A Loop handle	No decoration	The outer surface is reddish with spots of khaki. The inner surface is more of a reddish colour.
TFN.1954.B.272/5		Storage ware	Jar with ledge handle	A ledge handle	No decoration	The grain colour is lighter than the clay, where the clay is reddish brown and the grains are light khaki. The core in colour is a light khaki.
TFN.1959.L.718/31		Storage ware	*Pithos*, with grain wash decoration	Body	Blackish stripes paint decoration over a light khaki slip	The outer surface colour is light khaki while the inner surface is greyish khaki. The core colour resembles the inner surface colour.
TFN.1959.L.704/7		Storage ware	Holemouth Jar	Rim	No decoration	The outer surface colour is light khaki from the top whereas the bottom of the sherd has a reddish luster. The inner surface of the sherd has homogenous khaki colour. Both sides of the sherd have large grains. The core colour is similar to the inner surface of the sherd.
TFN.1959.L.718/3		Red Burnished ware	Bowl	Neck and Rim	No decoration	The outer surface has a reddish luster and beneath it a khaki greyish colour. The inner surface is darker khaki than the outer surface with big grains. The core colour resembles the inner surface.
TFN.1959.L.718/4		Storage ware	Bowl	Body	No decoration	The outer surface is reddish with big grains. The inner surface is a darker brown reddish colour. The core colour resembles the inner surface.

4.2 Microscopic investigation

SAMPLE TFN.1959.B.686/1

It displays a unimodal grain-size distribution of the inclusions, with an estimation of around 20%. They are equant and elongated, from angular to rounded and from single- to double-spaced, with no alignment. The inclusions are mainly characterized by calcareous rocks, with the predominant presence of equant to elongated calcite and a few nodules of iron oxides. Fossils are common, with size varying from 50 to 200 µm, and very rare elongated quartz crystals have also been identified in the calcareous matrix. The matrix is slightly optically active, heterogenous in colour ranging from dark orange to light brown (in PPL). The voids form approximately 5% of the matrix, consisting of micro-vesicles and macro-vughs aligned to the margin of the sample (Figure 26).

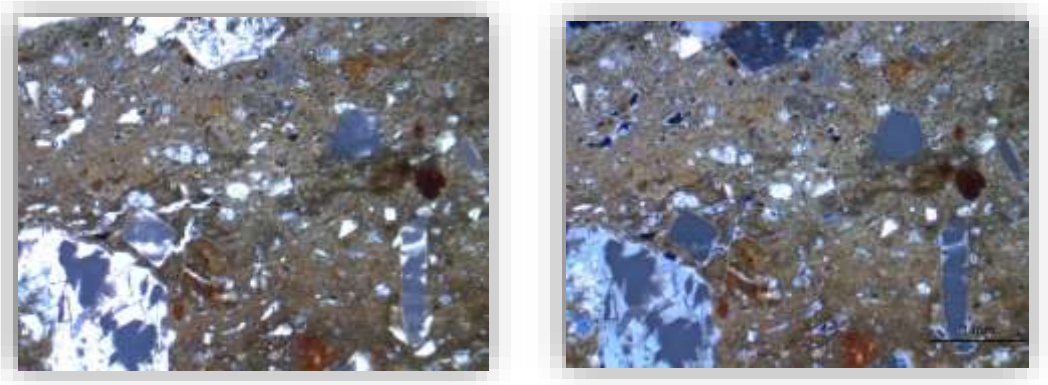

Figure 26 Optical light microscope images of sample TFN.1959.B.686/1 in plain polarized light (PPL) (left) and Crossed polarized light (XPL) (right)

SAMPLE TFN.1959.B.686/3

It displays a unimodal grain-size distribution of the inclusions, with an estimation of around 30%. They are equant and elongated, from angular to rounded and from single to double-spaced, with no alignment. The inclusions are mainly characterized by calcareous rocks, with the predominant presence of equant to elongated calcite, a frequent presence of elongated quartz, and a few nodules of iron oxides in the calcareous matrix. The matrix is slightly optically active, homogenous reddish brown in colour (in PPL). The voids form approximately 10% of the matrix, consisting of micro- to mega-vesicles and mega-vughs aligned to the margin of the sample (Figure 27).

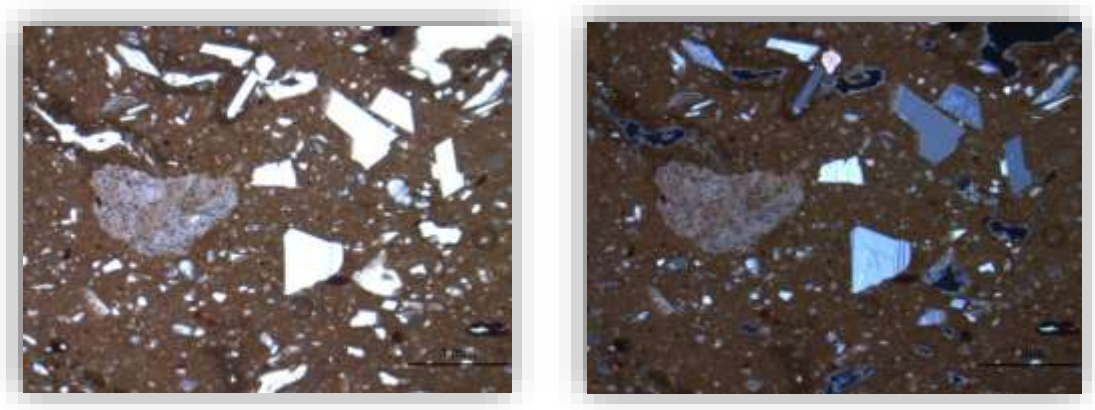

Figure 27 Optical light microscope images of sample TFN.1959.B.686/31 in PPL (left) and XPL (right).

SAMPLE TFN.1959.B.686/7

The sample displays a unimodal grain-size distribution of the inclusions, with an estimation of around 30%. They are equant and elongated, from angular to rounded and single-spaced, with no alignment. The inclusions are mainly characterized by calcareous rocks, with the predominant presence of equant-to-elongated calcite, a frequent presence of elongated quartz, and a common presence of iron oxides in the calcareous matrix. The matrix is slightly optically active, heterogenous in colour ranging from reddish to orange (in PPL). The voids form approximately 8% of the matrix, consisting of micro-vesicles, mega-vughs, planner voids and channel voids aligned to the margin of the sample (Figure 28).

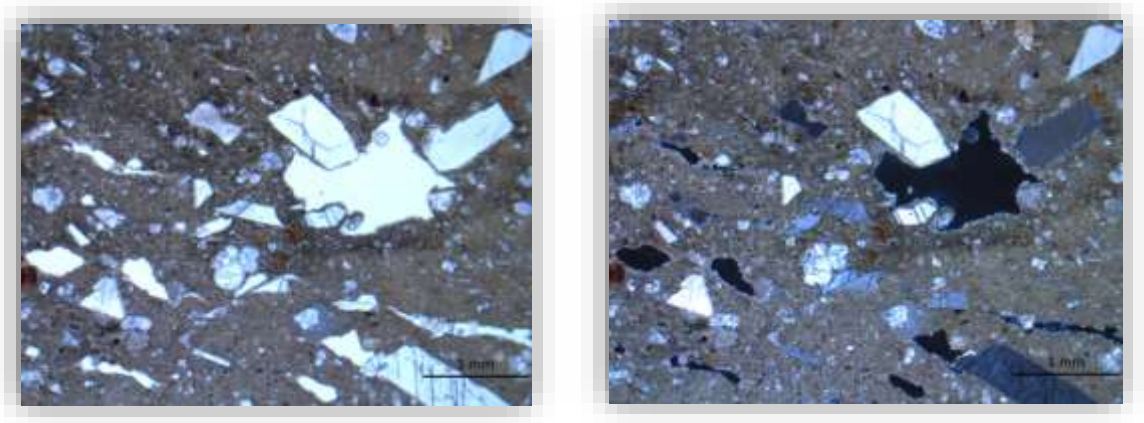

Figure 28 Optical light microscope images of sample TFN.1959.B.686/7 in PPL (left) and XPL (right).

SAMPLE TFN.1959.L.689sup./1

It displays a unimodal grain-size distribution of the inclusions, with an estimation of around 30%. They are equant and elongated, from very angular to rounded and single-spaced, with no alignment. The inclusions are mainly characterized by calcareous rocks, with the predominant presence of equant-to-elongated calcite, a common presence of elongated quartz, and a few nodules of iron oxide in the calcareous matrix. The matrix is slightly optically active, homogenous light brown colour (in PPL). The voids form approximately a range from 5%-10% of the matrix, consisting of micro- to mega-vesicles, aligned to the margin of the sample (Figure 29).

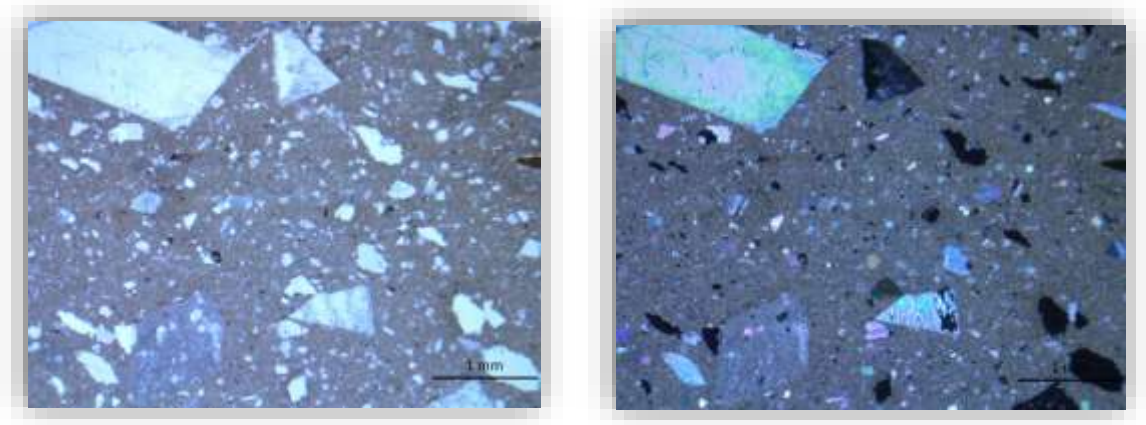

Figure 29 Optical light microscope images of sample TFN.1959.L.689sup./1 in PPL (left) and XPL (right).

SAMPLE TFN.1959.L.718/9

The sample displays a bimodal grain-size distribution of the inclusions, with an estimation of around 40%. They are equant and elongated, from very angular to well-rounded and close-spaced, with no alignment. The inclusions are mainly characterized by calcareous rocks, with the predominant presence of equant to elongated quartz, a common presence of elongated calcite, a very few nodules of iron oxides and a rare presence of fossils in the calcareous matrix. The matrix is slightly optically active, heterogenous in colour ranging from light brown, orange to dark brown (in PPL). The voids form approximately a range from 1%-3% of the matrix, consisting of micro-vesicles, mega-vughs and channel voids aligned to the margin of the sample (Figure 30).

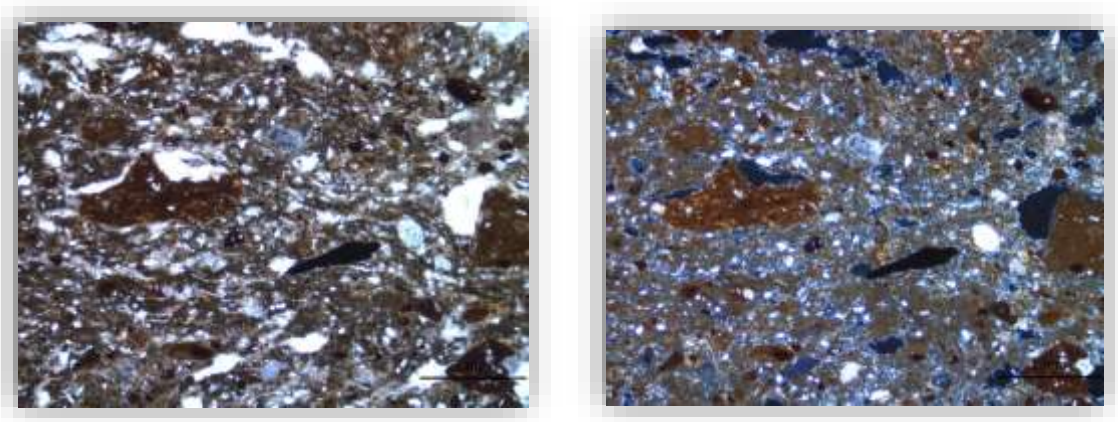

Figure 30 Optical light microscope images of sample TFN.1959.L.718/9 in PPL (left) and XPL (right).

SAMPLE TFN.1959.L.718/8

It displays a unimodal grain size distribution of the inclusions, with an estimation of around 35%. They are equant and elongated, from sub angular to well-rounded and single-spaced, with no alignment. The inclusions are mainly characterized by calcareous rocks, with the predominant presence of equant to elongated quartz, the presence of nodules of iron oxides. There is also few to common presence of calcite and rare presence of fragments of sedimentary calcareous rocks in the calcareous matrix. The matrix is slightly optically active, heterogenous in colour ranging from dark orange to light brown and dark brown and yellow (in PPL). The voids form approximately a range from 3%-7% of the matrix, consisting of micro-vesicles and mega-vughs aligned to the margin of the sample (Figure 31).

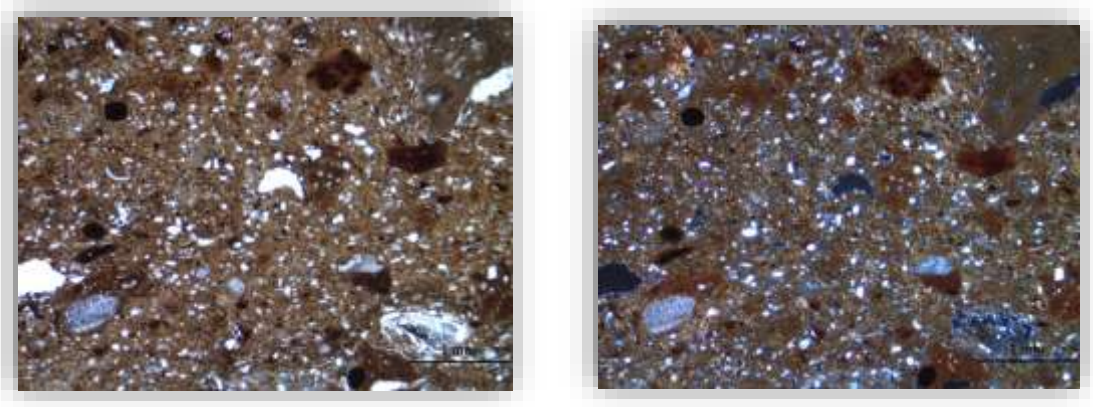

Figure 31 Optical light microscope images of sample TFN.1959.L.718/8 in PPL (left) and XPL (right).

SAMPLE TFN.1959.L.718/32

The sample displays a unimodal grain-size distribution of the inclusions, with an estimation of around 30%. They are equant and elongated, from angular to rounded and close-spaced, with no alignment. The inclusions are mainly characterized by calcareous rocks, with the predominant presence of equant to elongated quartz, the frequent presence of nodules of iron oxides and few to very few calcite in the calcareous matrix. The matrix is slightly optically active, heterogenous in colour ranging from dark brown to reddish light brown and yellow (in PPL). The voids form approximately the 7% of the matrix, consisting of micro- to mega-vesicles, micro- to mega-vughs and planar voids aligned to the margin of the sample (Figure 32).

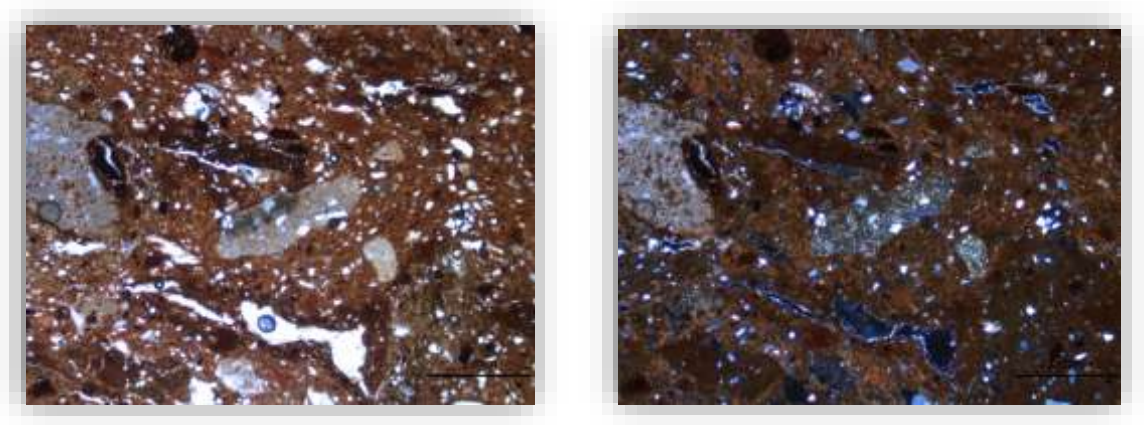

Figure 32 Optical light microscope images of sample TFN.1959.L.718/32 in PPL (left) and XPL (right).

SAMPLE TFN.1959.L.718/33

It displays a unimodal grain-size distribution of the inclusions, with an estimation of around 20%. They are equant and elongated, from angular to rounded and single to double-spaced, with no alignment. The inclusions are mainly characterized by calcareous rocks, with the predominant to dominant presence of quartz, the presence of frequent to common elongated mica, a frequent to common presence of nodules of iron oxide and few to very few of calcite have also been identified in the calcareous matrix. The matrix is slightly optically active, heterogenous in colour ranging from dark brown to light brown (in PPL). The voids form approximately 20% of the matrix, consisting of micro- to mega-vesicles, micro- to mega-vughs and macro-channels aligned to the margin of the sample (Figure 33).

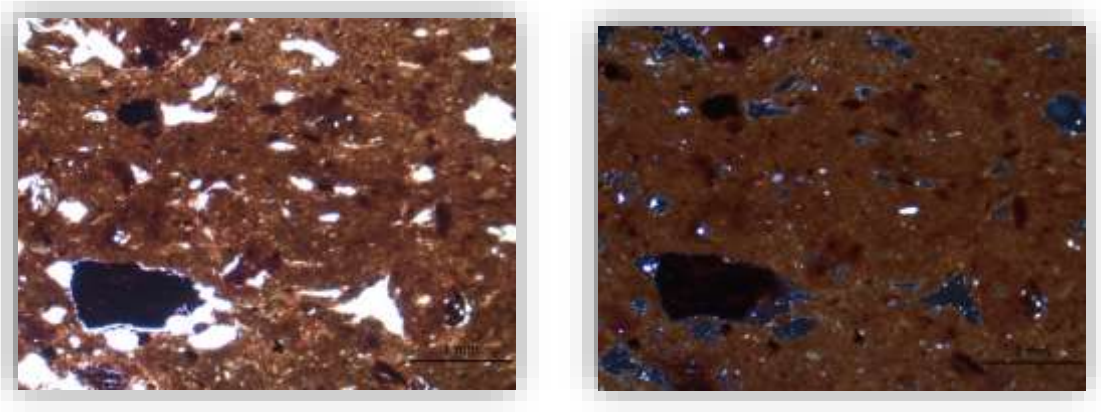

Figure 33 Optical light microscope images of sample TFN.1959.L.718/33 in PPL (left) and XPL (right).

SAMPLES TFN.1959.L.686/8

The sample displays a unimodal grain-size distribution of the inclusions, with an estimation of around 20%. They are equant and elongated, from angular to well-rounded and single to double-spaced, with no alignment. The inclusions are mainly characterized by calcareous rocks, with a predominant presence of quartz, a frequent to common presence of nodules of iron oxides, and few to very few calcite in the calcareous matrix. The matrix is slightly optically active, heterogenous in colour ranging from light brown to dark brown (in PPL). The voids form approximately 7% of the matrix, consisting of micro- to mega-vesicles, micro- to mega-vughs and mega-planar voids aligned to the margin of the sample (Figure 34).

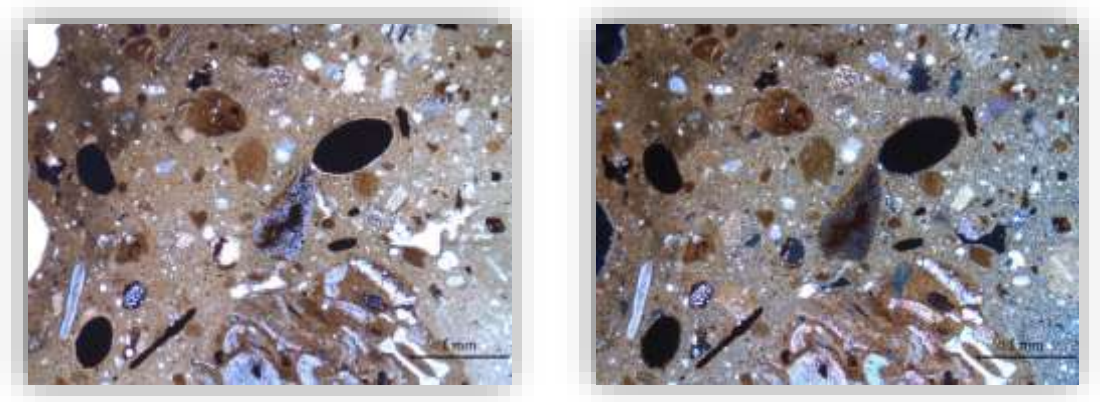

Figure 34 Optical light microscope images of sample TFN.1959.L.686/8 in PPL (left) and XPL (right).

SAMPLE TFN.1959.L.718/13

It displays a unimodal grain-size distribution of the inclusions, with an estimation of around 25%. They are equant and elongated, from sub-angular to well-rounded and single-spaced, with no alignment. The inclusions are mainly characterized by calcareous rocks, with predominant presence of quartz, common presence of calcite, a few to very few nodules of iron oxides and rare to very rare presence of fossils in the calcareous matrix. The matrix is slightly optically active, homogenous reddish brown (in PPL). The voids form approximately 10% of the matrix, consisting of micro- to mega-vesicles and micro- to mega-vughs aligned to the margin of the sample (Figure 35).

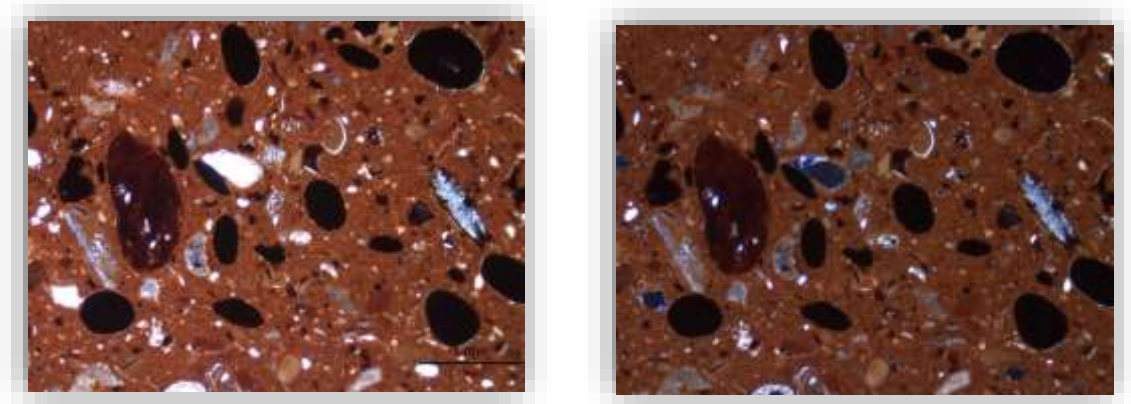

Figure 35 Optical light microscope images of sample TFN.1959.L.718/13 in PPL (left) and XPL (right).

SAMPLE TFN.1954.B.272/5

It displays a unimodal grain-size distribution of the inclusions, with an estimation of around 10%. They are equant and elongated, from sub-angular to rounded and single- to double-spaced, with no alignment. The inclusions are mainly characterized by calcareous rocks, with predominant presence of quartz, common presence of calcite, few to very few nodules of iron oxides, rare to very rare presence of hematite and very rare presence of mica in the calcareous matrix. The matrix is slightly optically active, heterogenous in colour ranging from yellowish brown to reddish brown (in PPL). The voids form approximately 7% of the matrix, consisting of micro- to mega-vesicles, micro- to mega-vughs and mega-channels aligned to the margin of the sample (Figure 36).

Figure 36 Optical light microscope images of sample TFN.1954.B. 272/5 in PPL (left) and XPL (right).

SAMPLE TFN.1959.L.718/31

It displays a unimodal grain-size distribution of the inclusions, with an estimation of around 15%. They are equant and elongated, from sub-angular to rounded and single- to close-spaced, with no alignment. The inclusions are mainly characterized by calcareous rocks, with predominant presence of quartz, common presence of calcite and rare presence of augite in the calcareous matrix. The matrix is slightly optically active, heterogenous in colour ranging from yellowish brown to reddish brown (in PPL). The voids form approximately 15% of the matrix, consisting of micro- to mega-vesicles, micro- to mega-vughs, micro- to mega-planar voids and macro-channels aligned to the margin of the sample (Figure 37).

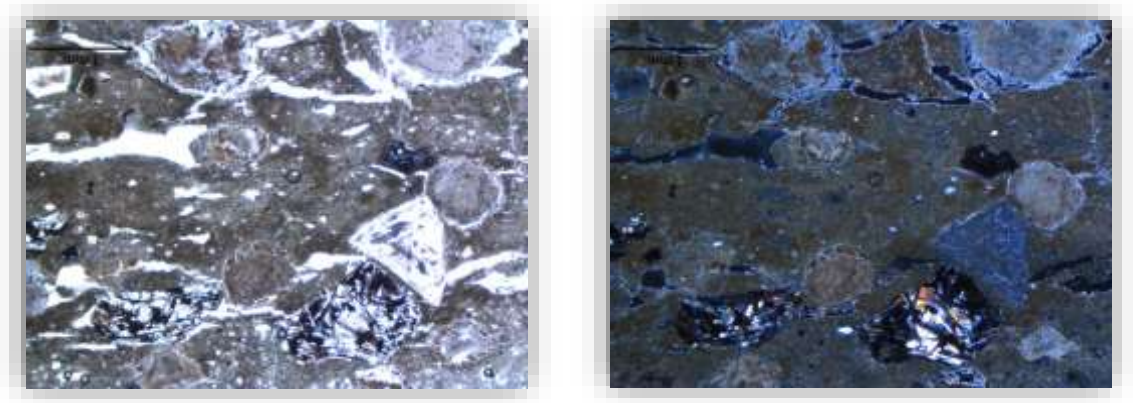

Figure 37 Optical light microscope images of sample TFN.1959.L.718/31 in PPL (left) and XPL (right).

Table 2 Summary of the main microscopic features of ceramic samples analysed by OM

Sample		Voids	Matrix	Inclusions	
TFN.1959.B.686/1	Fabric-A calcite	• 5% • Micro vesicles • Macro vughs • Secondary calcite • Aligned	• 75% • Heterogeneous • Calcareous • Slight optical activity	• 20% • Equant and elongated from angular to rounded, single spaced to double spaced not aligned to the margins, unimodal grain-size distribution	Predominant: calcite equant-elongated, sub-rounded /rounded, 2 mm- 50µm. Few: nodules of iron oxides, equant, rounded, 50µm-500µm Common: fossils, 50µm - 200µm. Very rare: quartz, elongated, from sub-rounded to rounded, 50µm.
TFN.1959.B.686/3		• 10% • Micro to mega vesicles • Mega vughs • Secondary calcite • Aligned	• 60% • Homogenous • Calcareous • Slight optical activity	• 30% • Equant and elongated from very angular to rounded, single-spaced, not aligned to the margins, unimodal grain-size distribution	Predominant: calcite equant-elongated, sub-angular to rounded, 2 mm- 50µm. Frequent: quartz, elongated, from angular to sub-angular, 2mm -500µm. Few: nodules of iron oxides, equant, rounded, 1mm-500µm.
TFN.1959.B.686/7		• 8% • Micro Vesicles • Mega vughs • Planner voids and channel voids • Secondary calcite • Aligned	• 62% • Heterogeneous • Calcareous • Slight optical activity	• 30% • Equant and elongated from angular to rounded, single spaced, not aligned to the margins, unimodal grain-size distribution	Predominant: calcite equant-elongated, angular to sub-rounded, 2 mm- 200µm. Frequent: Quartz, elongated, from angular to sub-angular, 2mm -500µm. Common: nodules of iron oxides, equant, rounded, 2mm-200µm.
TFN.1959.L.689sup./ 1		• 5%-10% • Micro vesicles to mega vesicles • Secondary Calcite • Aligned	• 60% • Homogenous • Calcareous • Optically active	• 30% • Equant and elongated from very angular to rounded, single-spaced, not aligned to the margins, unimodal grain-size distribution	Predominant: calcite equant-elongated, very angular to rounded, 2 mm- 200µm. Common: quartz, elongated, from angular to sub-angular, 2mm -50µm. Very few: nodules of iron oxides, equant, rounded, 3mm-50µm.
TFN.1959.L.718/9	Fabric-B calcareous	• 1%-3% • Micro Vesicles • Mega vughs • channel voids • Secondary calcite • Aligned	• 57% • Heterogeneous • Calcareous • Slight optical activity	• 40% • Equant and elongated from very angular to well rounded, close-spaced, not aligned to the margins, bimodal grain-size distribution	Predominant: quartz, elongated, from sub angular to sub rounded, 0.5 mm -200µm. Common: Calcite, equant-elongated, sub angular to rounded, 1mm- 200µm. Very few: nodules of iron oxides, equant, rounded, 1mm-200µm. Rare: fossils, 1mm-200µm.
TFN.1959.L.718/8		• 3%- 7% • Micro Vesicles • Mega vughs • Secondary calcite • Aligned	• 58% • Heterogeneous • Calcareous • Slight optical activity.	• 35% • Equant and elongated from sub-angular to well-rounded Rounded, single-spaced, not aligned to the margins, unimodal grain size distribution	Predominant: quartz, elongated from sub-angular to sub-rounded, 200 µm. Present: nodules of iron oxides, equant, rounded, 1mm to 200 µm. Few to common: calcite, equant to elongated, angular to rounded, 2 mm to 200 µm. Rare: fragments of sedimentary calcareous rocks, equant-elongated, sub rounded/ subangular, 2 mm to 200 µm.

TFN.1959.L.718/32	• 7% • Micro to mega vesicles • Micro to mega vughs • Planar voids • Secondary calcite • Aligned	• 63% • Heterogeneous • Calcareous • Slight optical activity	• 30% • Equant and elongated from angular to rounded, close-spaced, not aligned to the margins, unimodal grain-size distribution	Predominant: quartz angular to sub-rounded, 500µm to 25µm Present: calcite, equant-elongated, sub-angular to rounded, 25µm- 200µm. Few to very few: nodules of iron oxides, equant, sub-rounded to rounded, 3mm-50µm.
TFN.1959.L.718/33	• 20% • Micro vesicles to mega vesicles • Micro vughs to mega vughs • Macro channels to mega channels • Secondary calcite • Aligned	• 60% • Homogenous • Calcareous • Slight optical activity.	• 20% • Equant and elongated from angular to rounded, single-spaced to double-spaced, not aligned to the margins, unimodal grain-size distribution	Predominant to dominant: quartz, elongated, from sub-angular to rounded, 25µm -50µm. Frequent to common: nodules of iron oxides, equant, rounded, 1mm-50µm. Few to very few: mica, elongated, angular to rounded 20 µm to 50 µm. Very few: calcite equant-elongated, very angular to rounded, 200µm-50µm. Rare to very rare: sedimentary rocks fragments, sub-rounded to rounded, 50µm – 100 µm.
TFN.1959.L.686/8	• 7% • Mega planar voids • Micro vughs to mega vughs • Micro vesicles to mega vesicles • Secondary calcite • Aligned	• 83% • Heterogenous • Calcareous • Slight optical activity	• 20% • Equant and elongated from angular to well rounded, single-spaced to double-spaced, not aligned to the margins, unimodal grain-size distribution	Predominant: quartz, elongated, from sub-angular to rounded, 25µm -50µm. Frequent to common: nodules of iron oxides, equant, rounded, 500µm-30 µm. Few to very few: calcite elongated, angular to well-rounded 1mm to 10 µm.
TFN.1959.L.718/13	• 10% • Mico vesicles to mega vesicles • Micro vughs to mega vughs • Secondary calcite • Aligned	• 65% • Heterogenous • Not Calcareous • not optically active	• 25% • Equant from sub-angular to well-rounded Rounded, single-spaced, not aligned to the margins, unimodal grain-size distribution	Predominant: quartz, elongated, from sub-angular to rounded, 20 µm -100µm. Common: calcite equant-elongated, sub-angular to rounded, 50 µm- 500µm. Few to very few: nodules of iron oxides, equant, rounded, 50 µm -200µm. Rare to very rare: fossils, 200µm; hematite, sub-angular to sub-rounded, 150mm - 600 µm.
TFN.1954.B. 272/5	• 7% • Mico vesicles to mega vesicles • Micro vughs to mega vughs • Mega channels • Secondary calcite • Aligned	• 65% • Heterogenous • Calcareous • not optically active •	• 10% • Equant and elongated from sub-angular Angular to rounded, single-spaced to double-spaced, not aligned to the margins, unimodal grain-size distribution	Predominant: quartz, elongated, sub-rounded, 2mm -500µm Common: Calcite equant-elongated, angular to rounded, 500µm. Few to very rare: nodules of iron oxides, equant, sub-angular to sub-rounded, 50 µm Very rare: Hematite, sub-rounded, 500 µm; mica, angular 10µm.
TFN.1959.L.718/31	**LONER** • `15% • Micro vesicles to macro vesicles • Micro Macro vughs • Micro to Mega planar voids • Macro channels • Secondary calcite • Aligned	• 70% • Heterogenous • Not Calcareous • Not optically active	• 15% • Equant, from sub-angular to rounded, single-spaced to close-spaced, not aligned to the margins, unimodal grain-size distribution	Predominant: quartz, elongated, sub-angular Angular to well-rounded 400µm-10 µm Common: Calcite equant-elongated, sub-angular to sub-rounded, 100µm-50 µm Rare: K-feldspar, elongated, sub-angular to sub-rounded, 25 µm To 250 µm

4.3 XRPD analysis

SAMPLE TFN.1959.B.686/1

The Chalcolithic *bowl* is characterized by abundant calcite and scarce quartz (Figure 38).

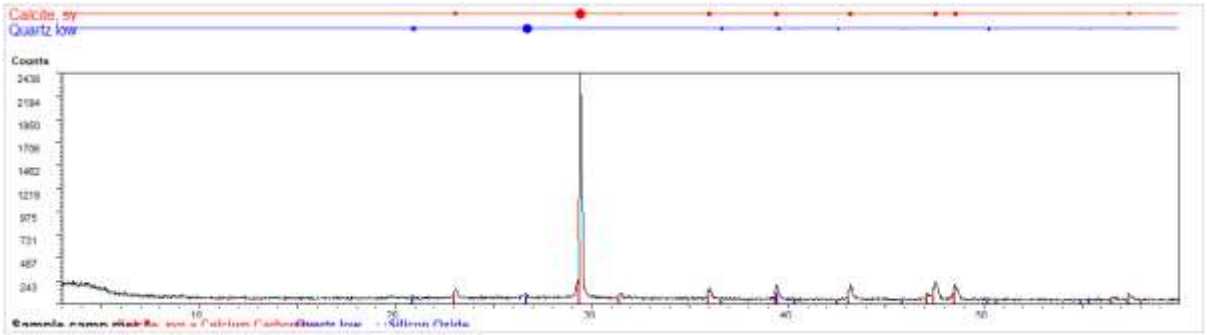

Figure 38 Diffraction pattern of sample TFN.1959.B.686/1

SAMPLE TFN.1959.B.686/3

The Chalcolithic jar is characterized by abundant calcite and traces of quartz (Figure 39).

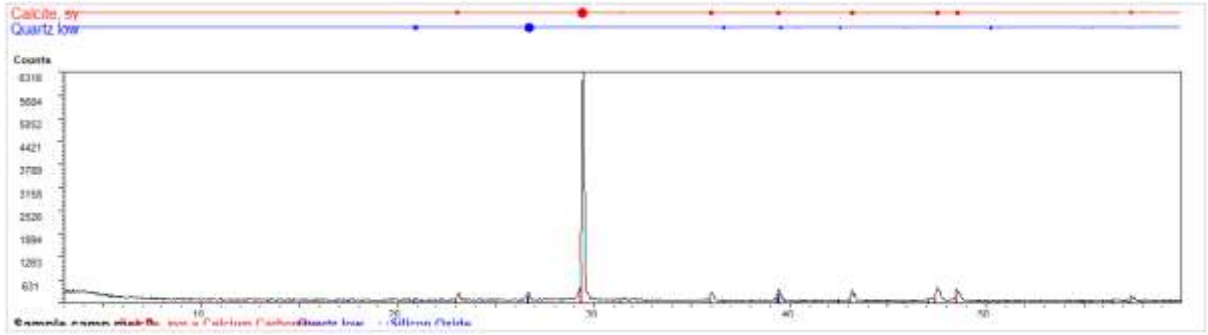

Figure 39 Diffraction pattern of sample TFN.1959.B.686/3

SAMPLE TFN.1959.B.686/7

The Chalcolithic *holemouth jar* is characterized by abundant calcite and traces of quartz (Figure 40).

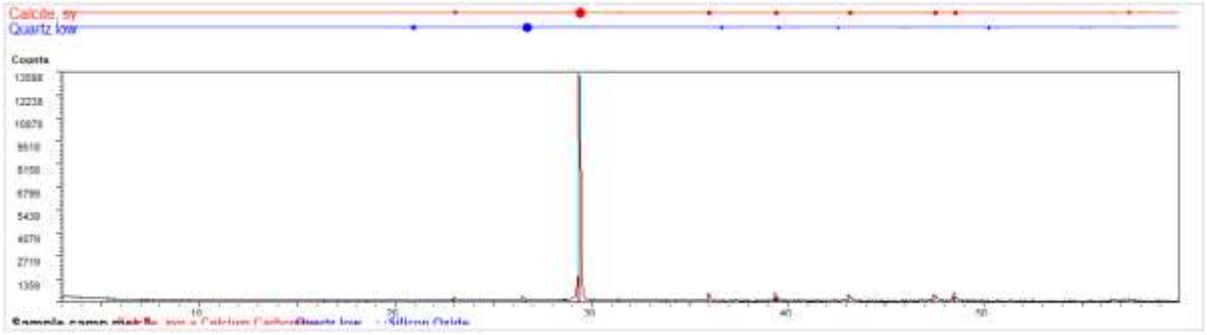

Figure 40 Diffraction pattern of sample TFN.1959.B.686/7

SAMPLE TFN.1959.L.689sup./1

The Chalcolithic *jar* is characterized by abundant calcite and traces of quartz (Figure 41).

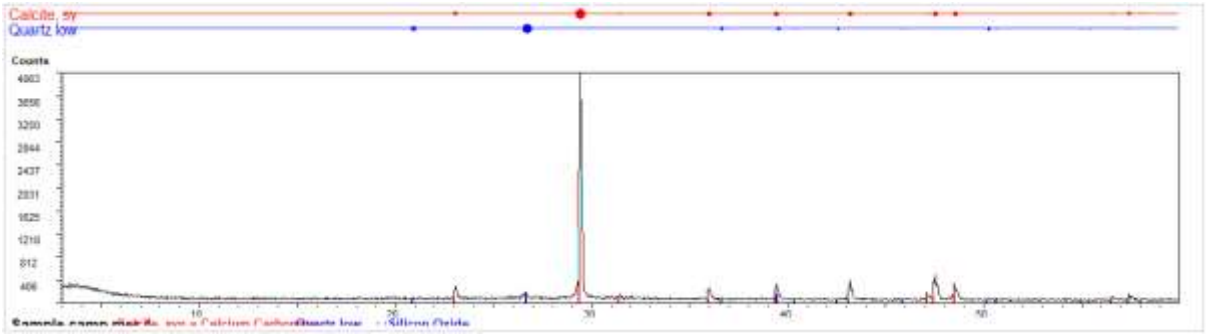

Figure 41 Diffraction pattern of sample TFN.1959.L.689sup./1

SAMPLE TFN.1959.L.689sup./2

The *holemouth jar* is characterized by abundant calcite and scarce quartz (Figure 42).

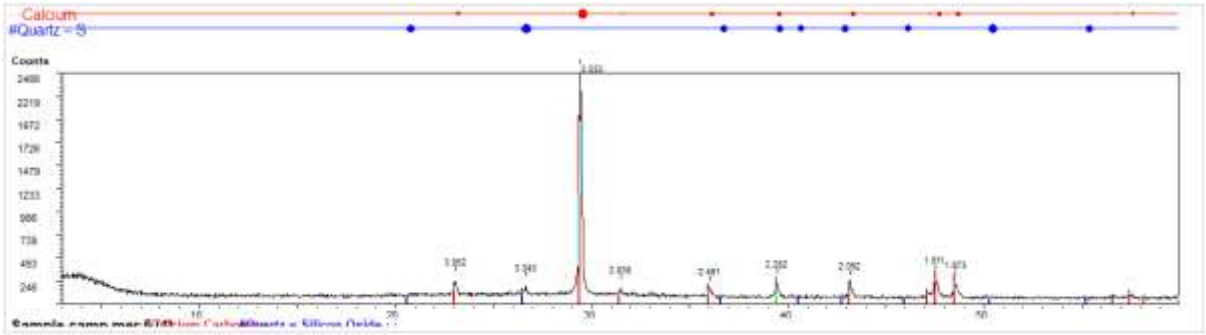

Figure 42 Diffraction pattern of sample TFN.1959.L.689sup./2

SAMPLE TFN.1959.L.689sup./3

The *holemouth jar* is characterized by abundant calcite and scarce quartz (Figure 43).

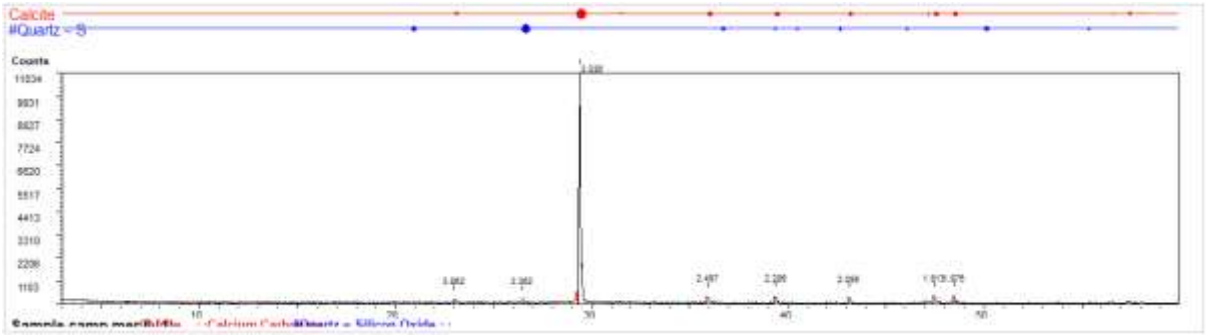

Figure 43 Diffraction pattern of sample TFN.1959.L.689sup./3

SAMPLE TFN.1959.L.689sup./4

The *red slip bowl* is characterized by abundant calcite and scarce quartz (Figure 44).

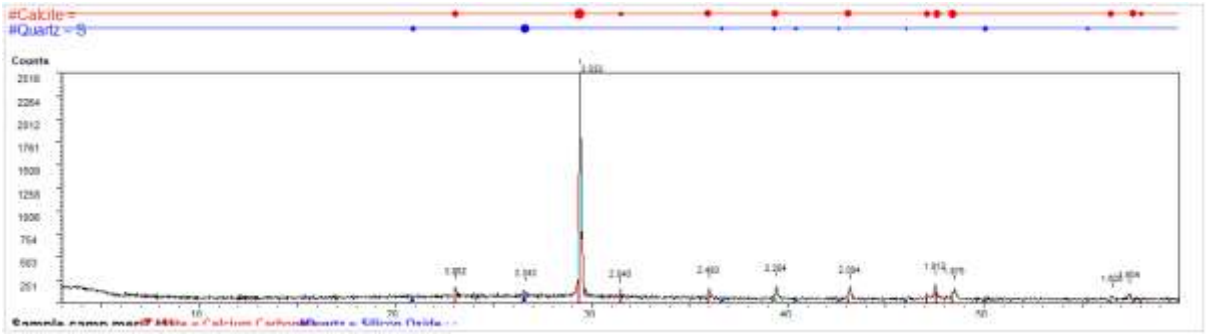

Figure 44 Diffraction pattern of sample TFN.1959.L.689sup./4

SAMPLE TFN.1959.L.718/9

The Early Bronze Age Um Hammad *jar* is characterized by abundant quartz and minor amounts of calcite (Figure 45).

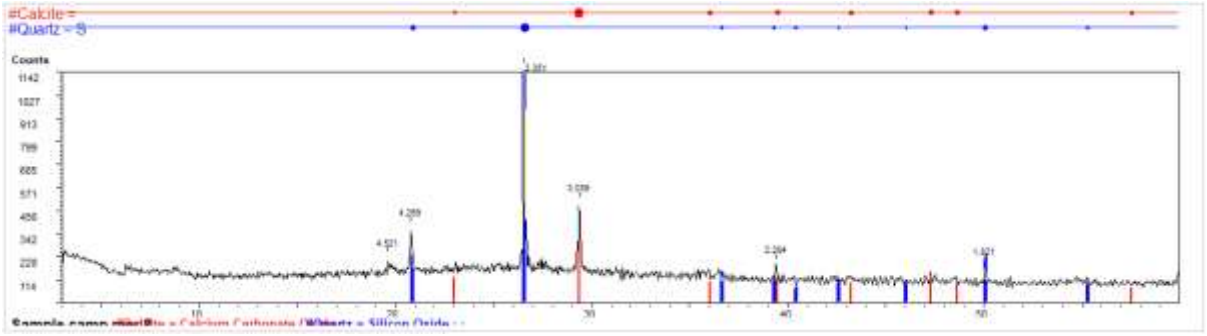

Figure 45 Diffraction pattern of sample TFN.1959.L.718/9

SAMPLE TFN.1959.L.718/8

The Early Bronze Age Um Hammad *jar* is characterized by abundant quartz, present K-feldspars and minor amounts of calcite (Figure 46).

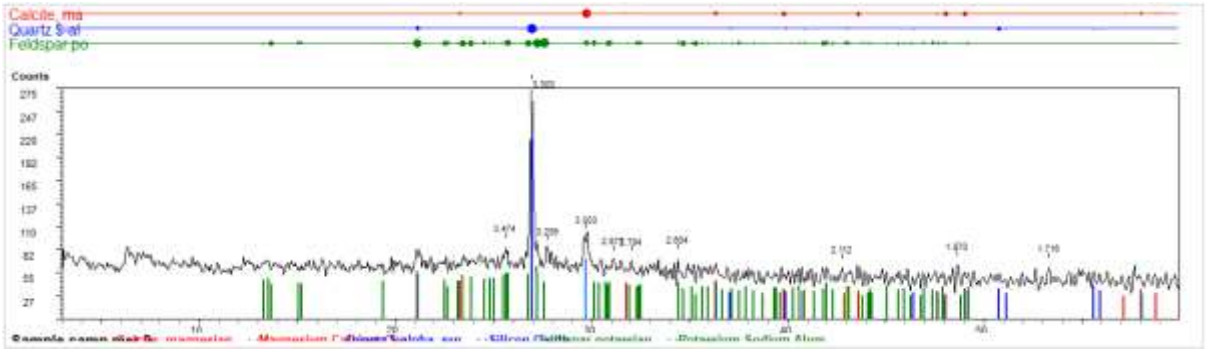

Figure 46 Diffraction pattern of sample TFN.1959.L.718/8

SAMPLE TFN.1959.L.718/32

The Early Bronze Age Um Hammad *jar* is very abundant in quartz, with minor presence of calcite and scarce of K-feldspars and anatase (Figure 47).

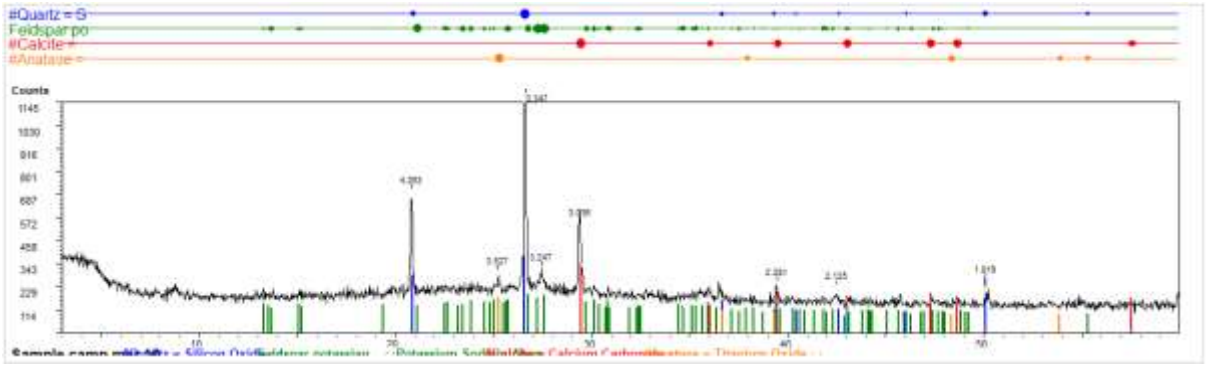

Figure 47 Diffraction pattern of sample TFN.1959.L.718/32

SAMPLE TFN.1959.L.718/33

The Early Bronze Age Um Hammad *jar* is very abundant in quartz, scarce in K-feldspars, calcite, mica and has minor presence of hematite (Figure 48).

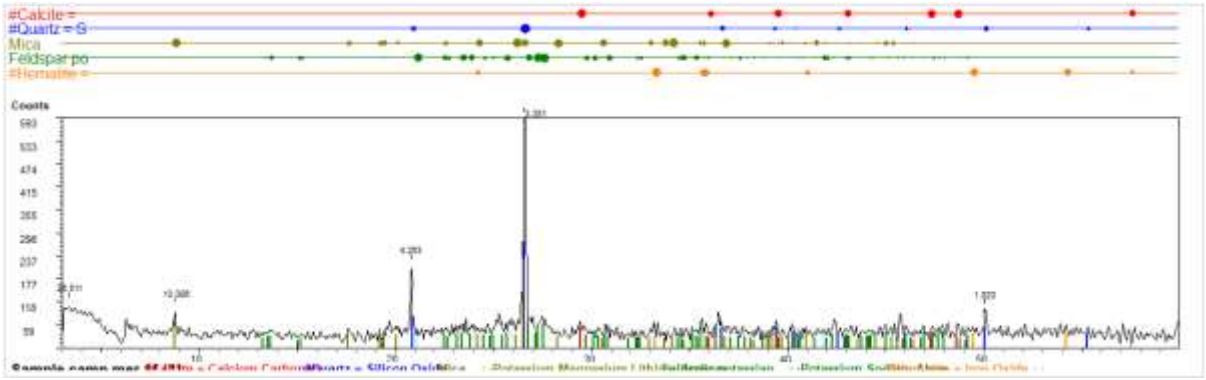

Figure 48 Diffraction pattern of sample TFN.1959.L.718/33

SAMPLE TFN.1959.L.718/35

The Early Bronze Age Um Hammad *jar* is very abundant in quartz, with minor presence of K-feldspars, scarce hematite and anorthite and traces of calcite (Figure 49).

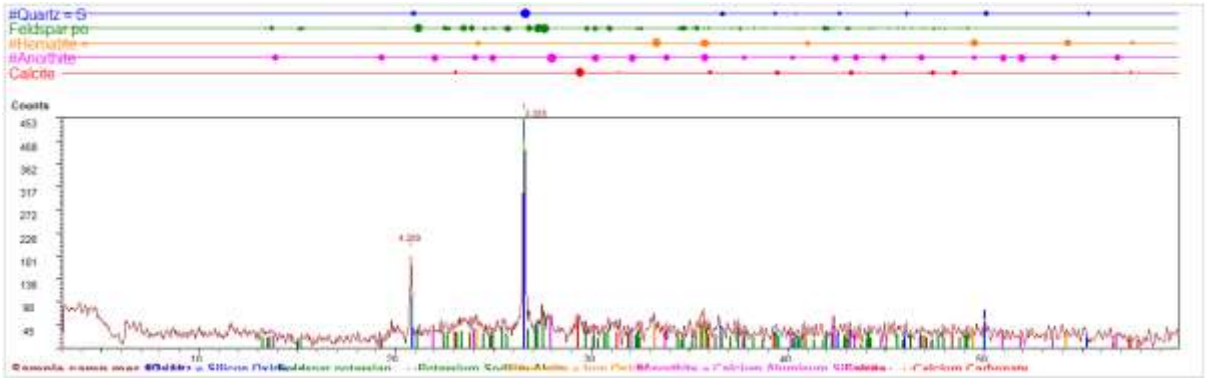

Figure 49 Diffraction pattern of sample TFN.1959.L.718/35

SAMPLE TFN.1959.B.672/4

The Early Bronze Age Um Hammad *bowl* is very abundant in quartz and has scarce K-feldspars, calcite, hematite, gehlenite and anorthite (Figure 50).

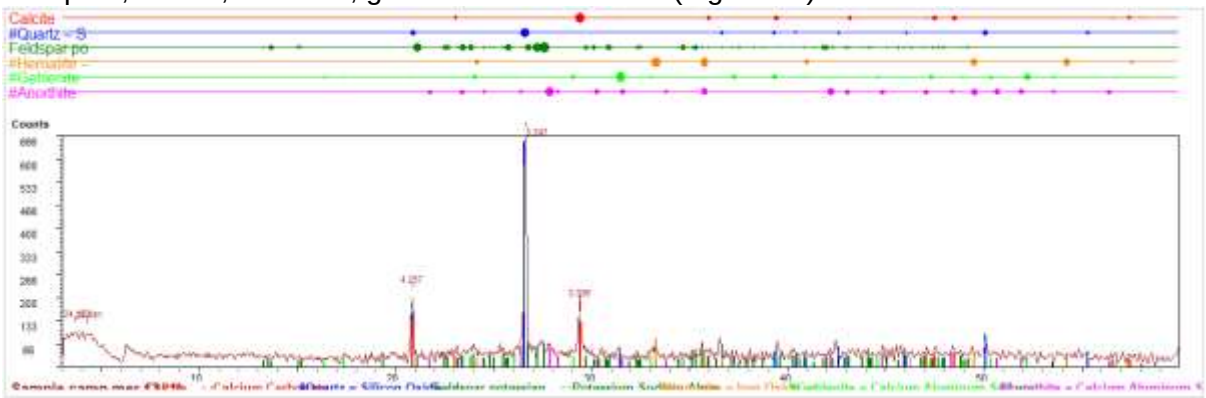

Figure 50 Diffraction pattern of sample TFN.1959.B.672/4

SAMPLE TFN.1959.L.686/8

The Early Bronze Age Um Hammad *bowl* is very abundant in calcite, with minor presence of quartz and scarce K-feldspars (Figure 51).

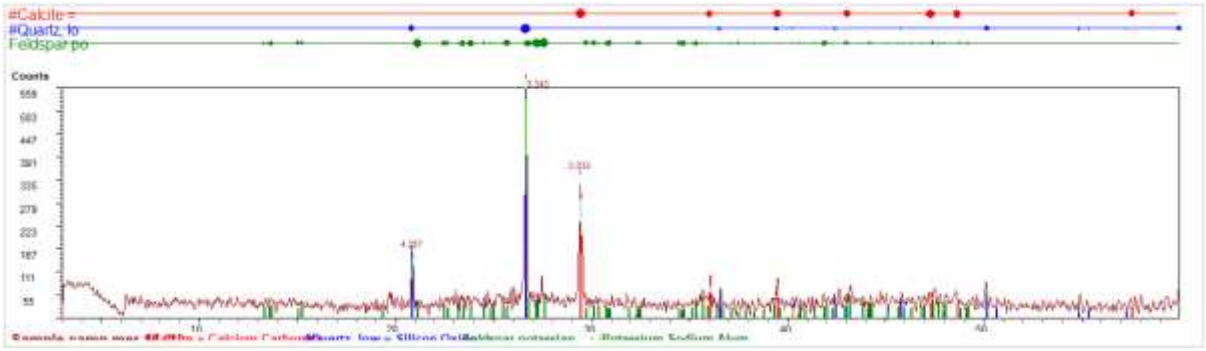

Figure 51 Diffraction pattern of sample TFN.1959.L.686/8

SAMPLE TFN.1959.L.686/6

The Early Bronze Age *pithos* is very abundant in calcite and scarce in quartz (Figure 52).

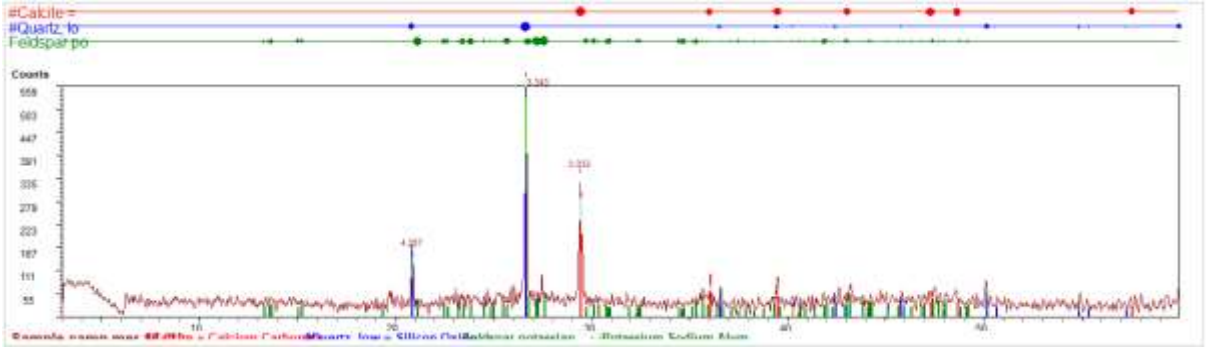

Figure 52 Diffraction pattern of sample TFN.1959.L.686/6

SAMPLE TFN.1959.L.718/13

The Early Bronze Age red slip *amphoriskos* is very abundant in calcite and has scarce quartz and hematite (Figure 53).

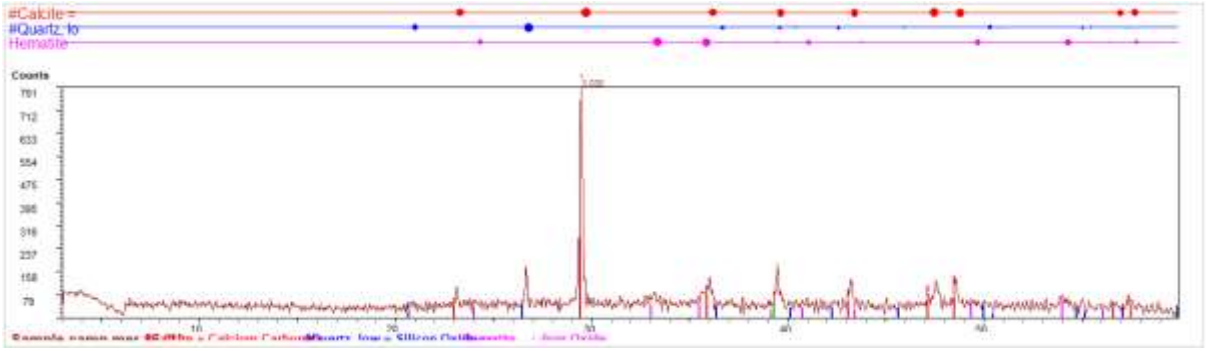

Figure 53 Diffraction pattern of sample TFN.1959.L.718/13

SAMPLE TFN.1954.B.272/5

The Early Bronze Age jar is very abundant in calcite and has scarce quartz and amphiboles (Figure 54).

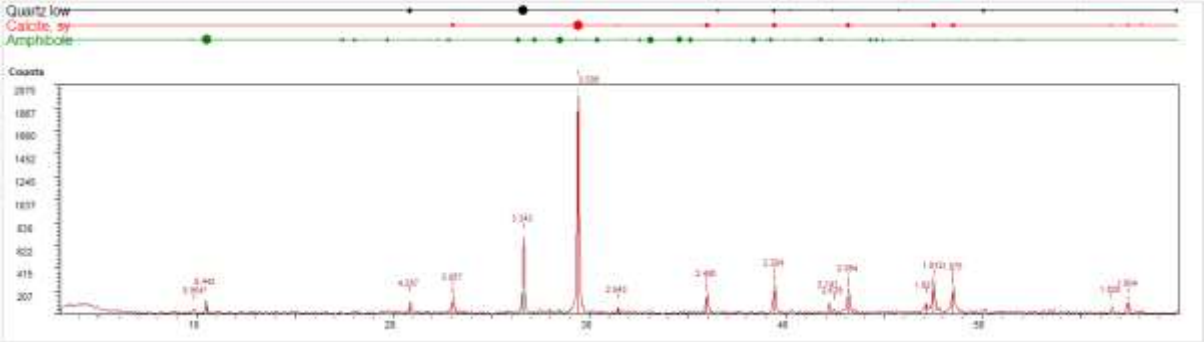

Figure 54 Diffraction pattern of sample TFN.1954.B.272/5

SAMPLE TFN.1959.L.718/31

The Early Bronze Age *pithos* is abundant in calcite, with minor presence of gehlenite and K-feldspars and scarce quartz and anorthite (Figure 55).

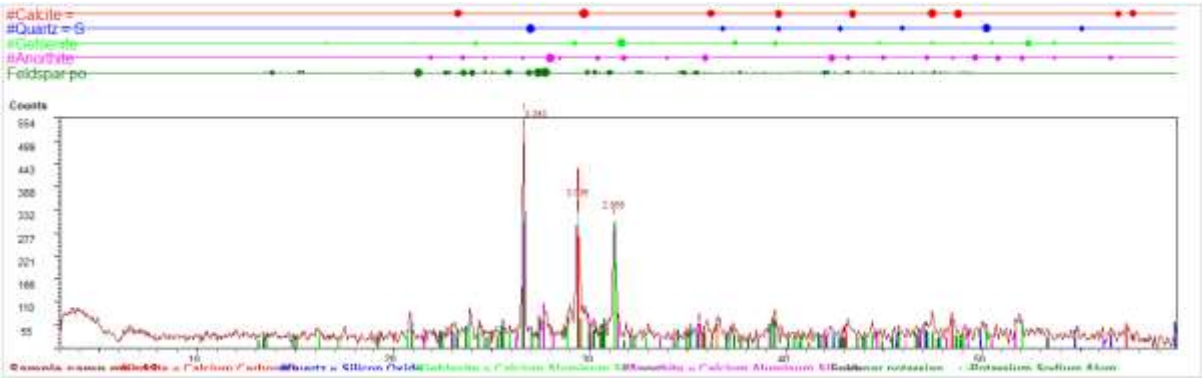

Figure 55 Diffraction pattern of sample TFN.1959.L.718/31

SAMPLE TFN.1959.L.704/7

The Early Bronze Age holemouth jar is abundant in calcite, with scarce pargasite and traces of quartz (Figure 56).

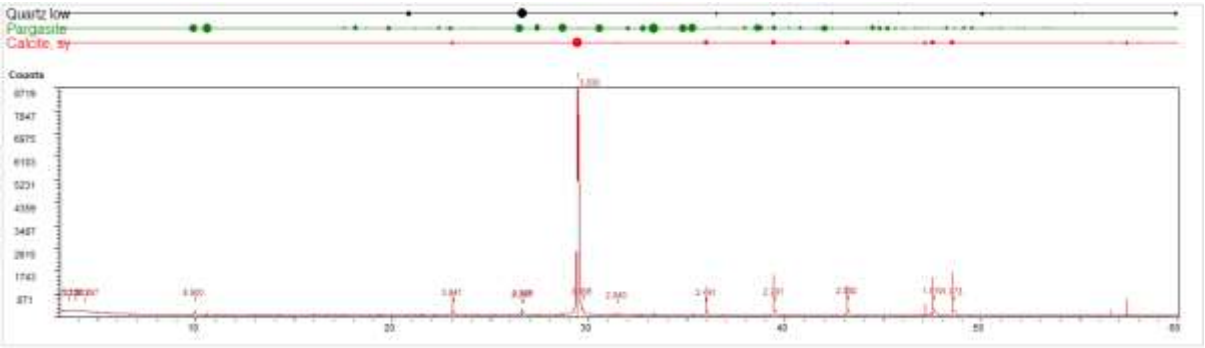

Figure 56 Diffraction pattern of sample TFN.1959.L.704/7

SAMPLE TFN.1959.L.718/3

The Early Bronze Age bowl is very abundant in calcite, with minor presence of sanidine and quartz and scarce illite (Figure 57).

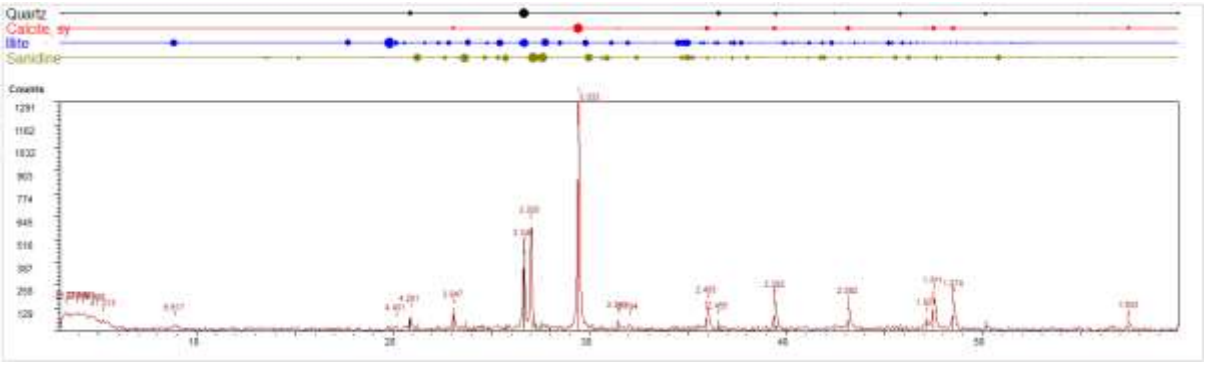

Figure 57 Diffraction pattern of sample TFN.1959.L.718/3

SAMPLE TFN.1959.L.718/30

The Early Bronze Age bowl is characterized by abundant calcite, minor presence of quartz and sanidine and scarce illite (Figure 58).

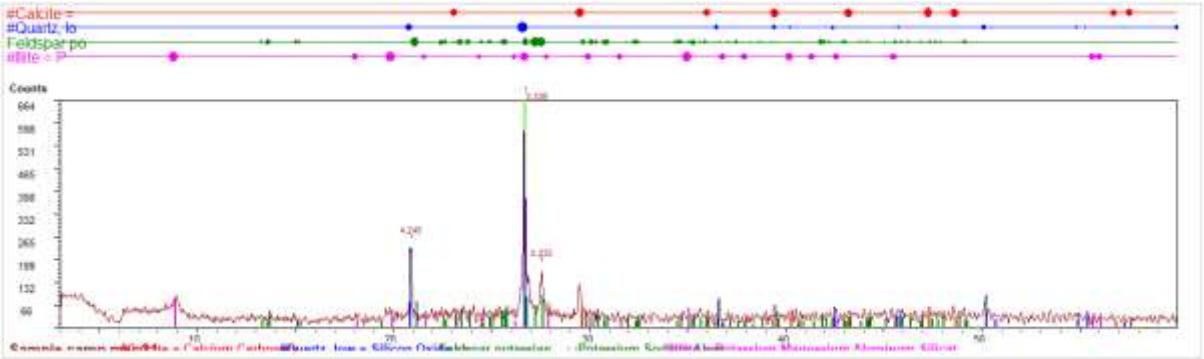

Figure 58 Diffraction pattern of sample TFN.1959.L.718/30

Table 3 XRPD results of the analysed ceramic samples: quartz: Qtz, calcite: Cal, K-Feldspars: Kfs, Plagioclase: Pl, illite: Ill, hematite: Hem, gehlenite: Gh, augite: Aug, mica: Mic, anatase: Anat, anthorite: An, amphibole: Amph, sanidine: Sa, pargasite: Prg

++++ very abundant +++ abundant ++ present + scarce tr. Traces

SAMPLE		Qtz	Cal	Kfs	Gh	Hem	Mic	Aug	Pl	Ill	Anat	An	Amph	Sa	Prg
TFN.1959.B.686/1	CHALCOLITHIC	+	++++												
TFN.1959.B.686/3		*tr*	++++												
TFN.1959.B.686/7		*tr*	++++												
TFN.1959.L.689sup./1		*tr*	++++												
TFN.1959.L.689sup./2		+	++++												
TFN.1959.L.689sup./3		*tr*	++++												
TFN.1959.L.689sup./4		+	++++												
TFN.1959.L.718/9	BRONZE AGE UM HAMMAD	++++	++												
TFN.1959.L.718/8		++++	++	+++											
TFN.1959.L.718/32		++++	++	+							+				
TFN.1959.L.718/33		++++	+	+		*tr*	+								
TFN.1959.L.718/35		++++	++	++		+						+			
TFN.1959.B.672/4		++++	+	+	+	+						+			
TFN.1959.L.686/8		++	++++	+											
TFN.1959.L.686/6	BRONZE AGE OTHER WARE	+	++++												
TFN.1959.L.718/13		+	++++			+									
TFN.1954.B. 272/5		+	++++										+		
TFN.1959.L.718/31		+	+++	++	++							+			
TFN.1959.L.704/7		*tr*	+++												+
TFN.1959.L.718/3		++	+++							+				++	
TFN.1959.L.718/4)		++	++	+++										+	

4.4 SEM-EDS analysis

SAMPLE TFN.1959.B.686/3

The EDS spectrum of the general composition is shown in Figure 59. It is characterized by a high amount of Ca, with minor abundance in Si and Al and lower amounts of Mg, Na, K, Fe and Ti.

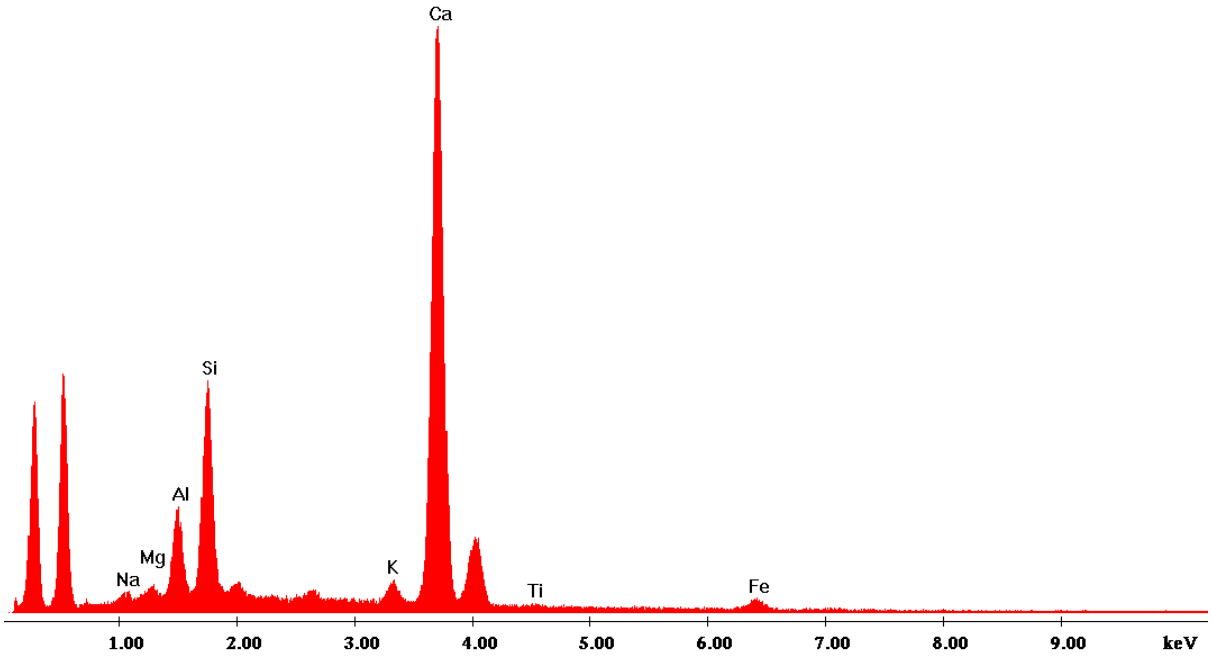

Figure 59 EDS spectrum of sample TFN.1959.B.686/3

Among the inclusions in sample TFN.1959.B.686/3 SEM-EDS allowed the identification of calcite, quartz and micro-fossils within the matrix (Fig. 66 and 67).

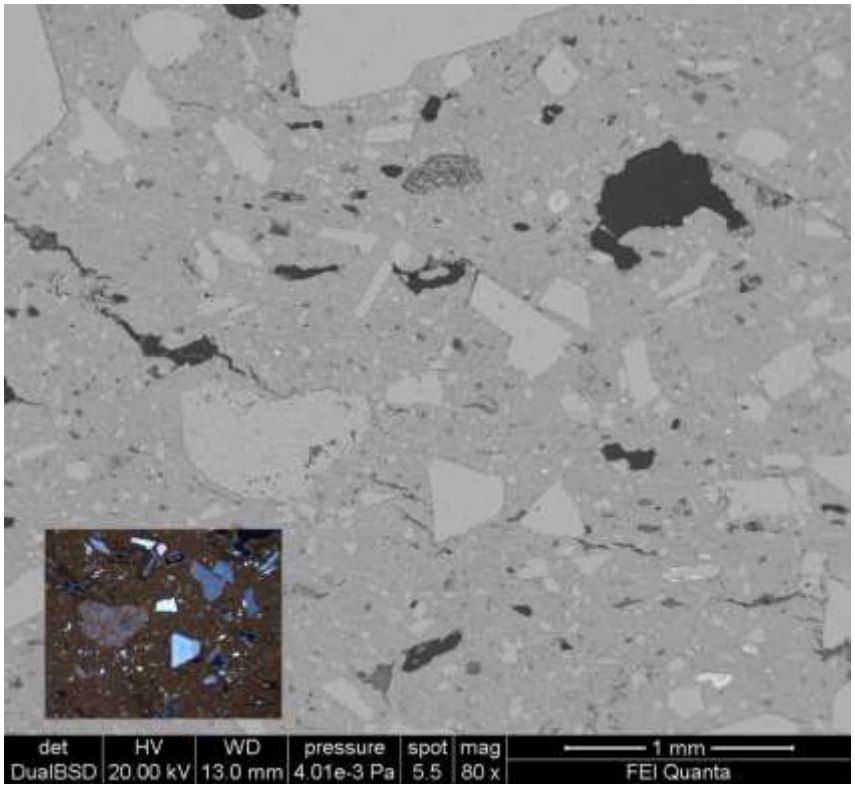

Figure 60 BSE image of sample TFN.1959.B.686/3, displaying calcite, quartz and some micro-fossils, together with the optical microscope image of the same area under XPL (bottom left).

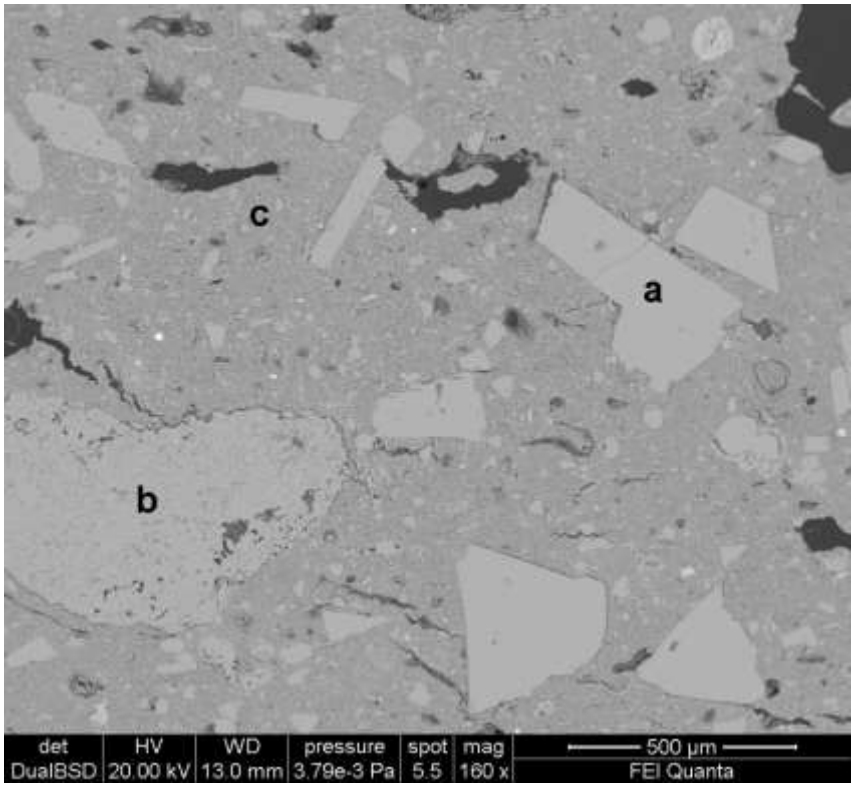

Figure 61 sample TFN.1959.B.686/3 marked with a calcite; b: calcareous fragment; c: matrix

The EDS spectrum (Figure 62) of point ”a” from Figure 61 is characterized by high amount of Ca, confirming the identification of a calcite crystal.

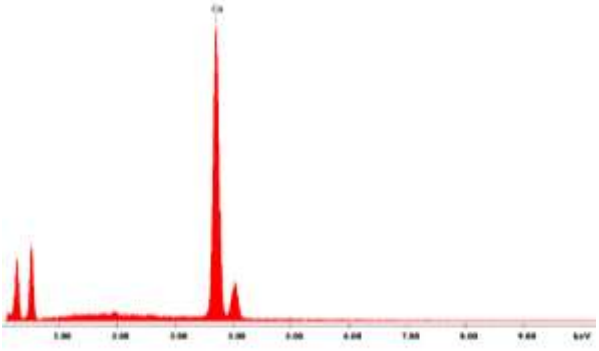

Figure 62 EDS spectrum of point ”a” of sample TFN.1959.B.686/3 identified as calcite

The EDS spectrum (Figure 63) of point ”b” from Figure 61 is characterized by high amount of Ca and minor amounts of Si, Al, Mg, K and Fe, representing the chemical composition of a calcareous rock fragment.

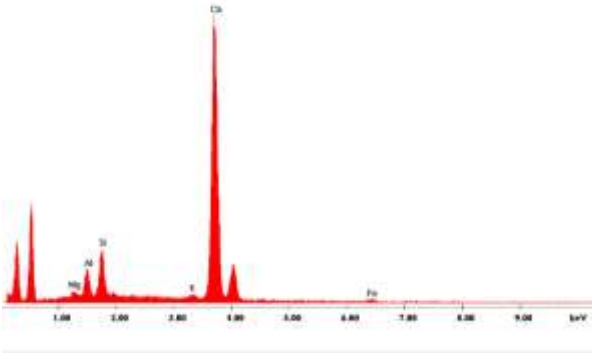

Figure 63 EDS spectrum of point ”b” of sample TFN.1959.B.686/3 identified as calcareous rock

The EDS spectrum (Figure 64) of point ”c” from Figure 61 is characterized by high amounts of Ca, Si and Al and minor amounts of K, Mg and Fe, reflecting the composition of the matrix.

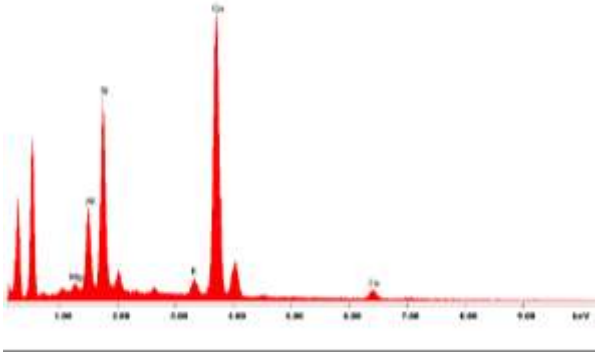

Figure 64 EDS spectrum of point ”c”, i.e. of the matrix of sample TFN.1959.B.686/3

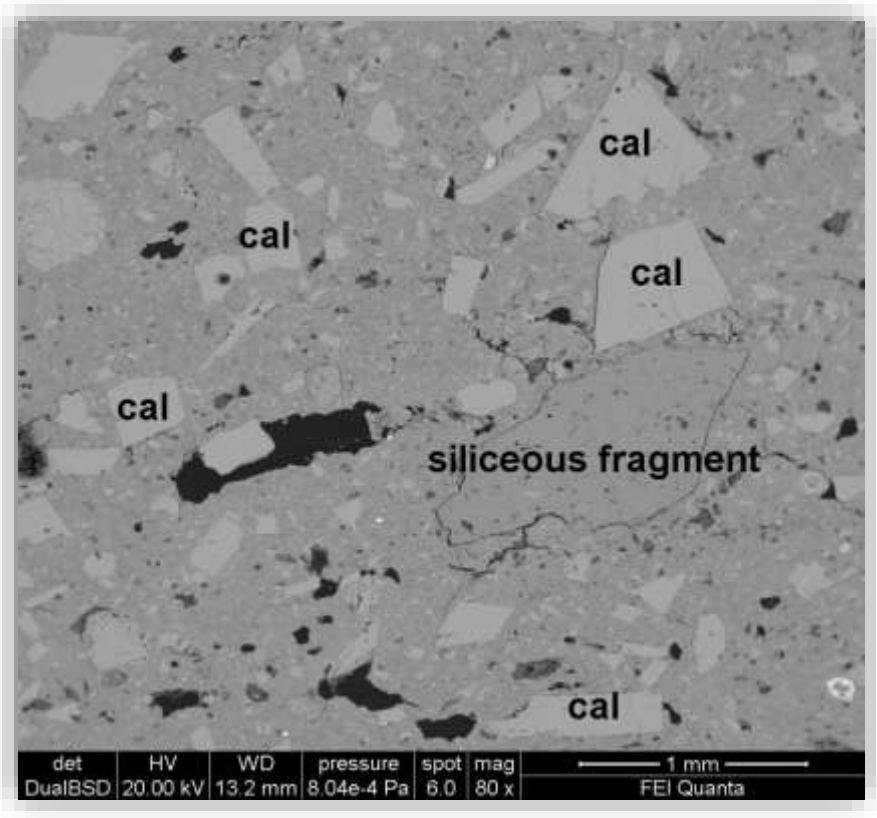

Figure 65 BSE image of sample TFN.1959.B.686/3 ,where calcite (cal) and siliceous fragments have been labelled.

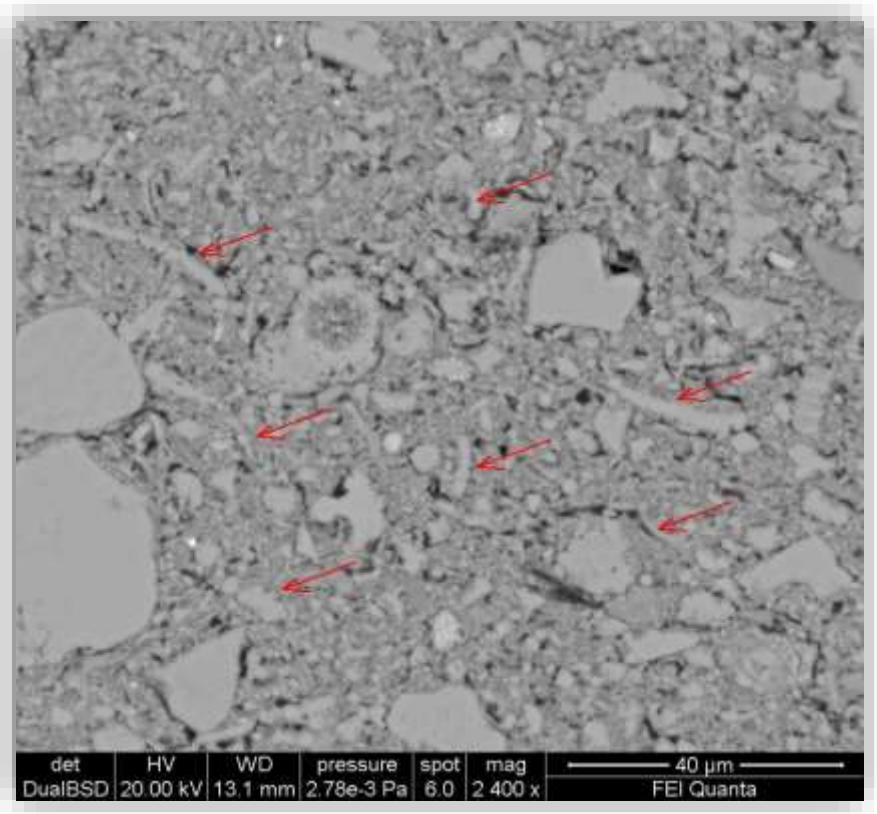

Figure 66 BSE image of sample TFN.1959.B.686/3 showing micro-fossils.

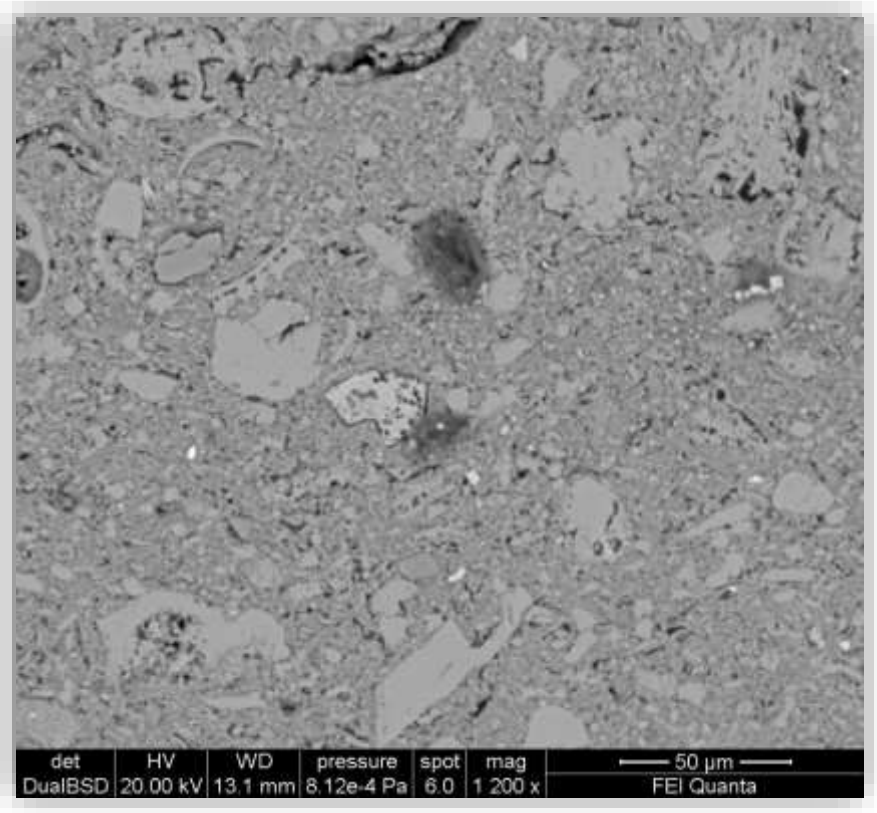

Figure 67 BSE image of sample TFN.1959.B.686/3 showing micro fossils, calcite, quartz and nodules of iron oxide.

SAMPLE TFN.1959.B.686/7

The EDS spectrum of the general composition is shown in Figure 68. It is characterized by high amounts of Ca, Si and Al, and minor amounts of Na, K, Fe and Ti.

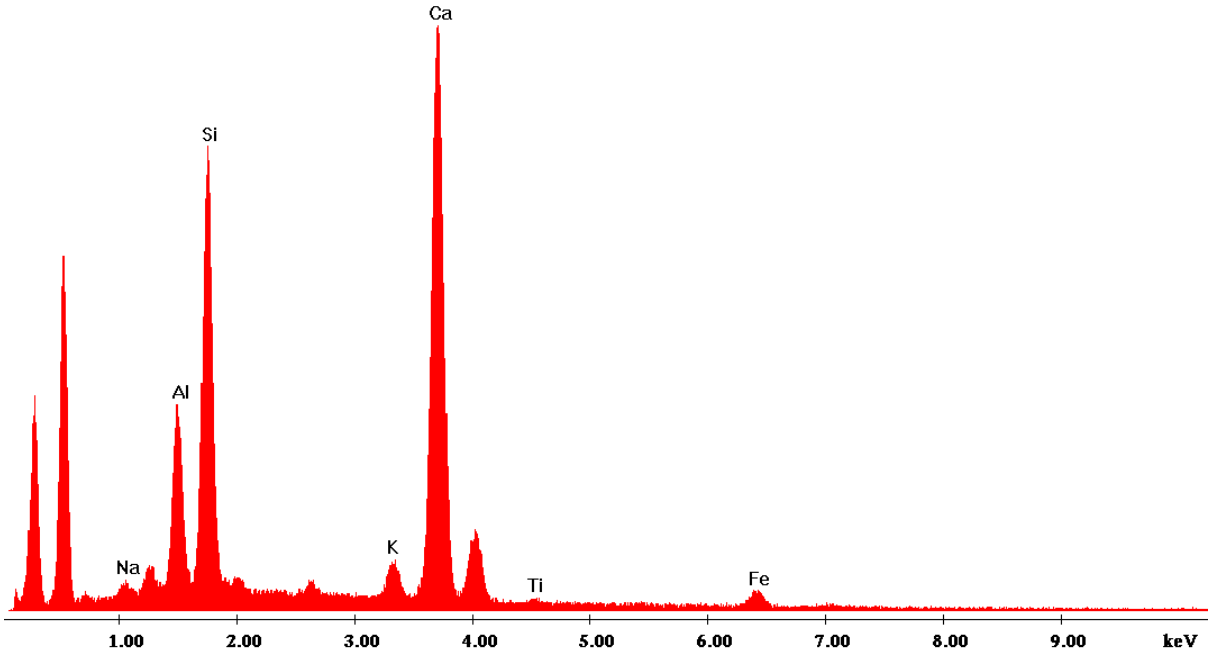

Figure 68 EDS spectrum of the general composition of sample TFN.1959.B.686/7

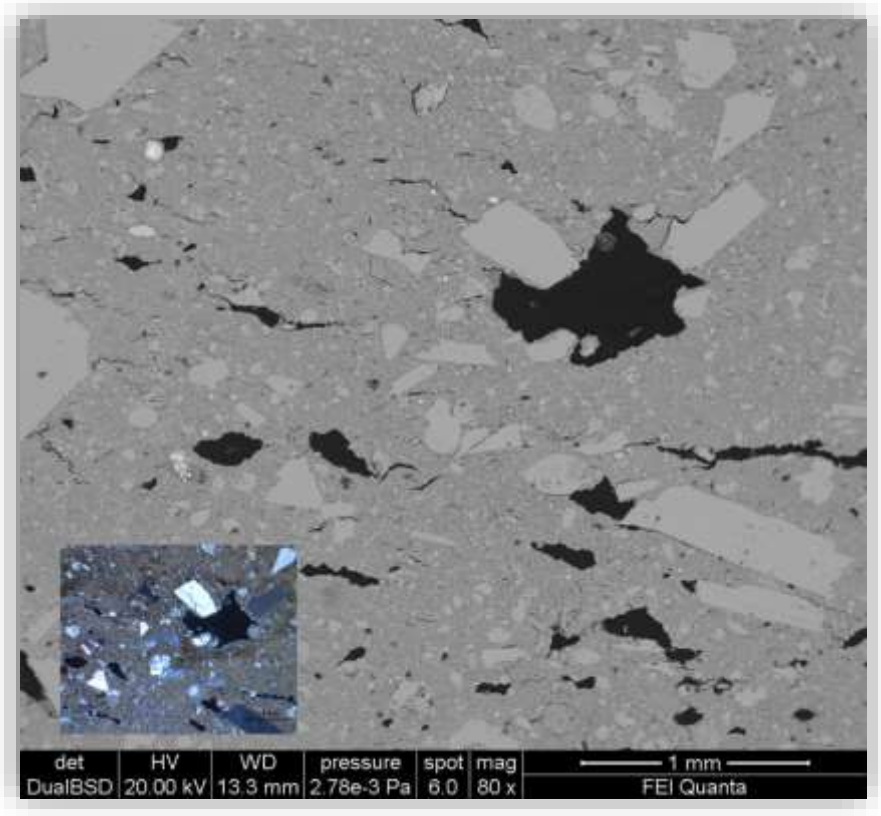

Figure 69 BSE image of sample TFN.1959.B.686/7 displaying calcite, secondary calcite, quartz and some micro-fossils, together with the optical microscope image of the same area under XPL (bottom left).

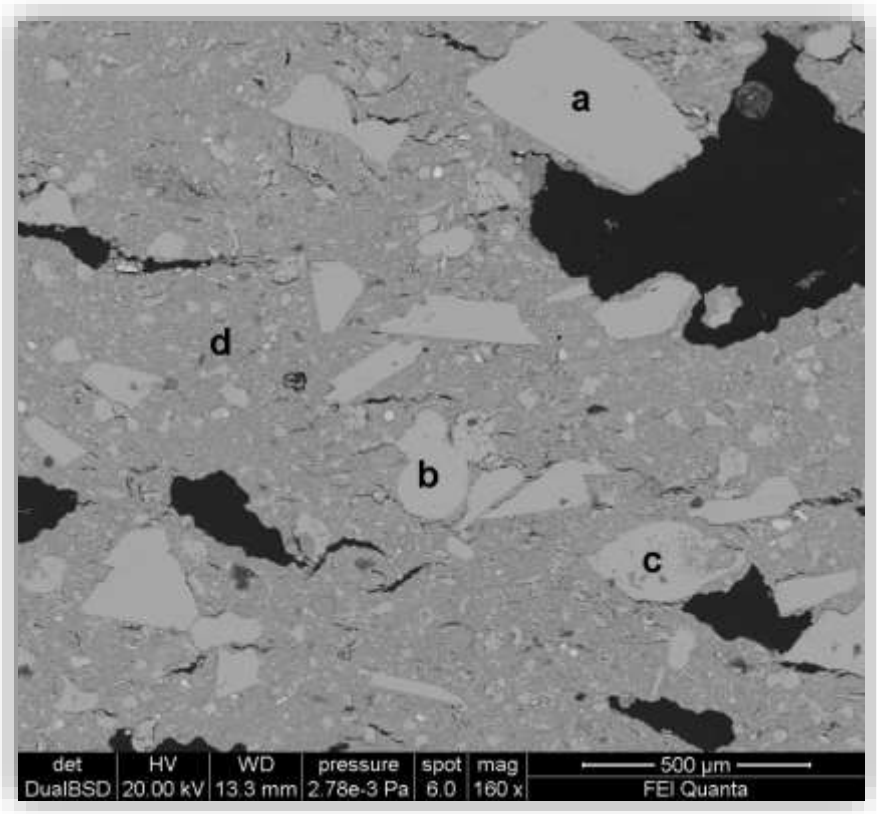

Figure 70 BSE image of sample TFN.1959.B.686/7; labelled a: calcite; b,c: microfossils and d: matrix

The EDS spectrum (Figure 71) of point ”a” from Figure 70 is characterized by high amount of Ca and minor amount of Mg, confirming the presence of calcite crystals.

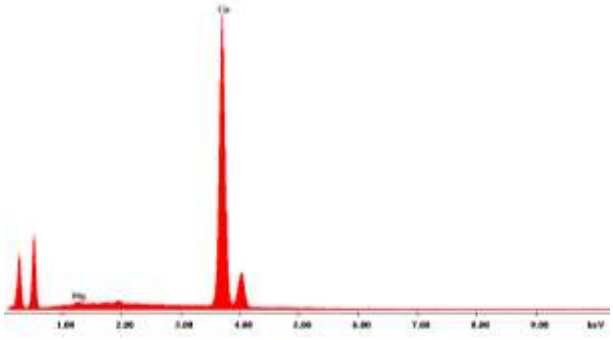

Figure 71 EDS spectrum of point ”a” of sample TFN.1959.B.686/7 identified as calcite

The EDS spectrum of point ”b” (Figure 72) and point “c” (Figure 73) from Figure 70 is characterized by high amount of Ca, as expected in microfossils.

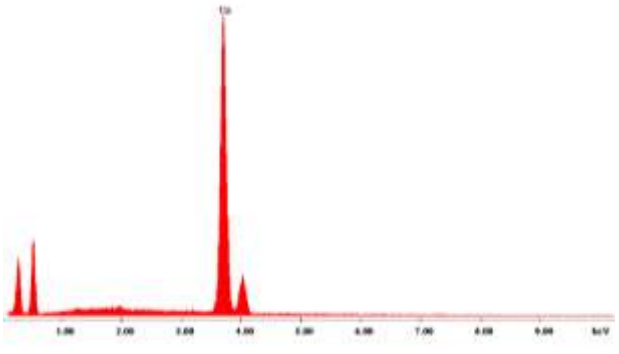

Figure 72 EDS spectrum of point ”b” of sample TFN.1959.B.686/7 identified as micro-fossils

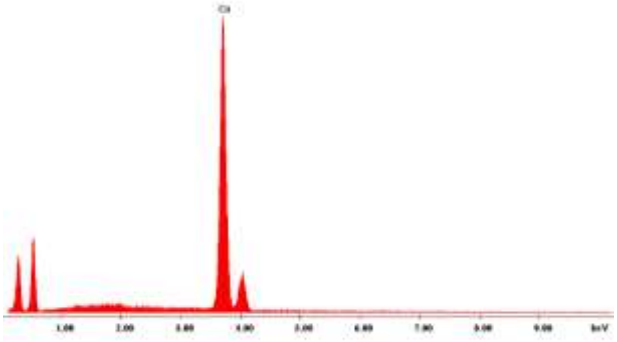

Figure 73 EDS spectrum of point "c" of sample TFN.1959.B.686/7 identified as micro-fossils

The EDS spectrum (Figure 74) of point "d" from Figure 70 is characterized by high amount of Si, abundance of Ca and Al and minor amounts of K, Na, Fe and Ti, reflecting the matrix composition.

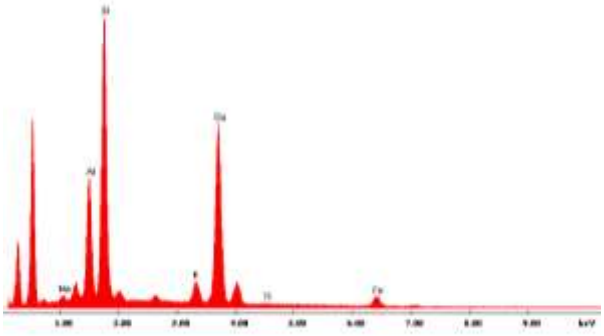

Figure 74 EDS spectrum of point "d" of sample TFN.1959.B.686/7

SAMPLE TFN.1959.L.718/8

The EDS spectrum of the general composition is shown in Figure 75. It is characterized by high amount of Ca and Al, minor abundance of Ca and lower amount of Mg, Na, K, Fe and Ti.

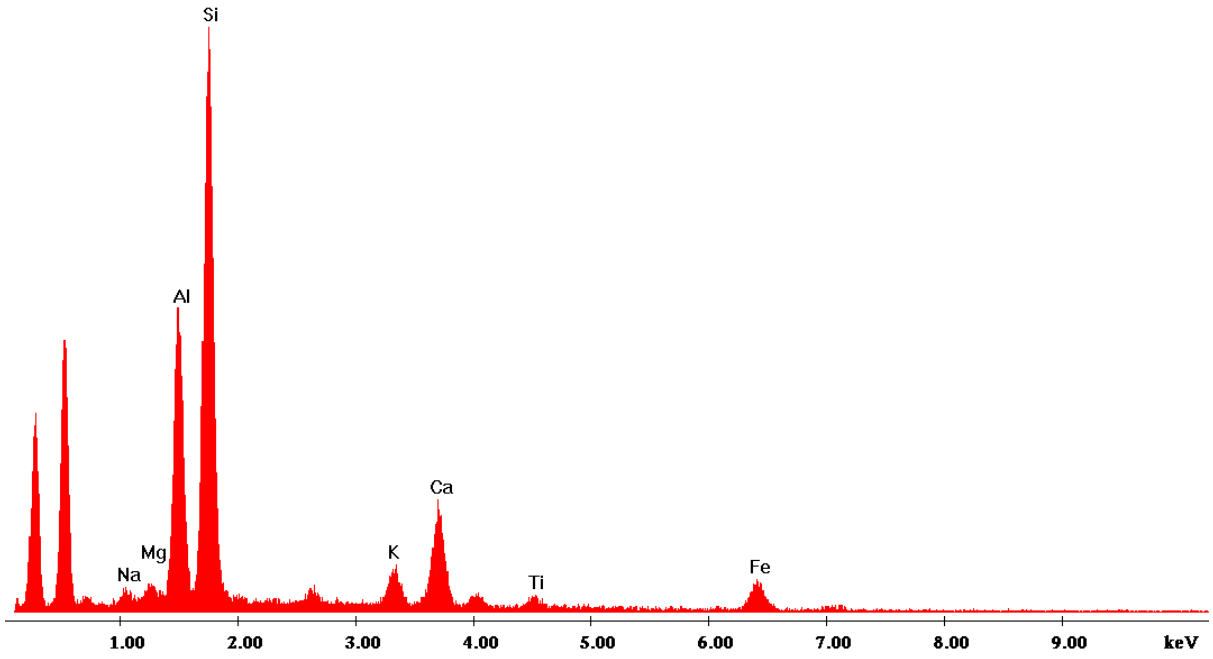

Figure 75 EDS spectrum of the general composition of sample TFN.1959.L.718/8

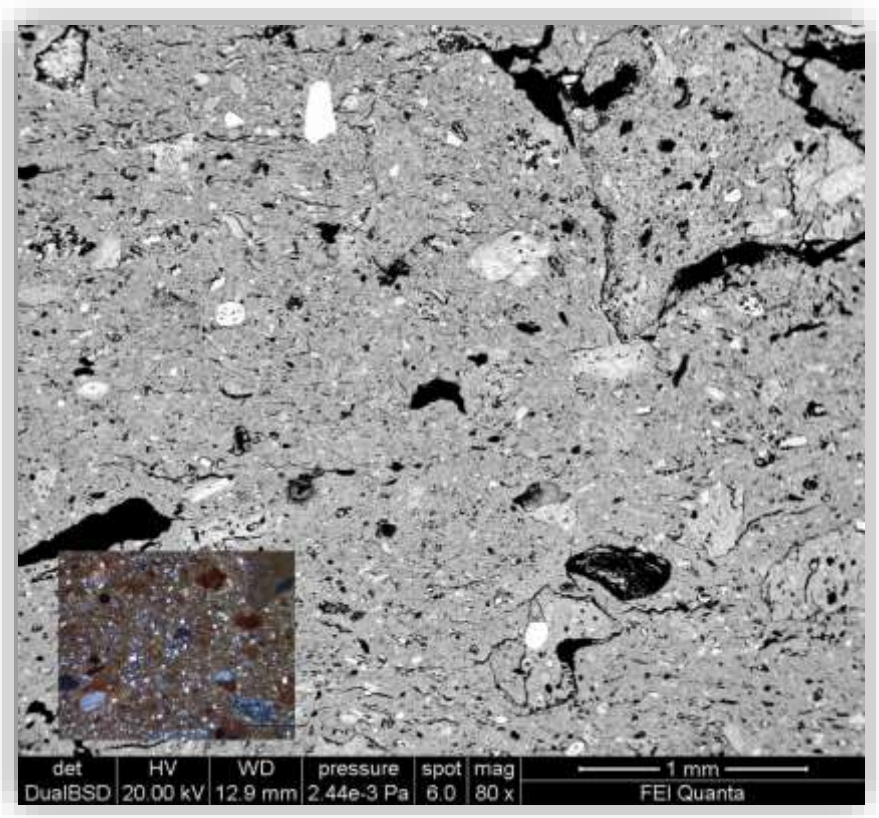

Figure 76 BSE image of sample TFN.1959.L.718/8 displaying calcite, quartz, nodules of iron oxides, fragments of unwell mixed clay and some micro-fossils, together with the optical microscope image of the same area under XPL (bottom left).

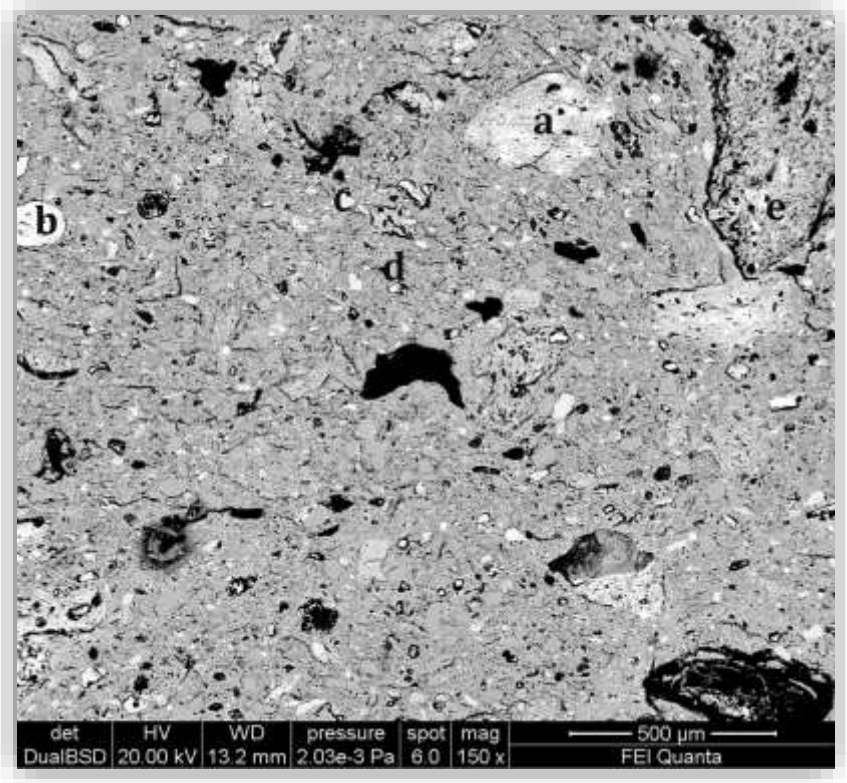

Figure 77 BSE image of sample TFN.1959.L.718/8; labelled a - b: nodules of iron oxides, c: K-felspar, d: quartz, e: fragment of unwell mixed clay

The EDS spectrum of points ”a” (Figure 78) and “b” (Figure 79) from Figure 77 are characterized by high amounts of Si and Al and minor amounts of Ca, Fe, K, Mg, Na and Ti,

reflecting the composition of iron oxide nodules which have composition similar to the matrix, but enriched in iron oxides.

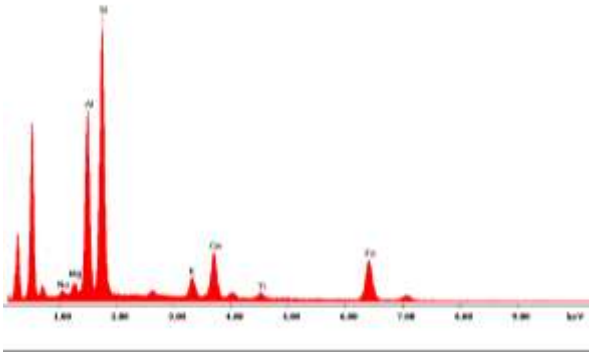

Figure 78 EDS spectrum of point "a" of sample TFN.1959.L.718/8 identified as a nodule of iron oxide

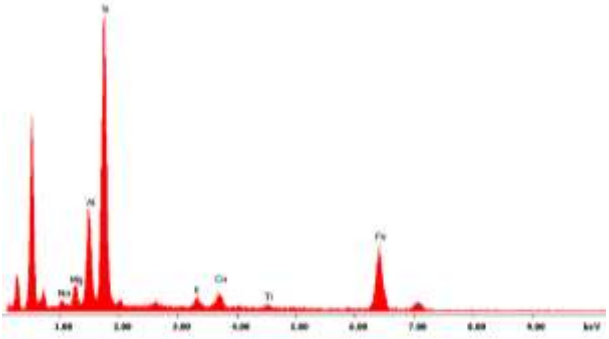

Figure 79 EDS spectrum of point "b" of sample TFN.1959.L.718/8 identified as a nodule of iron oxide

The EDS spectrum (Figure 80) of point "c" from Figure 77 is characterized by high amount of Si and abundance of Al and K.

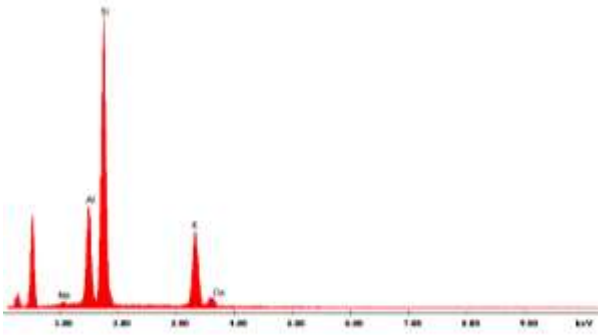

Figure 80 EDS spectrum of point "c" of sample TFN.1959.L.718/8 identified as k-feldspar

The EDS spectrum of point "d" shown in (Figure 81) from Figure 77 is characterized by a high amount of Si, confirming the presence of quartz.

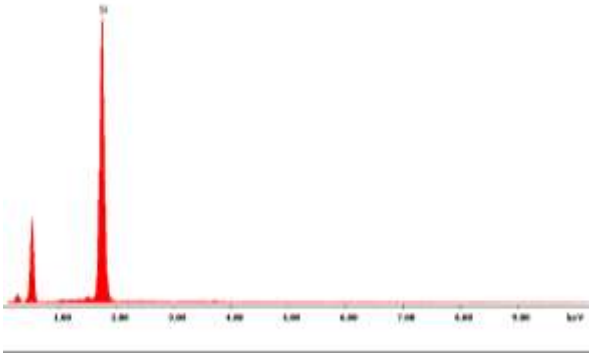

Figure 81 EDS spectrum of point "d" of sample TFN.1959.L.718/8

The EDS spectrum (Figure 82) of point "e" from Figure 77 is characterized by high amount of Si, abundance of Al and minor amounts of Fe, Mg, Ca, K, Na and Ti, reflecting the composition of unwell mixed clay.

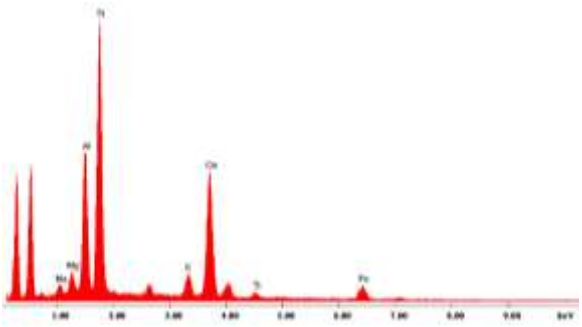

Figure 82 EDS spectrum of point "e" of sample TFN.1959.L.718/8

SAMPLE TFN.1959.L.718/13

The EDS spectrum of the general composition is shown in (Figure 83). It is characterized by high amounts of Si, Ca and Al, minor abundance of Fe and K and lower amounts of Mg, Na and Ti.

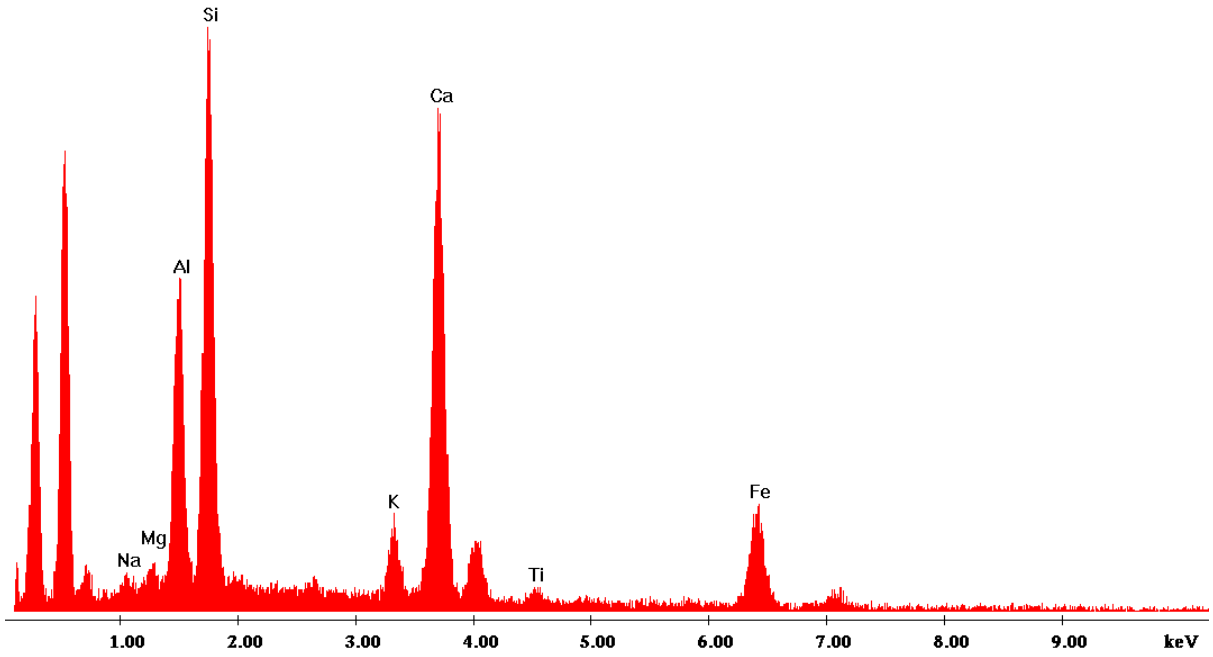

Figure 83 EDS spectrum of the general composition of sample TFN.1959.L.718/13

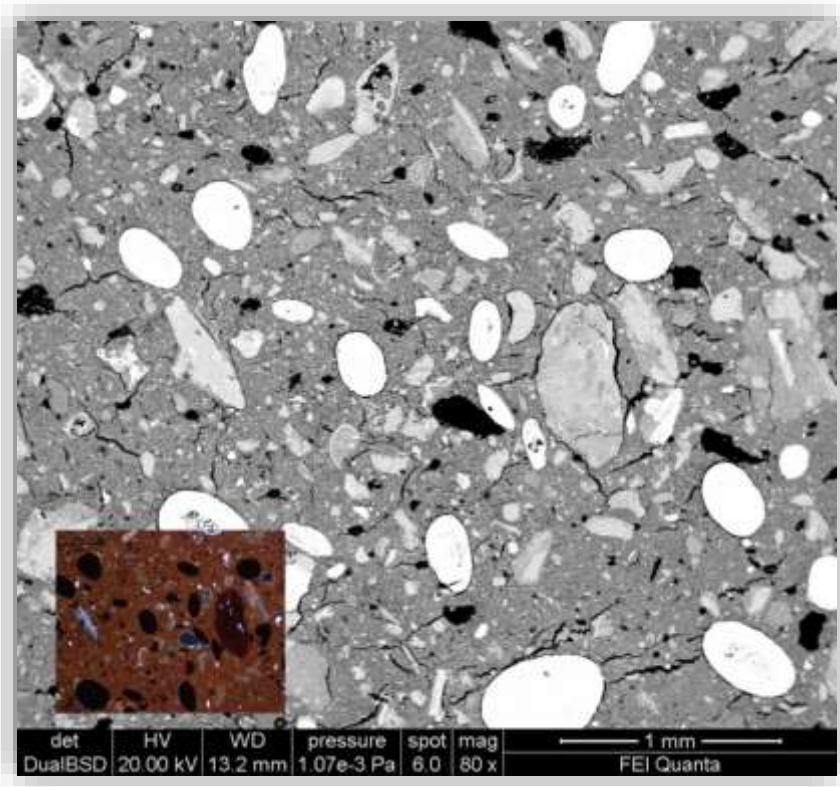

Figure 84 BSE image of sample TFN.1959.L.718/13, displaying calcite, iron oxide nodules, siliceous rock fragments, sedimentary calcareous rock fragments and some micro-fossils, together with the optical microscope image of the same area under XPL (bottom left).

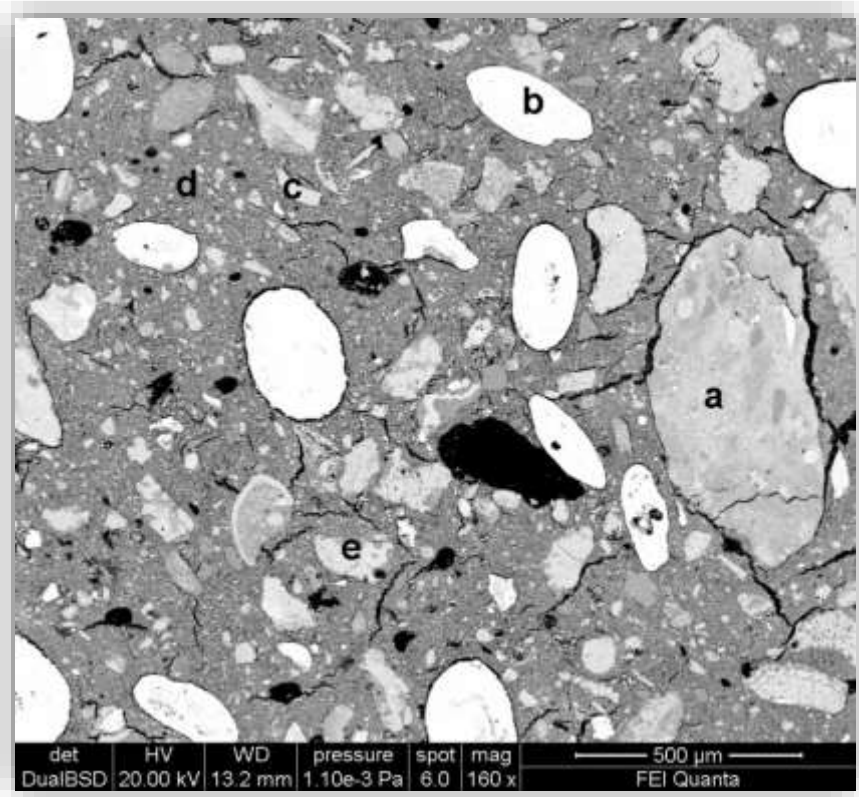

Figure 85 BSE image of sample TFN.1959.L.718/13; labelled a: siliceous rock fragment, b: a nodule of iron oxide, c: micro-fossil, d: quartz, e: sedimentary calcareous rock fragment

The EDS spectrum (Figure 86) of point ”b” from Figure 85 is characterized by high amount of Si, abundance of Al, presence of Ca and minor amounts of Fe, Mg, K, Na and Ti, reflecting the composition of a siliceous rock fragment.

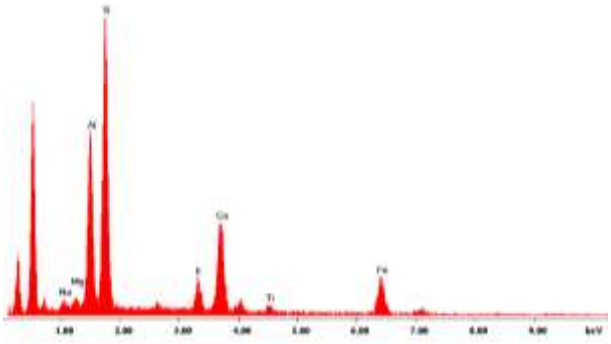

Figure 86 EDS spectrum of point ”a” of sample TFN.1959.L.718/13 identified as siliceous rock

The EDS spectrum (Figure 87) of point ”b” from Figure 85 is characterized by high amount of Fe, presence of Si and minor amounts of Al, Ca, Mg. K, Na and Ti, reflecting the composition of the nodules of iron oxides typical of this sample..

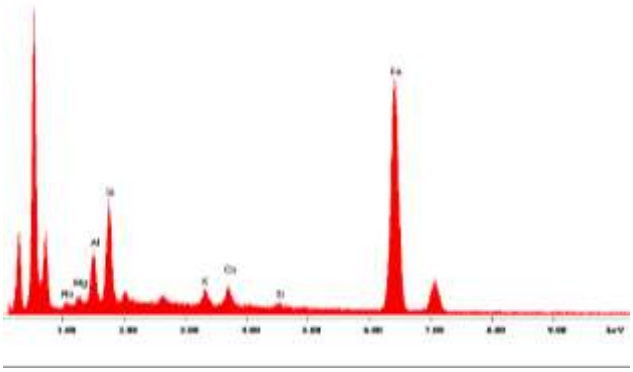

Figure 87 EDS spectrum of point ”b” of sample TFN.1959.L.718/13

The EDS spectrum (Figure 88) of point ”c” from Figure 85 is characterized by high amount of Ca, typical of microfossils.

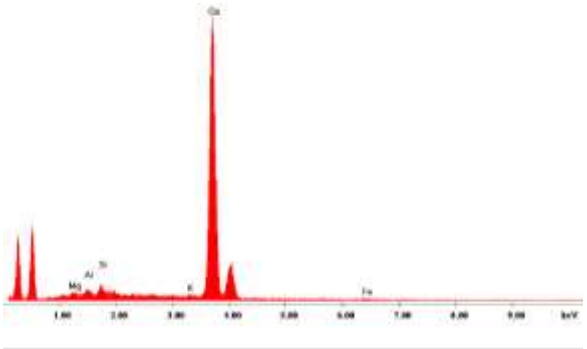

Figure 88 EDS spectrum of point ”c” of sample TFN.1959.L.718/13 from a micro-fossil

The EDS spectrum (Figure 89) of point ”d” from (Figure 85) is characterized by high amount of Si, confirming the presence of quartz.

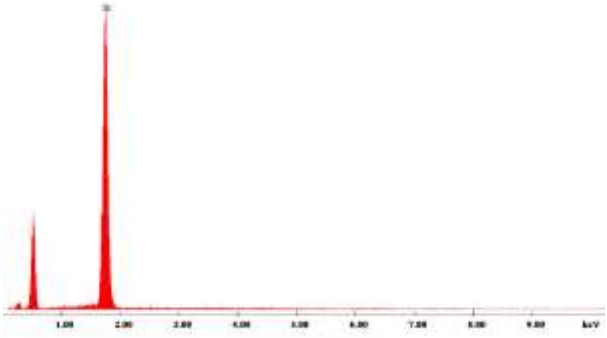

Figure 89 EDS spectrum of point "d" of sample TFN.1959.L.718/13

The EDS spectrum (Figure 90) of point "e" from Figure 85 is characterized by high amount of Ca and minor amounts of Si, Fe, Mg, Al and K, typical of calcareous rock fragments.

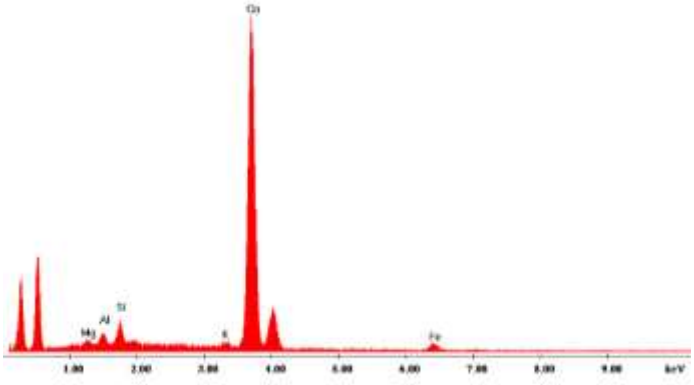

Figure 90 EDS spectrum of point "e" of sample TFN.1959.L.718/13 from a calcareous rock fragment

SAMPLE TFN.1954.B. 272/5

The EDS spectrum of the general composition is shown in Figure 91. It is characterized by high amount of Ca, Si, minor abundance of Al and lower amounts of K, Mg, Fe, Na and Ti.

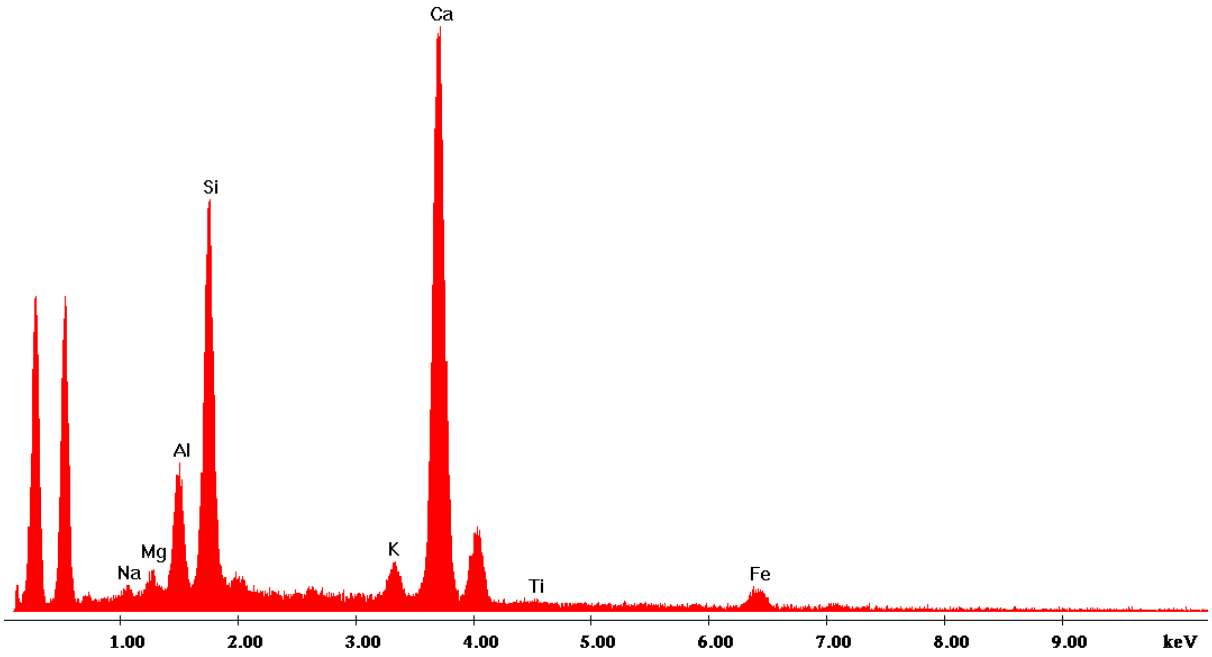

Figure 91 EDS spectrum of the general composition of sampleTFN.1954.B.272/5

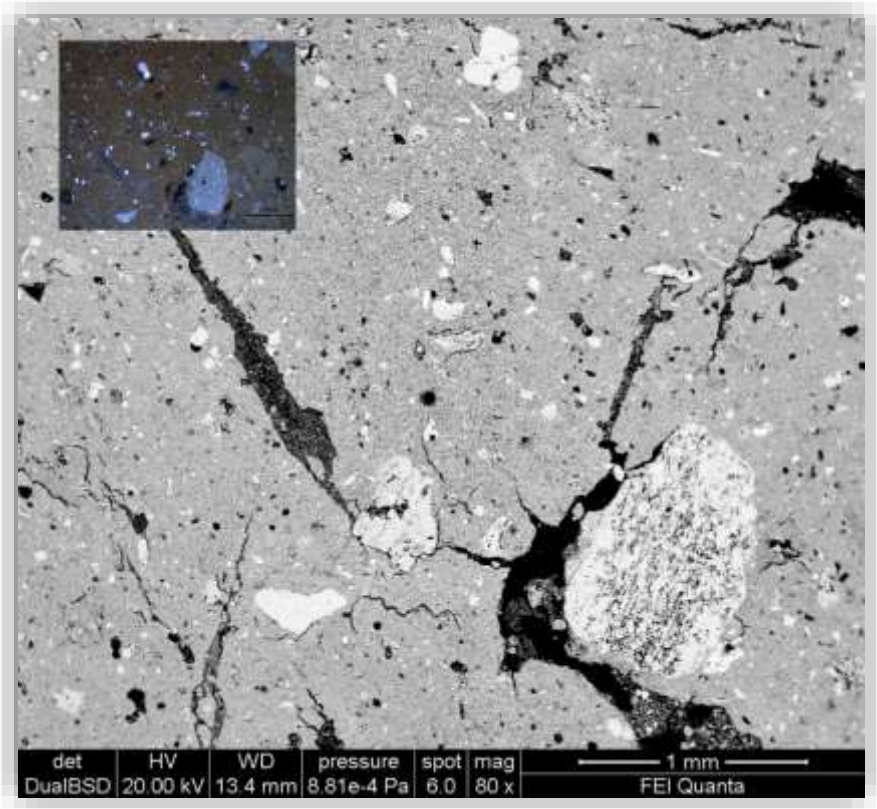

Figure 92 BSE image of sample TFN.1954.B. 272/5, displaying calcite, nodules of iron oxides and sedimentary calcareous rock fragments, together with the optical microscope image of the same area under XPL (top left).

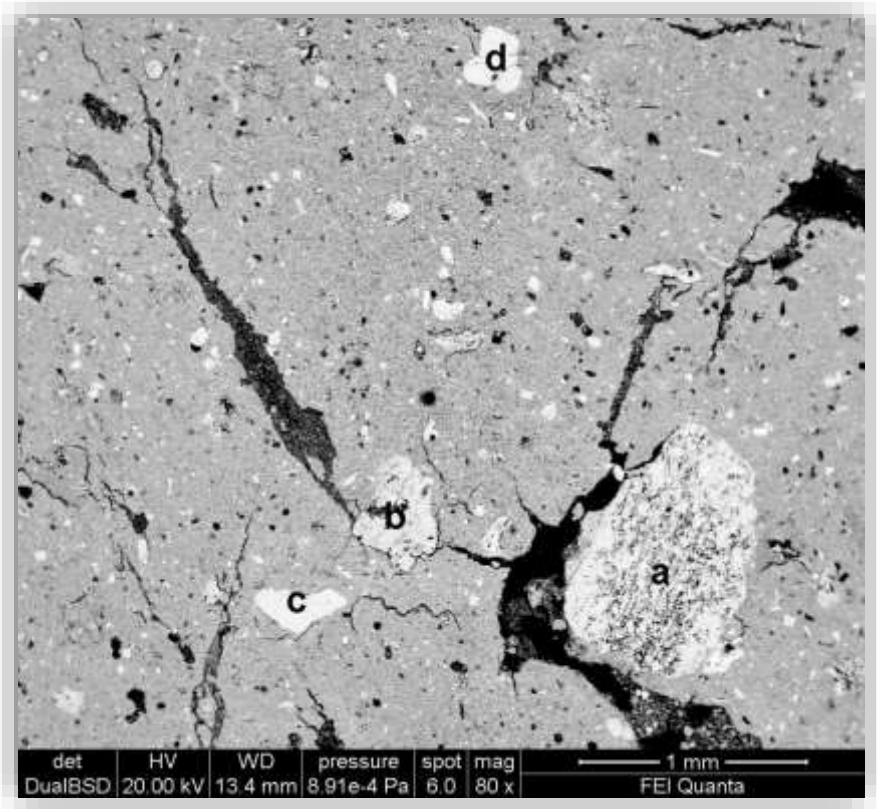

Figure 93 BSE image of sample TFN.1954.B. 272/5; labelled a, b, c, d, are all calcareous rock fragments.

The EDS spectra of points ”a” (Figure 94), “b” (Figure 95), “c” (Figure 96) and “d” (Figure 97) from Figure 93 are generally characterized by high amount of Ca and minor amounts of Mg, K, Na, Si, Ti and Fe, reflecting the composition of the calcareous rock fragments present in this sample.

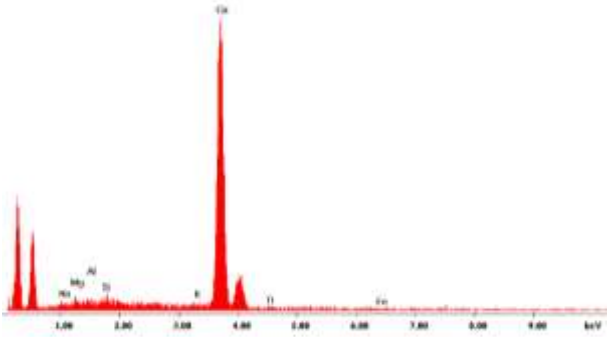

Figure 94 EDS spectrum of point ”a” of sample TFN.1954.B. 272/5 identified as calcareous rock

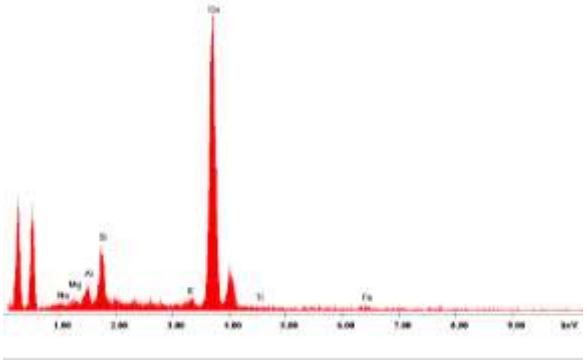

Figure 95 EDS spectrum of point ”b” of sample TFN.1954.B. 272/5 identified as calcareous rock

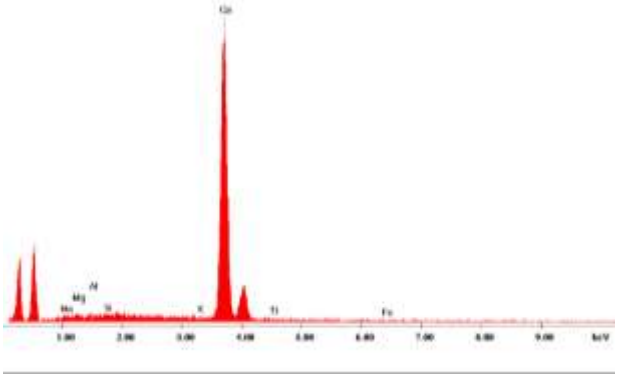

Figure 96 EDS spectrum of point ”c” of sample TFN.1954.B. 272/5 identified as calcareous rock

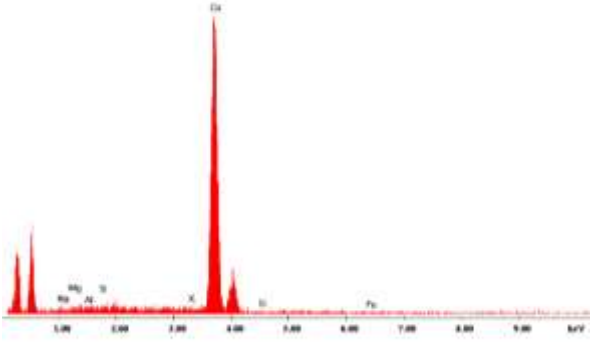

Figure 97 EDS spectrum of point ”d” of sample TFN.1954.B. 272/5 identified as calcareous rock

SAMPLE TFN.1959.L.718/31

The EDS spectrum of the general composition is shown in Figure 98. It is characterized by high amounts of Si and Ca, minor abundance of Al and lower amounts of Mg, Na, K, Fe and Ti.

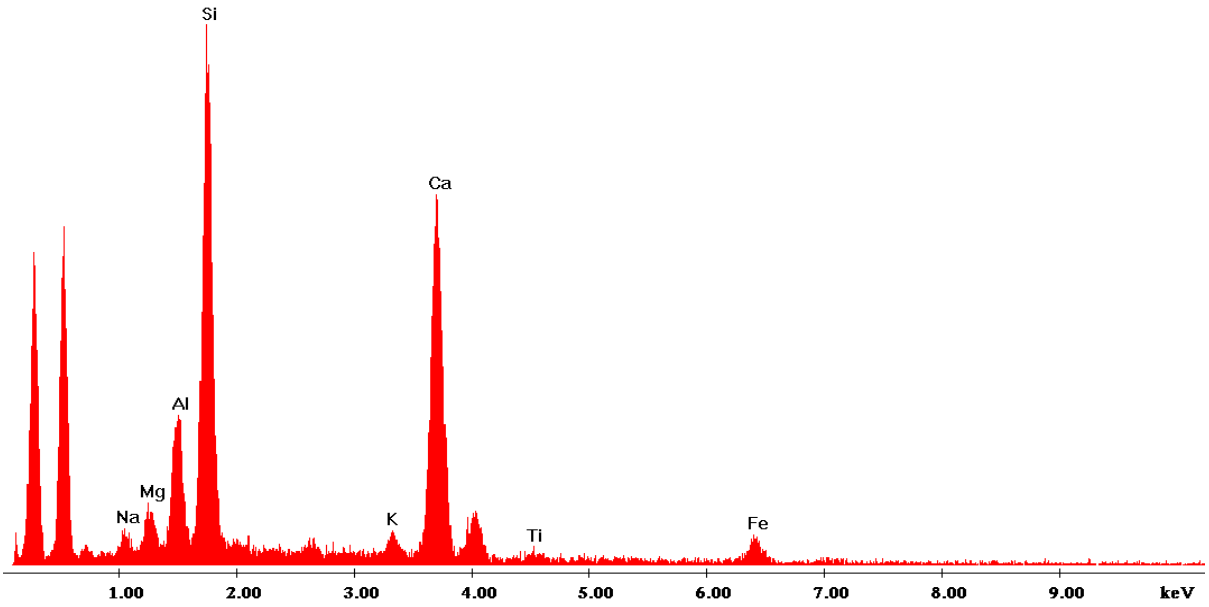

Figure 98 EDS spectrum of the general composition of sample TFN.1959.L.718/31

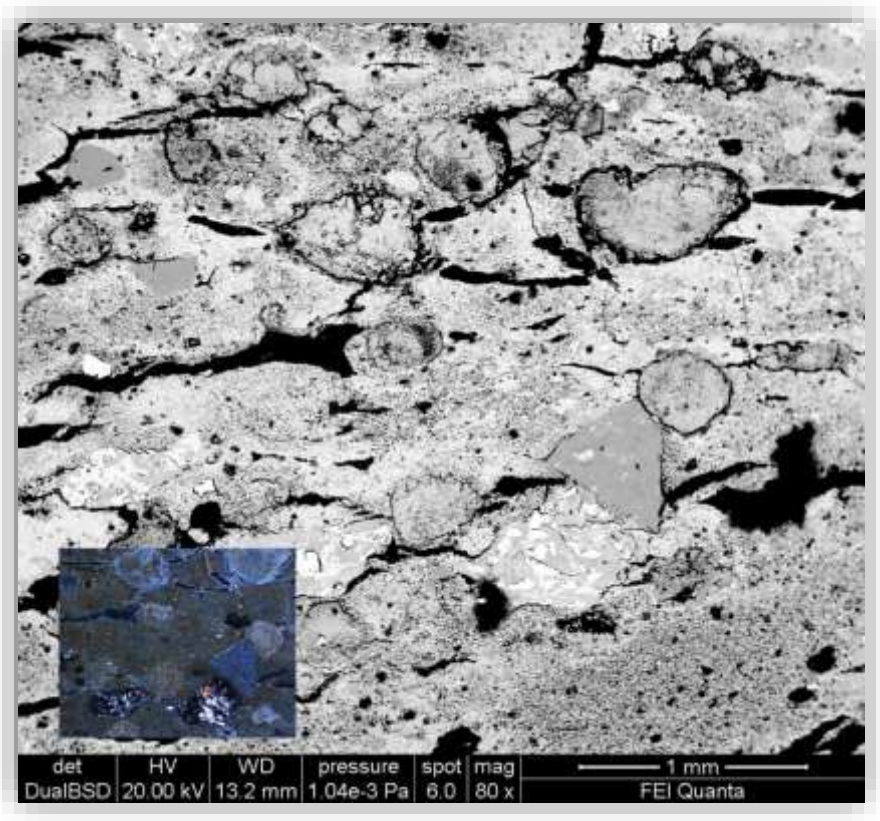

Figure 99 BSE image of sample TFN.1959.L.718/31, displaying calcite, siliceous rock fragments and fragments of basalt, together with the optical microscope image of the same area under XPL (bottom left).

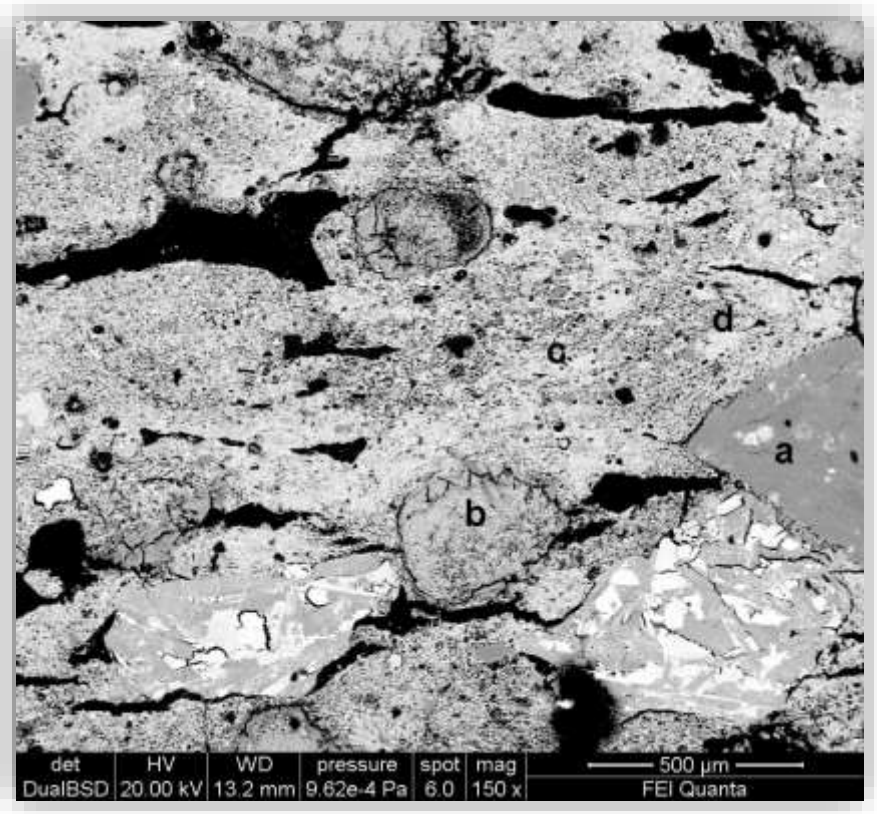

Figure 100: BSE image of sample TFN.1959.L.718/31; labelled a: siliceous rock fragment, b: calcareous rock fragment, c: matrix d: quartz.

The EDS spectrum (Figure 101) of point ”a” from Figure 100 is characterized by high amount of Si and minor amounts of Mg, Al, K, Na, Fe, Si, Ca and Ti, identified as a siliceous rock fragment.

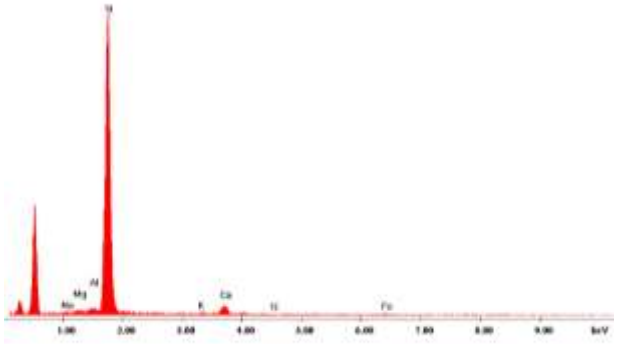

Figure 101 EDS spectrum of point ”a” of sample TFN.1959.L.718/31 identified as siliceous rock

The EDS spectrum (Figure 102) of point ”b” from Figure 100 is characterized by high amount of Ca and minor amounts of Mg, Al, K, Na, Fe, Si and Ti, thus suggesting a calcareous rock fragment.

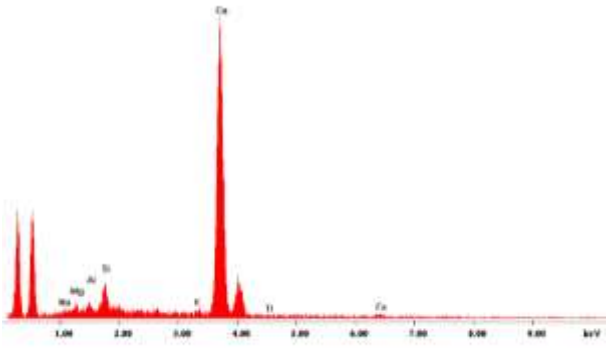

Figure 102 EDS spectrum of point ”b” of sample TFN.1959.L.718/31 is identified as calcareous rock fragment

The EDS spectrum (Figure 103) of point ”c” from Figure 100 is characterized by high amounts of Si and Ca with minor presence of Al, Mg and Na, reflecting the matrix composition.

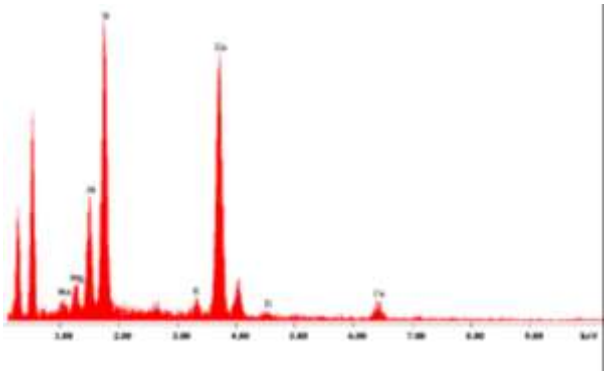

Figure 103 EDS spectrum of point ”c” of sample TFN.1959.L.718/31 representative of the matrix

The EDS spectrum (Figure 104) of point ”d” from Figure 100 is characterized by high amount of Si, confirming the presence of quartz.

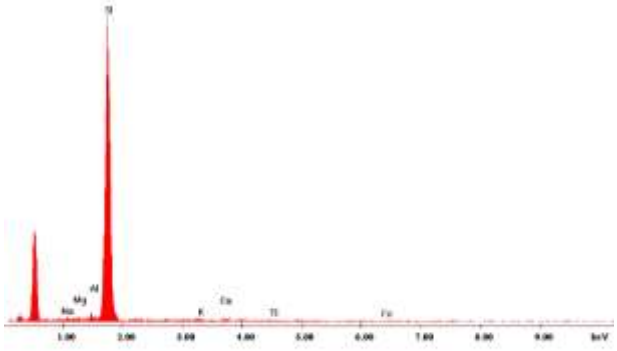

Figure 104 EDS spectrum of point ”d” of sample TFN.1959.L.718/31 identified as quartz

A basalt fragments is deeply analysed considering the minerals composing the rock.

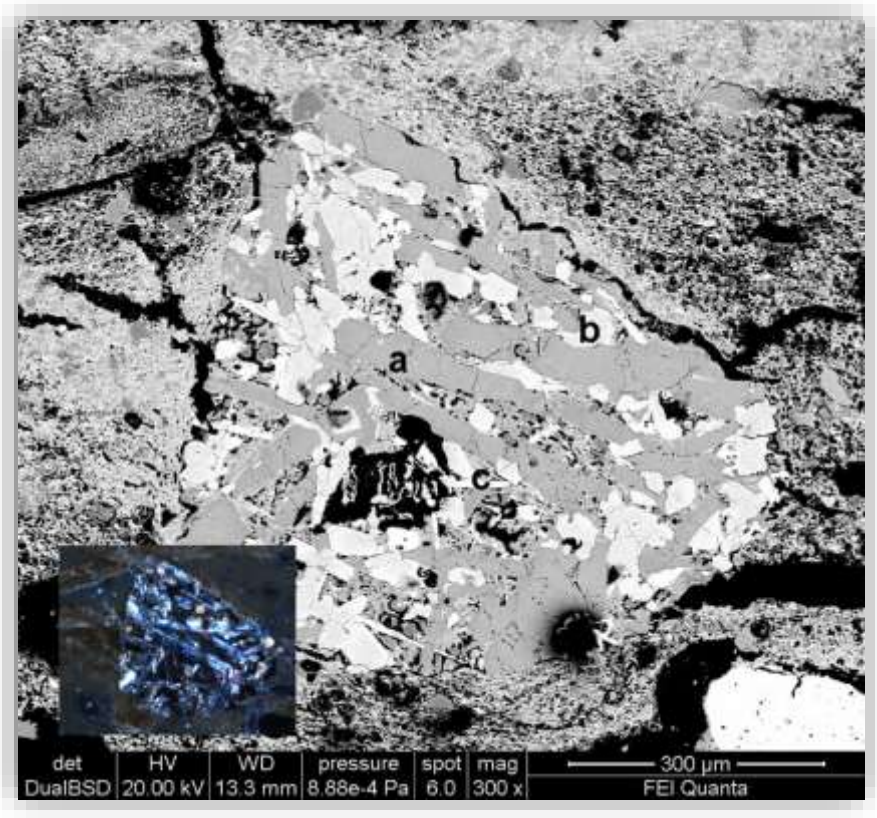

Figure 105 BSE image of sample TFN.1959.l.718/31, basalt fragment- labelled a:plagioclase, b:k-feldspar, quartz c:ilmenite

The EDS spectrum (Figure 106) of point ”a” from Figure 105 is characterized by high amount of Si and Al, as well as Ca and Na, confirming the presence of plagioclase crystals.

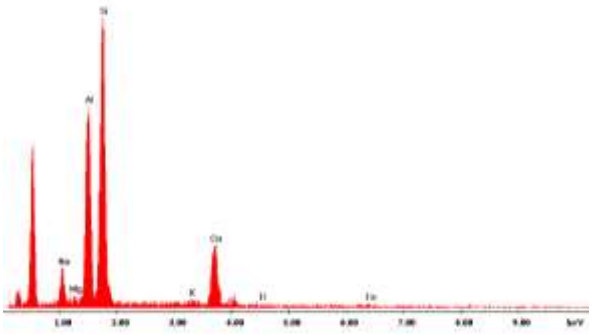

Figure 106 EDS spectrum of point ”a” of sample TFN.1959.L.718/31, identified as plagioclase.

The EDS spectrum (Figure 107) of point ”b” from Figure 105 is representative of a pyroxene crystal, and it is characterized by high amount of Si, lower amounts of Ca and Mg and minor amount of Al, K, Na, Fe and Ti.

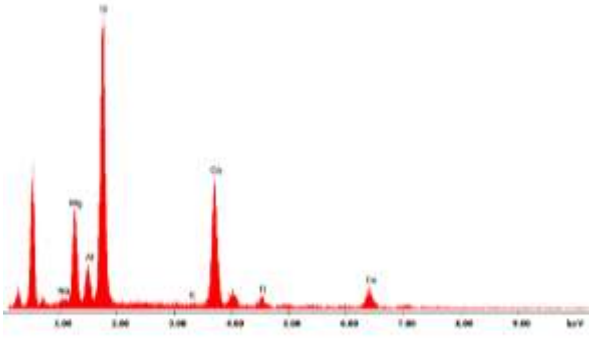

Figure 107 EDS spectrum of point ”b” of sample TFN.1959.L.718/31, identified as pyroxene.

The EDS spectrum (Figure 108) of point ”c” from Figure 105 is characterized by high amount of Ti, lower amounts of Si and Fe and minor amounts of Mg, Al, K, Na and Ca, suggesting the presence of ilmenite.

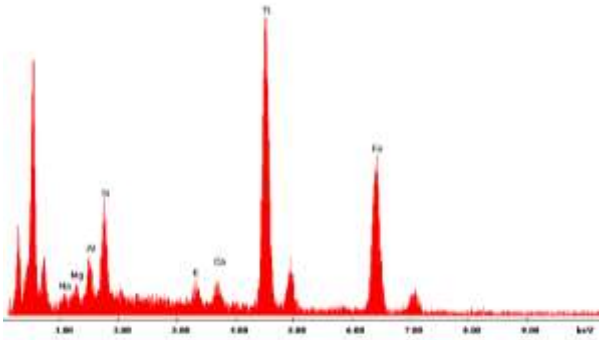

Figure 108 EDS spectrum of point ”c” of sample TFN.1959.L.718/31, identified as ilmenite.

Chapter 5: Discussion

Ceramics is the most studied type of artefact because it is the most enlightening source of information about the past (Cultrone et al., 2001; Barone et al., 2003; Maritan, 2004; Rathossi et al., 2004). Consequently, archaeometric applications are used in order to classify and characterize ceramic products as to provide data on the provenance of the raw material, ancient technologies for pottery production and possible function, as well as the social meaning of the product (Meloni et al., 2000; Zeinab, 2018).

5.1 Nature of the raw material

On the basis of the mineralogical and petrographic composition, two groups were identified as shown in Figure 109. Sample TFN.1959.L.718/31 is separated as a loner, characterized by coarse grain-size of inclusions, aligned to the margins and very abundant calcite, abundant K-feldspar and gehlenite, the presence of quartz and anorthite in addition to fragments of basalt rocks.

The other examined samples share a general similar mineralogical and petrographic composition, mainly characterized by the presence of calcite, quartz crystals and nodules of iron oxides. Nevertheless, the predominance of coarse and angular crystals of calcite allows distinguishing samples TFN.1959.B.686/1, TFN.1959.B.686/3, TFN.1959.B.686/7, TFN.1959.L.689sup./1 as fabric A-calcite. Of these, samples TFN.1959.B.686/3 and TFN.1959.B.686/7 are separated as fabric A-calcite/A1 from the other samples that belong to the same fabric due to the presence of diffuse microfossils. Fabric B-calcareous is the most populated fabric and includes the rest of the examined samples. Similarities among samples allowed us to include samples TFN.1959.L.718/9, TFN.1959.L.718/8 and TFN.1959.L.718/32 in fabric B-calcareous/B1 as they are characterized by the predominance of quartz and the presence of calcite in addition to nodules of iron oxides. On the other hand, fabric B-calcareous/B2 includes samples TFN.1959.L.718/8, TFN.1959.L.686/6 and TFN.1959.L.718/13, which show the presence of diffused micro-fossils. Finally, fabric B-calcareous/B3 includes sample TFN.1954.B.272/5 on the basis of the microfeatures of the calcareous matrix.

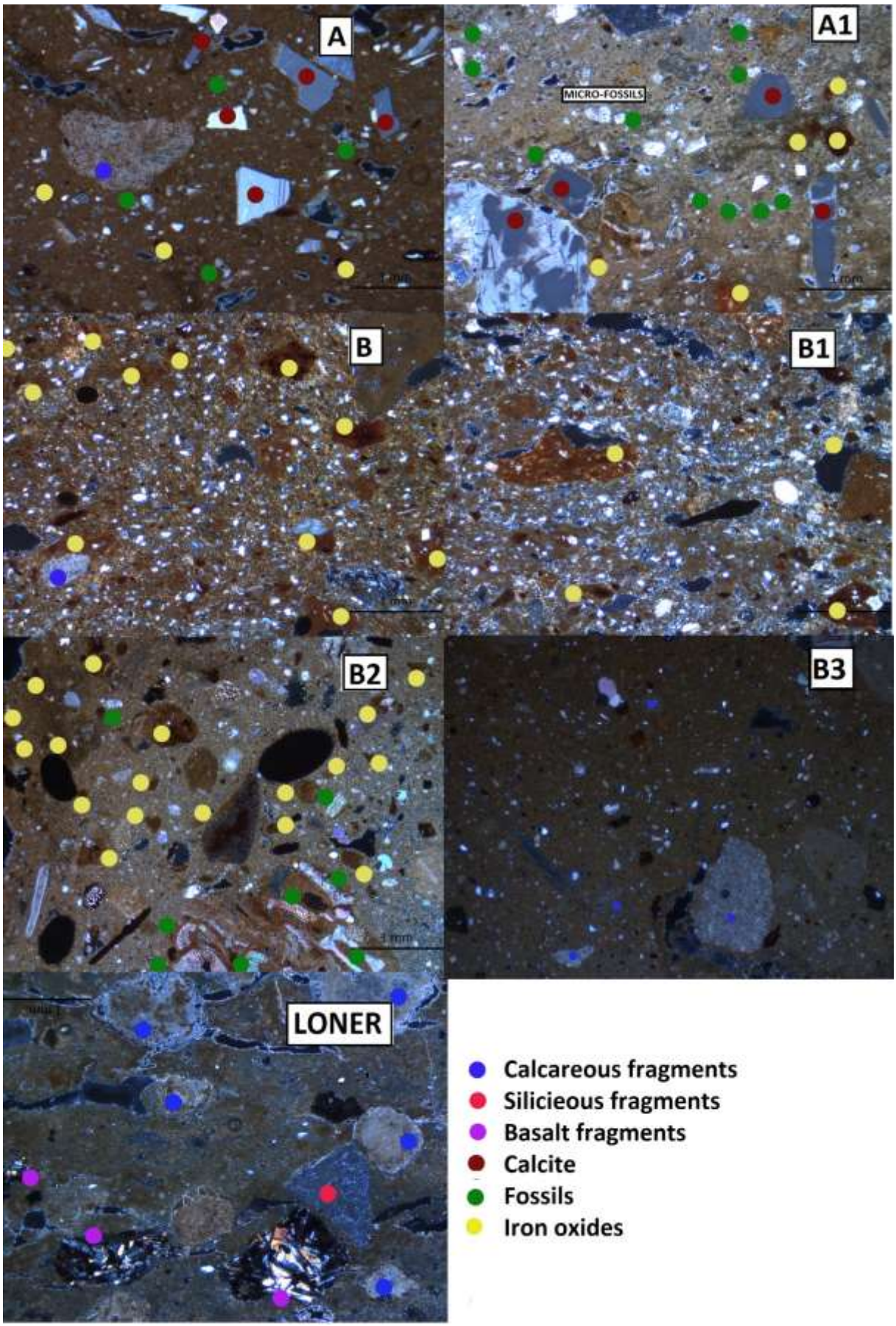

Figure 109 Microscopic images of representative samples for each petro-group identified: sample TFN.1959.B.686/3 (fabric A-calcite), sample TFN.1959.B.686/1 (fabric A-calcite/A1), sample TFN.1959.L.718/8 (fabric B-calcareous), sample TFN.1959.L.718/9 (fabric B-calcareous /B1), sample TFN.1959.L.686/8 (fabric B-calcareous/B2), sample TFN.1954.B. 272/5 (fabric B-calcareous/B3), sample TFN.1959.L.718/31 (loner).

According to the Scanning Electron Microscopy images, an overview of inclusions is given in Figure 110. Based on the presence or absence of microfossils within the matrix, clays can be sub-grouped into clay α and clay β, as previously reported by Medeghini et al. (2019). Indeed, samples TFN.1959.B.686/3 and TFN.1959.B.686/7 are identified as clay α, where diffused microfossils are present, whereas samples TFN.1959.L.718/8, TFN.1959.L.718/13, TFN.1954.B. 272/5 belong to clay β, where diffused crystals of quartz are present.

Finally, SEM images and EDS spectra confirmed that sample TFN.1959.L.718/31 is a loner characterized by coarse grain size of inclusions, aligned to the margins, where fragments of basalt rocks and siliceous rock fragments have been identified.

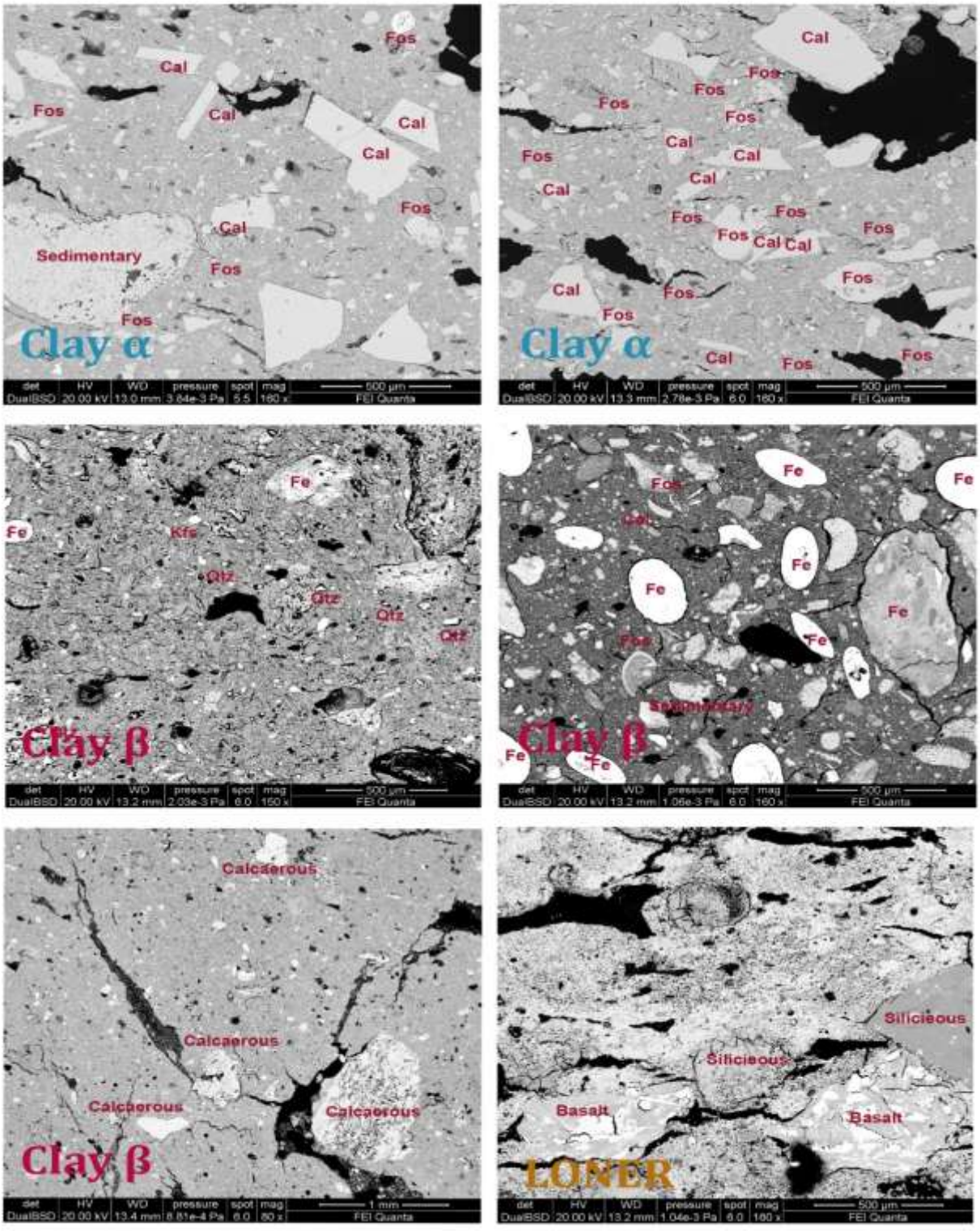

Figure 110 BSE images of sample TFN.1959.L.718/31 (loner), samples TFN.1959.B.686/3 and TFN.1959.B.686/7 (clay α), samples TFN.1959.L.718/8 ,TFN.1959.L.718/13 and TFN.1954.B. 272/5 (clay β)

5.2 Technological level

Once the materials are chosen, clay, inclusions and water are mixed to obtain the paste. The identification of clay pellets only in sample TFN.1959.L.718/13 suggests that the mixing was not complete for this sample, but it was generally a careful step in the production of the other vessels.

Another technological parameter to be considered is the utilization of the manual potter's wheel (i.e. slow wheel or *tournette*), which can be identified by the extent of kinetic energy testified by the alignment of voids and inclusions (Roux, & Miroschedji, 2009; Tite *et al.*, 2001). None of the samples shows alignment of the inclusions; however most of the voids are aligned to the margin, which suggest a manual modelling of the final shape.

The production technology is affected by the potter's preference when it comes to the raw materials used. According to technological studies of archaeological ceramics these choices are due to two reasons: firstly the environment e.g., the availability of raw materials (Matson 1965; Kolb 1989) and secondly an optimized function intended for the ceramics which is influenced by cultural considerations (Day, 1988).

Fabric A-calcite, which is characterized by angular and coarse calcite crystals that were added to the production of the typical storage ware such as large jars, hole-mouth jars, and *pithoi*, indicates that potters knew that the addition of calcite inclusions was to modify the plasticity of the clay and improve the hardness and resistance of the vessels for food storage. Likewise in Fabric B-Calcareous which is characterized by the predominance of diffused quartz crystals, the latter were added in the production of the typical Bronze age storage ware and simple table ware, such as bowls, hole-mouth jars, *pithoi* and *amphoriskos*. Quartz crystals were added as a temper, to improve the thermal expansion of the vessels producing items suitable to store foods.

This implies that A-calcite and B-calcareous do not correspond to macro-functional classes of the Tell El-Far'ah pottery assemblage, since the two fabrics are chronologically separate. Fabric A-calcite is associated with the Chalcolithic period, whereas Fabric B-calcareous with the Early Bronze Age I ceramics. However, the comparison with data from Medeghini et al. (2019) suggests that the subdivision of fabrics is not strictly related to the time periods, but probably due to a random selection of a low number of samples. In addition, a totally different fabric, separated as a loner, characterized by coarse grain size of inclusions, aligned to the margin and very abundant calcite, abundant K-feldspars and gehlenite, and the presence of quartz and anorthite in addition to fragments of basalt rocks is identified within the Early Bronze age assemblage.

An important step of ceramic production is represented by the firing process. Indeed, the firing conditions of ceramics, i.e. firing time, temperature and atmospheric conditions, influence the properties of the final product (Santos et al., 2009). The mineralogical composition can be used to estimate the approximate firing temperature, dependent on mineralogical and structural changes within the clayey material (Cogswell et al., 1996; Singh and Sharma, 2016). The atmosphere within the furnace, the maximum temperature reached, the firing time and the cooling rate are all factors that influence the colour of the matrix. The classification of archaeological ceramics through paste colour is widely used. The colour is not quantitatively measured and only comparative Munsell classification is occasionally given. Moreover, the validity of such classification depends on whether differences are related to different compositions, firing procedures, or uncontrolled conditions. Red colour is

associated with iron oxides, white with titanium oxide, yellow with iron hydroxides, and brown shows the difference in oxidation during the firing process (Uda, 2005). Ceramic colour is primarily determined by the iron content in raw materials and the redox conditions at the time of firing. Carbonate levels in raw materials also determine colour: pottery crafted with carbonate-poor clays becomes reddish-brown when fired in an oxidizing atmosphere, and dark grey or black when fired in a reducing atmosphere. In contrast, the colour of ceramics becomes creamy in an oxidizing atmosphere and brownish in a reducing atmosphere when carbonate-rich clays are used. When oxidizing firing conditions are appropriate, hematite is formed. Hematite is the mineral phase in the ceramics that gives the main pigmentation (Nodari et al., 2007).

The matrix of the analysed samples varies in colour, being mainly beige, khaki-reddish or beige, khaki-greyish which indicates that oxygen fugacity was completely non-controlled in a general oxidizing condition (Molera et al.1998). In addition, hematite, identified in the XRD pattern of samples TFN.1959.L.718/33, TFN.1959.L.718/35, TFN.1959.B.672/4 and TFN.1959.L.718/13, further support oxidizing conditions (De Benedetto et al., 2002).

Based on the nature and state of the inclusions identified in thin-section, the maximum firing temperature was estimated. A firing temperature below 850 °C is indicated by the presence of an optically active matrix as at 850 °C clay minerals completely lose their optical properties.

Thus, the examination of samples TFN.1959.B.686/1, TFN.1959.B.686/3, TFN.1959.B.686/7, TFN.1959.L.689sup./1, TFN.1959.L.718/9, TFN.1959.L.718/8, TFN.1959.L.718/32, TFN.1959.L.718/33 and TFN.1959.L.686/6 by optical microscopy, which showed a slightly optically active matrix, suggests a firing temperature lower than 850 °C, the temperature at which clay minerals and carbonates completely lose their optical properties. On the contrary, samples TFN.1959.L.718/13 and TFN.1959.L.718/31 do not show optical activity, indicating a firing temperature higher than 850 °C.

As far as inclusions are concerned, the diffused calcareous inclusions (calcite crystals, limestone fragments, microfossils) identified in these samples further support a possible firing temperature threshold lower than 850-900 °C, the upper limit of decarbonation process.

Another parameter that could be indicative of the firing temperature is the presence or absence of certain minerals. The XRD examination of samples TFN.1959.B.672/4 and TFN.1959.L.718/31 showed traces of gehlenite which further suggest high temperature of firing. Indeed, gehlenite forms between 800 and 950 °C as a result of the reaction among the products of carbonates and clay minerals decomposition (Medeghini & Nigro, 2017).

5.3 Provenance

Provenance studies on clay sources make it possible to define the raw material supplied and used in a specific ceramic production (Meloni et al.,2000). Microfossils hold a great potential in the determination of the nature and origin of raw materials, as they are highly indicative of geological age and palaeoenvironment (Quinn & Day, 2007). The microscopic features described for fabric A-calcite and fabric B-calcareous are highly compatible with resources in proximity of Tell El Far'ah North, supporting the hypothesis of local supplies. It is possible to infer a local, specialised ceramic industry, or even a specialised workshop, with high expertise in the selection of raw materials. Samples TFN.1959.B.686/3, TFN.1959.B.686/7, TFN.1959.L.686/6 and TFN.1959.L.718/13 showed the presence of diffused micro-fossils within the matrix. According to Medeghini et al. (2019) the raw materials used are local, due to the identification of micro-fossils as planktonic foraminifera and other benthic organisms, which are comparable to local sedimentary outcrops. In particular, the two types of clays used in the common ceramic *repertoire* at the site, are linked to local sedimentary outcrops belonging to the Lisan or alluvium formations. The presence of micro-fossils does not have any relation to the functional class or technological reasons, and suggests a natural variability in the deposits that include beds of microfossils (Medeghini et al.,2019.).

5.4 Chalcolithic vs Early Bronze Age Production

Mineralogical, petrographic and chemical results of this thesis suggested that there is no difference in the supply of the raw materials during the centuries. However, a predominant use of calcite is observed in the Chalcolithic period, then substituted by quartz in the Early Bronze age. The use of calcite could be intentional, to improve the plasticity and strength of the vessel, whereas the use of quartz to increase the thermal expansion of the vessel. In both cases the potters wanted to create a more durable vessel. Unfortunately, this hypothesis could be affected by the random selection of samples as previous work (Medeghini et al., 2019) proved that fabric A and B were attested in both periods.

Concerning the technological level of the production, no evident differences have been observed among the ceramics analysed dated in the two periods. Selection of the materials, mixing phase, modelling technique and firing procedure are quite similar in the two periods, suggesting similar procedure or *chaine operatoire*. However, the limited number of analysed samples requires further investigation before reaching conclusions on this issue.

Chapter 6 : Conclusion

Mineralogical, petrographic and chemical analyses were applied by means of optical microscopy (OM), X-Ray Powder Diffraction (XRPD) and Scanning Electron Microscopy coupled with Energy Dispersive Spectroscopy (SEM-EDS) to identify the petro-fabrics and finally assess the raw materials used in the manufacture and their provenance, as well as the maximum firing temperatures in the ceramic production.

Optical and Electron Microscopy allowed the identification of two fabrics used in the production, based on the mineralogical and petrographic composition, mainly characterized by the presence of calcite and quartz crystals and nodules of iron oxides. Fabric A-calcite is characterized by the predominance of coarse and angular crystals of calcite, and can be sub-divided in two sub-fabrics, A1 and A2, due to the presence or absence of microfossils, respectively. Fabric B-calcareous is mainly composed of calcareous inclusions, and it is sub-grouped into B1, with predominant quartz, B2 with micro-fossils and, B3 for the microfeatures of the matrix.

Sample TFN.1959.L.718/31 is a loner, characterized by coarse grain size of inclusions, aligned to the margin, very abundant calcite, abundant K-feldspars and gehlenite, and the presence of quartz and anorthite in addition to fragments of basalt rocks.

Moreover, two types of clays, α and β, can be described based on the presence or absence of microfossils within the matrix, suggesting that clays were collected from different sources.

A local supply of the raw materials is supported, probably connected to local sedimentary outcrops belonging to the Lisan or alluvium formations. However, the presence of microfossils does not have any relation to functional class or technological reasons, because it expresses the natural variability in the deposits.

A firing temperature below 850 °C is indicated for samples showing optical activity and not decomposed calcareous inclusions. Only three samples dated back to the Early Bronze age were probably fired at higher temperature, between 800 and 950 °C.

Finally, no evident differences have been observed among the ceramics produced in Chalcolithic and Early Bronze Age phase, suggesting a similar *chaine operatoire* along the centuries.

REFERENCES

Albright, W.F. (1931): “The Site Of Tirzah And The Topography Of Western Manasseh”, Journal Of The Palestine Oriental Society 11, 241-251.

Ambari, Assam. Journal of Archaeological Science: Reports, Vol. 5, pp. 557–563.

Amiet, P. Et Al. (1996): Tell El Far’ah. Histoire, Glyptique Et Céramologie, Fribourg.

Applied Research Institute Jerusalem, Environmental Profile For The West Bank, Nablus District, 1996.

Bar, S., 2010. Early Bronze Age I ‘Um Hammad Ware’: A Study In Regionalism. Palestine Exploration Quarterly, 142,(2), Pp.82–94.

Barone, G., Crupi, V., Galli, S., Majolino, D., Migliardo, P. And Venuti, V. (2003) Spectroscopic Investigation Of Greek Ceramic Artefacts. Journal Of Molecular Structure, Vol. 651–653, Pp. 449–458.

Beller, J. A., Greenfield, H. J., Shai, I., & Maeir, A. M. (2016). The life-history of basalt ground stone tools from early urban domestic contexts: A chronicle from the EBA III of Tell es-Safi/Gath, Israel. In Journal of Lithic Studies (Vol. 3, Issue 3, pp. 31–55). Edinburgh University Library.

Braun E. (2011a). The Transition From Chalcolithic To Early Bronze Age I: A “Lost Horizon” Slowly Revealed. In: LOVELL J.L. And ROWAN Y.M. (Eds.): 160-177

Braun E. (2011b) Of Pots And Towns: Old And New Perspectives On EB I Of The Southern Levant. In: CHESSON M. (Ed.), Daily Life, Materiality And Complexity In Early Urban Communities Of The Southern Levant: Papers In Honor Of Walter E. Rast And R. Thomas Schaub: 265-280. Winona Lake: Eisenbrauns.

Braun E. and Gophna R. (2004). Excavations At Ashqelon, Afridar—Area G. ‘Atiqot 45: 185-242.

Braun, E. (2001). Proto And Early Dynastic Egypt And Early Bronze I-II Of The Southern Levant: Uneasy 14C Correlations. Radiocarbon 43: 1202-1218.

Braun, E., (1996). Cultural Diversity And Change In The Early Bronze I of Israel and Jordan: Towards An Understanding Of The Chronological Progression And Patterns Of Regionalism In Early Bronze I Society. Unpublished Phd Dissertation, Tel Aviv University.

Cogswell, J.W., Neff, H. and Glascock, M.D. (1996) The Effect of Firing Temperature on the Elemental Char-acterization of Pottery. Journal of Archaeological Science, Vol. 23, pp. 283–287.

Contenson, H. de., 1960. ‘Three soundings in the Jordan valley’, Annual of the Department of Antiquities of Jordan 4–5,12–98

Day, P. M., (1988), Ceramic Analysis And Pottery Systems: The Case Of Minoan Crete, In New Aspects of archaeological Science In Greece (4s. R. E. Jones And H. W. Catling), 39-45, Fitch Lab. Occas. Pap., 3, Athens.

De Benedetto, G.E., Laviano, R., Sabbatini, L. and Zambonin, P.G. (2002) Infrared spectroscopy in the miner-alogical characterization of ancient pottery. Journal of Cultural Heritage, Vol. 3, pp.177–186.

De Vaux, R. (1976): “El-Far’a, tell, North”, in Avi-Yonah, M. ed., Encyclopedia of Archaeological Excavations in the Holy Land, vol. 2, Jerusalem, 395-404

G. Cultrone, C. Rodriguez-Navarro, E. Sebastian, O. Cazalla, M.J. De La Torre, (2001) . Carbonate and Silicate Phase Reactions During Ceramic Firing, Eur. J. Mineral 13 621–634,

Garfinkel, Y., (1999). Neolithic And Chalcolithic Pottery Of The Southern Levant, Qedem, Vol. 39, Jerusalem: Institute Of Archaeology: Hebrew University Of Jerusalem.

Gilead, I.,(1988). The Chalcolithic Period In The Levant. Journal Of World Prehistory, 2(4), Pp.397-443.

Glueck, N., (1951). 'Explorations In Eastern Palestine IV (Part I: Text)', Annual Of The American Schools Of Oriental Research, Vols. XXV–XXVIII (For 1945–1949), New Haven: American Schools Of Oriental Research.

Golani A. and Nagar Y. (2011). Newly Discovered Burials Of The Chalcolithic And The Early Bronze Age I In Southern Canaan – Evidence Of Cultural Continuity In: LOVELL J.L. And ROWAN Y.M. (Eds.): 84-96

Golani, A., (2004). 'Salvage Excavations At The Early Bronze Age Site Of Ashqelon, Afridar — Area E', 'Atiqot 45, 9–62.

I.K. Whitbread, The characterization of argillaceous inclusions in ceramic thin sections, Archaeometry 28 (1986) 79–88, https://doi.org/10.1111/j.1475-4754.1986.tb00376.x

Kolb, C. C. 1989, Ceramic ecology in retrospect: a critical review of methodology and results, in Ceramic ecology 1988: current research on ceramic materials (ed. C. C. Kolb), British Archaeological Reports, S-513, Oxford.

Macdonald, E. (1932) Prehistoric Fara, Beth Pelet 11. London: The British School Of Archaeology In Egypt.

Mallon A., Koeppel S.J. and Neuville R. (1934). Teleilat Ghassul I. Rome: Pontifical Biblical Institute.

Maritan, L.,(2004). Archaeometric Study Of Etruscan-Padan Type Pottery From The Veneto Region: Petrographic, Mineralogical And Geochemical–Physical Characterisation. Eur. J. Mineral. 16, 297–307.

Matson, F. R., 1965, Ceramic ecology: an approach to the study of early culture in the near east, in Ceramics and man (ed. F. Matson), 202–17, Wenner–Gren Foundation for Anthropology Research, Viking Fund Publications in Anthropology 41, New York

Medeghini L. & Nigro L. (2017) Khirbet al-Batrawy ceramics: a systematic mineralogical and petrographic study for investigating the material culture. Periodico di Mineralogia, 86,19–35.

Medeghini, L., Sala, M., Mignardi, S. And De Vito, C., (2019). A Forgotten Centre Of Ceramic Production In Southern Levant: Preliminary Analytical Study Of The Early Bronze Age Pottery From Tell El-Far'ah North (West Bank). Elsevier, (Ceramics International 45), Pp.11457–11467.

Mellaart, J. (1962) Preliminary Report Of The Archaeological Survey In The Yarmouk And Jordan Valleys. Annual Of The Department Of Antiquities Of Jordan 6–7, 126–57.

Meloni, S., Oddone, M., Genova, N. And Cairo, A. (2000) The Production Of Ceramic Materials In Roman Pa- Via: An Archaeometric NAA Investigation Of Clay Sources And Archaeological Artifacts. Journal Of Ra- Bioanalytical And Nuclear Chemistry, Vol. 244, Pp. 553-558

Milevski, I., (2013). The Transition From The Chalcolithic To The Early Bronze Age Of The Southern Levant In Socioeconomic Context. Paléorient, Vol. 39, N°1., Pp. 193-208;.

Mimran, Y., Shaliv, G., Sakal, E., Sneh, A., (2016). The Geological Map Of Israel, 1: 50,000. Sheet 6-III, IV, Beqa'ot. In: Rosensaft, M., Vectorial Format Of The 1: 50,000 Geological Map Of Israel. Isr. Geol. Surv., Jerusalem. (Partly Revised, 2020).

Miroschedji, Pierre de, and Alain Chambon. "Far'ah, Tell el- (North)." In The New Encyclopedia of the Archaeological Excavations in the Holy Land, edited by Ephraim Stern, pp. 433–441. Jerusalem: Israel Exploration Society, 1993.

Miroschedji, Pierre R. de: L'Époque pré-Urbaine en Palestine. Cahiers de la Revue Biblique 13. Paris: Galbalda, 1971. 152 pp., 30 figs. F59.

Molera, J. (1998). The colours of CA-rich ceramic pastes: Origin and characterization. Applied Clay Science, 13(3), 187–202. https://doi.org/10.1016/s0169-1317(98)00024-6

Moore, A. M. T. (1985). The Development Of Neolithic Societies In The Near East. In Wendorf, F., And Close, A. E. (Eds.), Advances In World Archaeology, Vol 4, Academic Press, Orlando, Fla., Pp. 1-69.

Munita, C.S., Paiva, R.P., Alves, M.A., De Oliveira, P.M.S. & Momose, E.F. (2003) Provenance Study Of Archaeological Ceramic, Journal Of Trace And Microprobe Techniques, Vol. 21(4), Pp. 697-706.

Neff, H., (1993). Theory, Sampling, And Analytical Techniques In The Archaeological Study Of Prehistoric Ceramics. American Antiquity, Vol. 58(No. 1), Pp.23-44.

Nodari, L., Marcuz, E., Maritan, L., Mazzoli, C. and Russo, U. (2007) Hematite nucleation and growth in the firing of carbonate-rich clay for pottery production. Journal of the European Ceramic Society, Vol. 27, pp. 4665–4673.

Perrot, J. (1955). The Excavations At Teil Abu Matar Near Beersheba. Israel Exploration Journal 5: 17-40, 73-84, 167-189.

Quinn, P. S., & Day, P. M. (2007). Calcareous Microfossils In Bronze Age Aegean Ceramics: Illuminating Technology And Provenance. Archaeometry, 49(4), 775–793. Https://Doi.Org/10.1111/J.1475-4754.2007.00335.X

Rathossi,C., Tsolis-Katagas, P., Katagas,C. (2004).Technology and composition Of Roman Pottery In Northwestern Peloponnese, Greece. Applied Clay Science ,24, N 3–4, Pp. 313–326.

Regev, J, P De Miroschedji, R Greenberg, E Braun, Z Greenhut, & E Boaretto,(2012). "Chronology Of The Early Bronze Age In The Southern Levant: New Analysis For A High Chronology.". In Radiocarbon, 54, , 525-566.

Rice, P.M. (1987) Pottery Analysis: A Sourcebook. The University Of Chicago Press, Chicago And London.

Rosenberg D. & Golani A., (2012). Ground stone Tools Of A Bronze Smiths' Community – Under-Standing Stone-Related Aspects Of The Early Bronze Age Site Of Ashqelon Barnea. Journal Of Mediterranean Archaeology 25,1: 27-51.

Roux, V, & P De Miroschedji, (2009). "Revisiting The History Of The Potter's Wheel In The Southern Levant.". In Levant, 41, 155-173.

Rowan, Y, & J Golden, , (2009). "The Chalcolithic Period Of The Southern Levant: A Synthetic Review.". In Journal Of World Prehistory, 221-92.

Santos, J.O., Munita, C.S., Toyota, R.G., Vergne, C., Silva, R.S. and Oliveira, P.M.S. (2009) The archaeometry study of the chemical and mineral composition of pottery from Brazil's Northeast. J Radioanal Nucl Chem, Vol. 281, pp.189–192

Singh, P., & Sharma, S. (2016). Thermal and spectroscopic characterization of archaeological pottery from Ambari, Assam. In Journal of Archaeological Science: Reports (Vol. 5, pp. 557–563). Elsevier BV.

Sneh, A., Bartov, Y., Weissbrod, T. And Rosensaft, M., 1998. Geological Map Of Israel, 1:200,000. Isr. Geol. Surv. (4 Sheets).

Tite, M. S., Kilikoglou, V., & Vekinis, G. (2001). Strength, Toughness And Thermal Shock Resistance Of Ancient Ceramics, And Their Influence On Technological Choice. Archaeometry, 43(3), 301-324.

Uda, M. (2005) Characterization of Pigments Used in Ancient Egypt. In X-rays for Archaeology, M. Uda, G. Demortier, I. Nakai (ed.), The Netherlands: Springer, Nr. 1, pp. 3-26

Zeinab Javanshah (2018) Chemical And Mineralogical Analysis For Provenaning Of The Bronze Age Pottery From Shahr-I-Sokhta, South Eastern Iran. SCIENTIFIC CULTURE, Vol. 4, No 1, Pp. 83-92 (Early View 2017).